symmetry

MDPI

Article

Circuit Complexity in Z_2 EEFT

Kiran Adhikari [1], Sayantan Choudhury [2,3,4,*], Sourabh Kumar [5,6], Saptarshi Mandal [7,8], Nilesh Pandey [9], Abhishek Roy [10], Soumya Sarkar [11], Partha Sarker [12] and Saadat Salman Shariff [13,14]

1 Department of Physics, RWTH Aachen University, Otto-Blumenthal-Straße, 52074 Aachen, Germany
2 Centre For Cosmology and Science Popularization (CCSP), SGT University, Delhi-NCR, Gurugram 122505, India
3 National Institute of Science Education and Research, Bhubaneswar 752050, India
4 Homi Bhabha National Institute, Training School Complex, Anushakti Nagar, Mumbai 400085, India
5 Department of Physics and Astronomy, University of Calgary, Calgary, AB T2N 1N4, Canada
6 Institute for Quantum Science and Technology, University of Calgary, Calgary, AB T2N 1N4, Canada
7 Department of Physics, Jadavpur University, Kolkata 700032, India
8 Department of Physics, Indian Institute of Technology Kharagpur, Kharagpur 721302, India
9 Department of Applied Physics, Delhi Technological University, Delhi 110042, India
10 Department of Physics, Indian Institute of Technology Jodhpur, Karwar, Jodhpur 342037, India
11 National Institute of Technology Karnataka, Mangalore 575025, India
12 Department of Physics, University of Dhaka, Curzon Hall, Dhaka 1000, Bangladesh
13 Department of Theoretical Physics, University of Madras, Guindy Campus, Chennai 600025, India
14 Department of Physics, Indian Institute of Science and Educational Research, Behrampur 760010, India
* Correspondence: sayantan_ccsp@sgtuniversity.org or sayanphysicsisi@gmail.com

Abstract: Motivated by recent studies of circuit complexity in weakly interacting scalar field theory, we explore the computation of circuit complexity in $\mathcal{Z}_2$ Even Effective Field Theories ($\mathcal{Z}_2$ EEFTs). We consider a massive free field theory with higher-order Wilsonian operators such as ϕ^4, ϕ^6, and ϕ^8. To facilitate our computation, we regularize the theory by putting it on a lattice. First, we consider a simple case of two oscillators and later generalize the results to N oscillators. This study was carried out for nearly Gaussian states. In our computation, the reference state is an approximately Gaussian unentangled state, and the corresponding target state, calculated from our theory, is an approximately Gaussian entangled state. We compute the complexity using the geometric approach developed by Nielsen, parameterizing the path-ordered unitary transformation and minimizing the geodesic in the space of unitaries. The contribution of higher-order operators to the circuit complexity in our theory is discussed. We also explore the dependency of complexity on other parameters in our theory for various cases.

Keywords: circuit complexity; effective field theory; AdS/CFT correspondence

Citation: Adhikari, K.; Choudhury, S.; Kumar, S.; Mandal, S.; Pandey, N.; Roy, A.; Sarkar, S.; Sarker, P.; Shariff, S.S. Circuit Complexity in Z_2 EEFT. *Symmetry* **2023**, *15*, 31. https://doi.org/10.3390/sym15010031

Academic Editor: Abraham A. Ungar

Received: 24 November 2022
Revised: 12 December 2022
Accepted: 14 December 2022
Published: 22 December 2022

1. Prologue

In recent years, tools and techniques from quantum information have played a vital role in developing new perspectives in areas such as quantum field theory and holography, particularly for AdS/CFT duality. A particular line of study in the context of AdS/CFT correspondence is deciphering the emergence of bulk physics using information from the boundary CFT [1]. It was shown in [2–4] that the codimension-2 extremal surfaces in the AdS are associated with the entanglement entropy (EE) of the boundary CFT. However, in recent years, studies in black hole physics have suggested that EE is not sufficient to capture the complete information, which led Susskind et al. to introduce a new measure known as Quantum Computational Complexity (QCC) [5–13]. In the context of AdS/CFT, the QCC of the dual CFT is proposed to be associated with the properties of the codimension-0 and codimension-1 extremal surfaces. This aroused the study of QCC in QFTs.

The complexity of quantum states has aroused a significant amount of interest not only in the context of holography but across different subfields of physics (from quantum computing and information to many-body physics), as it appears to be a better measure of information. In [14,15], the notion of circuit complexity was defined and studied for free bosonic field theory, and in [16,17], it was defined and studied for free fermionic field theory. For a weakly interacting field theory, the authors of [18] extended the study to the ϕ^4 theory, where in addition to the study of QCC, its relationship with renormalization group flows was also explored. The growth of complexity in the quantum circuit model was studied in [19]. Circuit complexity was also discussed in the context of chaos, quantum mechanics, and quantum computing in [20–23]. It has been probed in relation to conformal and topological field theories and the Chern–Simmons theory [24–27]. Active study in the context of many-body quantum systems has been also gaining interest in recent years [28]. QCC has been studied in many other contexts. It has been explored extensively in holography [29–57]. The thermodynamic properties of QCC were studied in [58–60]. In addition, various applications and properties of QCC were investigated in [61–84].

In this paper, we extend the work in [18] by including even higher-order Wilsonian operators, which we denote with $\mathcal{Z}_2$ EEFT (Even Effective Field Theory). Our theory contains the interaction terms ϕ^4, ϕ^6, and ϕ^8. These are weakly coupled to the free scalar field theory via the coupling constants λ_4, λ_6, and λ_8 respectively. The primary motivation for studying QCC in this context is to compute and understand QCC by including higher-order terms. The organization of the paper is as follows. In Section 2, we summarize Nielsen's method for computing circuit complexity. In Section 3, we briefly discuss the pertinent details of EFT related to our work. In Section 4, we illustrate the computation of QCC for our theory by first giving an example of two coupled oscillators. In Section 5, we generalize the calculation to the N oscillator case. Since we could not observe any analytical expression for the relevant eigenvalues for N oscillators, in Section 6, we resort to numerical computation of the QCC. We plot the corresponding graphs of QCC with the relevant parameters in our theory. We finish up by summarizing and providing possible future prospects for our work.

2. Circuit Complexity and Its Purposes

Computationally, circuit complexity is defined as a measure of the minimum number of elementary operations required by a computer to solve a certain computational problem [85–90]. In quantum computation, a quantum operation is described by a unitary transformation. Therefore, quantum circuit complexity is the length of the optimized circuit that performs this unitary operation. As the size of the input increases, if the complexity grows polynomially, then the problem is called "easy", but if it grows exponentially, then the problem is called "hard".

Quantum information-theoretic concepts, such as entanglement, have proven to be helpful in areas other than quantum computing [91–94]. Quantum circuit complexity (QCC) is emerging as one such quantum information-theoretic concept that has the potential to explain phenomena in several areas of quantum physics. However, the lower bounding quantum circuit complexity is an extremely challenging open problem.

For our purpose, we will consider the geometric approach to computing quantum circuit complexity developed by Nielsen et al. [85,87]. The prime reason to consider a geometric approach is that it is much easier to minimize a smooth function in a smooth space than to minimize an arbitrary function in a discrete space. Since the unitaries are continuous, this method of optimization suits our needs well. Interestingly, this approach allows us to formulate the optimal circuit-finding problem in the language of the Hamiltonian control problem, for which a mathematical method called the calculus of variations can be employed to find the minima. Another reason is that this method is similar to the general Lagrangian formalism, where the motion of the test particle is obtained from minimizing a global functional. For example, in general relativity, test particles move along geodesics of spacetime described by the following geodesic equation:

$$\frac{d^2x^j}{dt^2} + \Gamma^j_{kl}\frac{dx^k}{dt}\frac{dx^l}{dt} = 0$$

where x^j represents the coordinates for the position on the manifold and Γ^j_{kl} represents the Christoffel symbols given by the geometry of the spacetime. Thus, the problem of finding an optimal quantum circuit is related to "freely falling" along the minimal geodesic curve connecting the identity to the desired operation, and the path is given by the "local shape" of the manifold. If we have information about the local velocity and the geometry, then it is possible to predict the rest of the path. In this regard, geometric analysis of quantum computation is quite powerful, as it allows one to design the rest of the shortest quantum circuit with information about only part of it.

2.1. Main Mathematical Ideas

Our goal is to understand how difficult it is to implement an arbitrary unitary operation $\mathbb{U}$ generated by a time-dependent Hamiltonian $H(t)$:

$$\mathbb{U}(s) = \overleftarrow{\mathcal{P}} \exp\left[-i \int_0^s ds' \, H(s') \right] \tag{1}$$

where $\overleftarrow{\mathcal{P}}$ is the path-ordering operator and the space of the circuits is parameterized by s. The path-ordering operator $\overleftarrow{\mathcal{P}}$ is the same as the time-ordering operator, which indicates that the circuit runs from right to left. We can expand the Hamiltonian $H(s)$ as follows:

$$H(s) = \sum_I Y^I(s) M_I \tag{2}$$

where M_I represents the generalized Pauli matrices and the coefficient $Y^I(s)$ represents the control functions that tell us the gate to be applied at particular values of s.

The Schrödinger equation $d\mathbb{U}/dt = -iH\mathbb{U}$ describes the evolution of the unitary operation:

$$\frac{d\mathbb{U}(s)}{ds} = -iY(s)^I M_I \mathbb{U}(s) \tag{3}$$

where at the final time t_f, $\mathbb{U}(t_f) = \mathbb{U}$.

We can impose a cost function $F(\mathbb{U}, \dot{\mathbb{U}})$ on the Hamiltonian control $H(t)$ which will tell us how difficult it is to apply a specific unitary operation $\mathbb{U}$. One can then define a Riemannian geometry in the space of the unitary operations with this cost function. Then, the problem of finding an optimal control function is translated to the problem of finding the minimal geodesic in this geometry, and we can define a notion of distance in $SU(2^n)$. For this, we have to define a curve $\mathbb{U}$ between the identity operation I and the desired unitary $\mathbb{U}$, which is a smooth function $\mathbb{U} : [0, t_f] \to SU(2^n)$ such that $\mathbb{U}(0) = I$ and $\mathbb{U}(t_f) = \mathbb{U}$. The length of this curve is defined as

$$d([\mathbb{U}]) = \int_0^{t_f} dt F(\mathbb{U}, \dot{\mathbb{U}}) \tag{4}$$

This length $d([\mathbb{U}])$ gives the total cost of synthesizing the Hamiltonian that describes the motion along the curve. In particular, the distance $d(I, \mathbb{U})$ is also a lower bound on the number of one- and two-qubit quantum gates necessary to exactly simulate U. The proof is available in the original papers of Nielsen [85]. Therefore, one can also consider the distance $d([\mathbb{U}])$ as an alternative description of the complexity.

The cost function F has to satisfy certain properties, such as continuity, positivity, positive homogeneity, and triangle inequality [77]. If we also demand F to be smooth (i.e., $F \in C^\infty$), then the manifold is referred to as the Finsler manifold. Since the field of differential geometry is relatively mature, we hope that borrowing tools from differential geometry can provide a unique perspective on quantum complexity.

In the literature, there are several alternative definitions of the cost function $F(\mathbb{U}, v)$. Some of them are

$$\begin{aligned} F_1(\mathbb{U}, Y) &= \sum_I |Y^I| \\ F_p(\mathbb{U}, Y) &= \sum_I p_I |Y^I| \\ F_2(\mathbb{U}, Y) &= \sqrt{\sum_I |Y^I|^2} \\ F_q(\mathbb{U}, Y) &= \sqrt{\sum_I q_I |Y^I|^2} \end{aligned} \tag{5}$$

where F_1, the linear cost functional measure, is the concept closest to the classical concept of counting gates, while F_2, the quadratic cost functional, can be understood as the proper distance in the manifold. F_p is similar to F_1 but with penalty parameters p_I used to favor certain directions over others.

In Figure 1 the left figure represents a unitary transformation from a reference state to a target state using quantum gates, and the right figure represents geometrizing the problem of calculating the minimum number of gates representing the transformation.

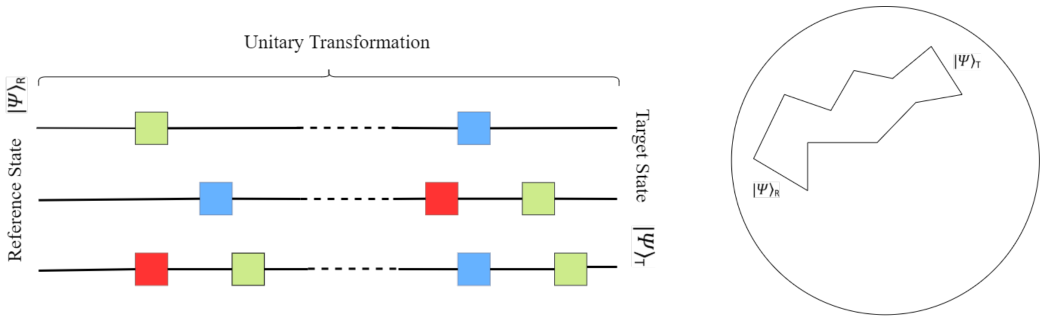

Figure 1. The left figure represents a unitary transformation from a reference state to a target state using quantum gates (square blocks), and the right figure represents geometrizing the problem of calculating the minimum number of gates representing the transformation.

2.2. Geometric Algorithm to Compute Circuit Complexity

We will now describe the algorithm for computing the circuit complexity. These algorithms are not rigorously proven, but from an operational point, these general steps are implemented to calculate the circuit complexity:

1. Give the Hamiltonian corresponding to a particular physical system;
2. Specify the reference state $|\psi\rangle_R$, the target state $|\psi\rangle_T$, and the unitary operation $\mathbb{U}$ that takes the former to the latter, where $|\psi\rangle_T = \mathbb{U}\,|\psi\rangle_R$;
3. Now, we need to choose some set of elementary gates $Q_{ab} = \exp[\epsilon M_{ab}]$, where M_I represents the generators of the group corresponding to the choice of gates and ϵ is a controllable parameter. For simplicity, we often choose generators satisfying $Tr[M_I M_J^T] = \delta_{IJ}$.
4. With the basis of generators M_I, we parametrize the unitary operation $\mathbb{U}$ as $\mathbb{U}(s)$;
5. The velocity component $Y^I(s)$ can be explicitly computed using

$$Y^I(s) M_I = i(\partial_s \mathbb{U}(s)) \mathbb{U}^{-1}(s)) \rightarrow Y^I(s) = \frac{1}{\mathrm{Tr}\left[M^I (M^I)^T\right]} \mathrm{Tr}\left[\partial_s \mathbb{U}(s) \mathbb{U}^{-1} \left(M^I\right)^T\right] \tag{6}$$

For generators obeying $Tr[M_I M_J^T] = \delta_{IJ}$, $Y^I(s)$ reduces to

$$Y^I(s) = \mathrm{Tr}[i(\partial_s \mathbb{U}(s)) \mathbb{U}^{-1}(s) M_I^T] \tag{7}$$

The right invariant metric in the space is given by

$$ds^2 = G_{IJ} Y^I Y^J \tag{8}$$

where G_{IJ} gives the penalty parameters. If $G_{IJ} = \delta_{IJ}$ (i.e., assigning an equal cost to every choice of gate), and having an extra condition $Tr[M_I M_J^T] = \delta_{IJ}$, we obtain a metric of the reduced simple form

$$ds^2 = \delta_{IJ} \mathrm{Tr}[i(\partial_s \mathbb{U}(s))\mathbb{U}^{-1}(s) M_I^T] \mathrm{Tr}[i(\partial_s \mathbb{U}(s))\mathbb{U}^{-1}(s) M_J^T] \tag{9}$$

6. The general form of the circuit complexity would be

$$\mathcal{C}[\mathbb{U}] = \int_0^1 ds \sqrt{G_{IJ} Y^I(s) Y^J(s)} \tag{10}$$

The circuit complexity for the F_2 metric (i.e., $G_{IJ} = \delta_{IJ}$) is then

$$\mathcal{C}[\mathbb{U}] = \int_0^1 ds \sqrt{g_{ij} \dot{x}^i \dot{x}^j} \tag{11}$$

7. From the boundary conditions of the evolution of unitary operations, we can compute the geodesic path and geodesic length. This length then gives a measure of circuit complexity.

In the literature, circuit complexity, using this geometric approach, is computed mostly for Gaussian wave functions because of its simpler structure compared with non-Gaussian wave functions. A Gaussian wave function can be represented as follows:

$$\psi \approx \exp\left[-\frac{1}{2} v_a A(s)_{ab}\, v_b\right], \text{ where } v = \{x_a, x_b\} \tag{12}$$

where x_a and x_b are the bases of vector v. If we can simultaneously diagonalize the reference and target states, then a common pattern observed in the complexity is that it will be given by some function of the ratio of the eigenvalues of $A(s=0)$ and $A(s=1)$. Here, $A(s=0)$ represents the reference state, and $A(s=1)$ represents the target state.

We would like to mention that our approach to computing complexity is based on Nielsen's geometric approach, which suffers from ambiguity in choosing the elementary quantum gates and states. However, these choices of our gates significantly simplify the calculation. Furthermore, the previous works on complexity in QFT and interacting QFT [14,18], using similar quantum gates to ours, have been connected to a holographic proposal, which is the original motivation to study quantum circuit complexity in QFT. Recently, Krylov complexity has been proposed as a tool for studying operator growth and associated quantum chaos [95–103]. Contrary to Nielsen's geometric approach, the Krylov complexity is independent of such arbitrary choices, making it a good candidate for complexity in QFT and holography. However, Krylov complexity does not have a good operational meaning, such as in Nielsen's geometric measure. Nielsen's measure not only gives the state complexity but also gives us a method of constructing an optimal quantum circuit. This feature makes it more appealing than the Krylov complexity. In the future, we would like to study the Krylov complexity for our case too.

3. Effective Field Theory in a Nutshell

An effective field theory (EFT) is a theory corresponding to the dynamics of a physical system at energies that are smaller than the cutoff energy. EFTs have made a significant impact on several areas of theoretical physics, including condensed matter physics [104], cosmology [105–111], particle physics [112,113], gravity [114,115], and hydrodynamics [116,117]. The idea behind an EFT is that we can compute results without knowing the full theory. In the context of quantum field theory, this implies that using the method of

EFTs, one can study the low energy aspect of the theory without having a full theory in the high energy limit. If the high-energy theory is known, then one can obtain an EFT using the "top-down" approach [118], where one has to eliminate high-energy effects. Using the "bottom-up" approach, one can obtain an EFT if the theory for high energy is not available. Here, one has to impose constraints given by symmetry and "naturalness" on suitable Lagrangians.

The Hamiltonian of our theory is

$$H = \frac{1}{2}\int d^{d-1}x\left[\pi(x)^2 + (\nabla\phi(x))^2 + m^2\phi^2(x) + 2\sum_{n=2}^{4} C_{2n}\phi^{2n}(x)\right] \tag{13}$$

where the coefficients $C_{2n} = 2\hat{\lambda}_{2n}/(2n)!$ are called the "Wilson coefficients" for the $\mathcal{Z}_2$ EEFTs in arbitrary dimensions. These coefficients depend on the scaling of the theory. These coefficients are expected to be functions of the λs, the cutoffs of our theory, and this functional dependence can be found by solving the renormalization group equations or Callan–Symanzik equations. ϕ^{2n}s are called the "Wilson operators" in $\mathcal{Z}_2$ EEFTs. $\phi^2(x)$ and $\phi^4(x)$ are called "relevant operators of EEFTs", and this theory is renormalizable up to $\phi^4(x)$. Beyond that, all the higher-order even terms, which are $\phi^6(x)$ and $\phi^8(x)$ in our case, are called "non-renormalizable irrelevant operators of $\mathcal{Z}_2$ EEFTs". However, it should be noted that even though this theory goes up in the "Wilson operator" order, the contributions from those terms decrease gradually. Therefore, it is an infinite convergent series. Building upon this, we go on to compute the circuit complexity in the $\mathcal{Z}_2$ EEFT.

4. Circuit Complexity with $(\hat{\lambda}_4\phi^4 + \hat{\lambda}_6\phi^6 + \hat{\lambda}_8\phi^8)$ Interaction for the Case of Two Harmonic Oscillators

We work with massive scalar field theory and with the even interaction terms ϕ^4, ϕ^6, and ϕ^8, which are weakly coupled to the free field theory via the coupling constants $\hat{\lambda}_4$, $\hat{\lambda}_6$, and $\hat{\lambda}_8$, respectively. The inequality between the coupling constants is $\frac{\hat{\lambda}_4}{4!} > \frac{\hat{\lambda}_6}{6!} > \frac{\hat{\lambda}_8}{8!}$. The Hamiltonian for this scalar field in d spacetime dimensions is

$$H = \frac{1}{2}\int d^{d-1}x\left[\pi(x)^2 + (\nabla\phi(x))^2 + m^2\phi(x)^2 + 2\sum_{n=2}^{4} C_{2n}\phi^{2n}(x)\right] \tag{14}$$

where the mass of the scalar field ϕ is m. We work in the weak coupling regime $(\hat{\lambda} \ll 1)$ so that perturbative methods can be used to investigate the theory. The system can be reduced to a chain of harmonic oscillators if we regulate the theory by placing it on a $(d-1)$ dimensional square lattice with lattice spacing δ. We are taking the infinite system in Equation (14) and discretizing it to a finite N oscillator system because if we have an infinite convergent theory and an infinite number of terms in the Hamiltonian, then we do not have the finite symmetries that we are interested in. Therefore, the discretized Hamiltonian becomes

$$H = \frac{1}{2}\sum_{\vec{n}}\left\{\frac{\pi(\vec{n})^2}{\delta^{d-1}} + \delta^{d-1}\left[\frac{1}{\delta^2}\sum_i(\phi(\vec{n}) - \phi(\vec{n}-\hat{x}_i))^2 + m^2\phi(\vec{n})^2 + \frac{2\hat{\lambda}_4}{4!}\phi(\vec{n})^4 + \frac{2\hat{\lambda}_6}{6!}\phi(\vec{n})^6 + \frac{2\hat{\lambda}_8}{8!}\phi(\vec{n})^8\right]\right\} \tag{15}$$

where $\vec{n}$ denotes the spatial position vectors of the points on the lattice in d dimensions and $\hat{x}_i$ represents the unit vectors along the lattice. We make the following substitutions to simplify the form of the Hamiltonian:

$$X(\vec{n}) = \delta^{d/2}\phi(\vec{n}) \qquad P(\vec{n}) = \pi(\vec{n})/\delta^{d/2} \qquad M = \frac{1}{\delta}, \omega = m, \Omega = \frac{1}{\delta}$$

$$\lambda_4 = \frac{\hat{\lambda}_4}{4!}\delta^{-d} \qquad \lambda_6 = \frac{\hat{\lambda}_6}{6!}\delta^{-2d} \qquad \lambda_8 = \frac{\hat{\lambda}_8}{8!}\delta^{-3d}$$

After the substitutions, we obtain

$$H = \sum_{\vec{n}} \left\{ \frac{P(\vec{n})^2}{2M} + \frac{1}{2} M \Big[\omega^2 X(\vec{n})^2 + \Omega^2 \sum_i (X(\vec{n}) - X(\vec{n} - \hat{x}_i))^2 + 2\big\{ \lambda_4 X(\vec{n})^4 + \lambda_6 X(\vec{n})^6 + \lambda_8 X(\vec{n})^8 \big\} \Big] \right\} \tag{16}$$

We observe that the Hamiltonian obtained is identical to that of an infinite family of coupled anharmonic oscillators. The nearest term interaction comes from the kinetic part, and the self-interactions come from the remaining portion of the Hamiltonian. We start with the simple case of two coupled oscillators and generalize it to the case of N oscillators later in this paper. By setting $M = 1$, the Hamiltonian takes the form

$$H = \tfrac{1}{2}\Big[p_1^2 + p_2^2 + \omega^2 (x_1^2 + x_2^2) + \Omega^2 (x_1 - x_2)^2 + 2\big\{ \lambda_4 (x_1^4 + x_2^4) + \lambda_6 (x_1^6 + x_2^6) + \lambda_8 (x_1^8 + x_2^8) \big\} \Big] \tag{17}$$

Now, let us consider the normal mode basis:

$$\begin{aligned} \bar{x}_0 &= \frac{1}{\sqrt{2}}(x_1 + x_2), \quad \bar{x}_1 = \frac{1}{\sqrt{2}}(x_1 - x_2), \\ \bar{p}_0 &= \frac{1}{\sqrt{2}}(p_1 + p_2), \quad \bar{p}_1 = \frac{1}{\sqrt{2}}(p_1 - p_2) \\ \tilde{\omega}_0^2 &= \omega^2, \quad \tilde{\omega}_1^2 = \omega^2 + 2\Omega^2 \end{aligned} \tag{18}$$

In the normal mode basis, the unperturbed Hamiltonian becomes decoupled. Then, the eigenfunctions and eigenvalues for the unperturbed Hamiltonian can be easily solved, which is just a product of the ground-state eigenfunctions of the oscillators in the normal basis:

$$\psi^0_{n_1,n_2}(\bar{x}_0, \bar{x}_1) = \frac{1}{\sqrt{2^{n_1+n_2} n_1! n_2!}} \frac{(\tilde{\omega}_0 \tilde{\omega}_1)^{1/4}}{\sqrt{\pi}} e^{-\frac{1}{2}\tilde{\omega}_0 \bar{x}_0^2 - \frac{1}{2}\tilde{\omega}_1 \bar{x}_1^2} H_{n_1}\big(\sqrt{\tilde{\omega}_0}\bar{x}_0\big) H_{n_2}\big(\sqrt{\tilde{\omega}_1}\bar{x}_1\big) \tag{19}$$

Here, $H_n(x)$s denote Hermite polynomials of an order n. The ground state wavefunction with first-order perturbative correction in λ_4, λ_6, and λ_8 has the following expression:

$$\psi_{0,0}(\bar{x}_0, \bar{x}_1) = \psi^0_{0,0}(\bar{x}_0, \bar{x}_1) + \lambda_4 \psi^1_{0,0}(\bar{x}_0, \bar{x}_1)_4 + \lambda_6 \psi^1_{0,0}(\bar{x}_0, \bar{x}_1)_6 + \lambda_8 \psi^1_{0,0}(\bar{x}_0, \bar{x}_1)_8 \tag{20}$$

Here, $\psi^1_{0,0}(\bar{x}_0, \bar{x}_1)_4$, $\psi^1_{0,0}(\bar{x}_0, \bar{x}_1)_6$, and $\psi^1_{0,0}(\bar{x}_0, \bar{x}_1)_8$ are the terms representing the first-order perturbative corrections to the ground state wavefunction due to the ϕ^4, ϕ^6, and ϕ^8 interactions, respectively, which are as follows:

$$\begin{aligned} \psi^1_{0,0}(\bar{x}_0, \bar{x}_1)_4 = &- \frac{3(\tilde{\omega}_0 + \tilde{\omega}_1)}{4\sqrt{2}\tilde{\omega}_0 \tilde{\omega}_1^3} \psi^0_{0,2} - \frac{\sqrt{3}}{8\sqrt{2}\tilde{\omega}_1^3} \psi^0_{0,4} - \frac{3(\tilde{\omega}_0 + \tilde{\omega}_1)}{4\sqrt{2}\tilde{\omega}_0^3 \tilde{\omega}_1} \psi^0_{2,0} - \frac{3}{4\tilde{\omega}_0(\tilde{\omega}_0 + \tilde{\omega}_1)\tilde{\omega}_1} \psi^0_{2,2} \\ &- \frac{\sqrt{3}}{8\sqrt{2}\tilde{\omega}_0^3} \psi^0_{4,0} \end{aligned}$$

$$\begin{aligned} \psi^1_{0,0}(\bar{x}_0, \bar{x}_1)_6 = &- \frac{45(\tilde{\omega}_0 + \tilde{\omega}_1)^2}{32\sqrt{2}\tilde{\omega}_0^2 \tilde{\omega}_1^4} \psi^0_{0,2} - \frac{15\sqrt{3}(\tilde{\omega}_0 + \tilde{\omega}_1)}{32\sqrt{2}\tilde{\omega}_0 \tilde{\omega}_1^4} \psi^2_{0,4} - \frac{\sqrt{5}}{16\tilde{\omega}_1^4} \psi^0_{0,6} - \frac{45(\tilde{\omega}_0 + \tilde{\omega}_1)^2}{32\sqrt{2}\tilde{\omega}_0^4 \tilde{\omega}_1^2} \psi_{2,0} \\ &- \frac{45(\tilde{\omega}_0 + \tilde{\omega}_1)}{16\tilde{\omega}_0^2(\tilde{\omega}_0 + \tilde{\omega}_1)\tilde{\omega}_1^2} \psi^0_{2,2} - \frac{15\sqrt{3}}{16\tilde{\omega}_0(\tilde{\omega}_0 + 2\tilde{\omega}_1)\tilde{\omega}_1^2} \psi^0_{2,4} - \frac{15\sqrt{3/2}(\tilde{\omega}_0 + \tilde{\omega}_1)}{32\tilde{\omega}_0^4 \tilde{\omega}_1} \psi^0_{4,0} \\ &- \frac{15\sqrt{3}}{16\tilde{\omega}_0^2(2\tilde{\omega}_0 + \tilde{\omega}_1)\tilde{\omega}_1} \psi^0_{4,2} - \frac{\sqrt{5}}{16\tilde{\omega}_0^4} \psi^0_{6,0} \end{aligned}$$

$$\begin{aligned}\psi^1_{0,0}(\bar{x}_0,\bar{x}_1)_8 =&\Big(\frac{105\sqrt{2}}{8\tilde{\omega}_0^5}+\frac{315\sqrt{2}}{8\tilde{\omega}_0^4\tilde{\omega}_1}+\frac{315\sqrt{2}}{8\tilde{\omega}_0^3\tilde{\omega}_1^2}+\frac{105\sqrt{2}}{8\tilde{\omega}_0^2\tilde{\omega}_1^3}\Big)\psi^0_{2,0}+\Big(\frac{105\sqrt{2}}{8\tilde{\omega}_1^5}+\frac{105\sqrt{2}}{8\tilde{\omega}_0^3\tilde{\omega}_1^2}+\frac{315\sqrt{2}}{8\tilde{\omega}_0^3\tilde{\omega}_1^2}\\&+\frac{315\sqrt{2}}{8\tilde{\omega}_1^4\tilde{\omega}_0}\Big)\psi^0_{0,2}+\Big(\frac{315}{4\tilde{\omega}_0^3\tilde{\omega}_1(\tilde{\omega}_0+\tilde{\omega}_1)}+\frac{315}{2\tilde{\omega}_0^2\tilde{\omega}_1^2(\tilde{\omega}_0+\tilde{\omega}_1)}+\frac{315}{4\tilde{\omega}_1^3\tilde{\omega}_0(\tilde{\omega}_0+\tilde{\omega}_1)}\Big)\\&*\psi^0_{2,2}+\Big(\frac{105\sqrt{6}}{16\tilde{\omega}_0^5}+\frac{105\sqrt{6}}{8\tilde{\omega}_0^4\tilde{\omega}_1}+\frac{105\sqrt{6}}{16\tilde{\omega}_0^3\tilde{\omega}_1^2}\Big)\psi^0_{4,0}+\Big(\frac{105\sqrt{6}}{16\tilde{\omega}_1^5}+\frac{105\sqrt{6}}{8\tilde{\omega}_1^4\tilde{\omega}_0}+\frac{105\sqrt{6}}{16\tilde{\omega}_0^2\tilde{\omega}_1^3}\Big)\\&*\psi^0_{0,4}+\Big(\frac{105\sqrt{3}}{2\tilde{\omega}_0^3\tilde{\omega}_1(2\tilde{\omega}_0+\tilde{\omega}_1)}+\frac{105\sqrt{3}}{2\tilde{\omega}_0^2\tilde{\omega}_1^2(2\tilde{\omega}_0+\tilde{\omega}_1)}\Big)\psi^0_{4,2}+\Big(\frac{105\sqrt{3}}{2\tilde{\omega}_1^3\tilde{\omega}_0(2\tilde{\omega}_1+\tilde{\omega}_0)}\\&+\frac{105\sqrt{3}}{2\tilde{\omega}_0^2\tilde{\omega}_1^2(\tilde{\omega}_0+2\tilde{\omega}_1)}\Big)\psi^0_{2,4}+\frac{105}{4\tilde{\omega}_0^2\tilde{\omega}_1^2(\tilde{\omega}_0+\tilde{\omega}_1)}\psi^0_{4,4}+\Big(\frac{7\sqrt{5}}{2\tilde{\omega}_0^5}+\frac{7\sqrt{5}}{2\tilde{\omega}_0^4\tilde{\omega}_1}\Big)\psi^0_{6,0}+\\&\Big(\frac{7\sqrt{5}}{2\tilde{\omega}_1^5}+\frac{7\sqrt{5}}{2\tilde{\omega}_1^4\tilde{\omega}_0}\Big)\psi^0_{0,6}+\frac{21\sqrt{10}}{2\tilde{\omega}_1^3\tilde{\omega}_0(3\tilde{\omega}_1+\tilde{\omega}_0)}\psi^0_{2,6}+\frac{21\sqrt{10}}{2\tilde{\omega}_1^3\tilde{\omega}_0(3\tilde{\omega}_1+\tilde{\omega}_0)}\psi^0_{2,6}\\&+\frac{3\sqrt{70}}{\tilde{\omega}_0^5}\psi^0_{8,0}+\frac{3\sqrt{70}}{\tilde{\omega}_1^5}\psi^0_{0,8}\end{aligned}$$

We can approximate the total ground state wave function in Equation (20) in exponential form as the values of λ_4, λ_6, $\lambda_8 \ll 1$:

$$\begin{aligned}\psi_{0,0}(\bar{x}_0,\bar{x}_1)\approx\frac{(\tilde{\omega}_0\tilde{\omega}_1)^{1/4}}{\sqrt{\pi}}\exp[\alpha_0]\exp\Big[-\frac{1}{2}\Big(\alpha_1\bar{x}_0^2+\alpha_2\bar{x}_1^2+\alpha_3\bar{x}_0^2\bar{x}_1^2+\alpha_4\bar{x}_0^4+\alpha_5\bar{x}_1^4+\alpha_6\bar{x}_0^4\bar{x}_1^2+\alpha_7\bar{x}_0^2\bar{x}_1^4\\+\alpha_8\bar{x}_0^6+\alpha_9\bar{x}_1^6+\alpha_{10}\bar{x}_0^2\bar{x}_1^6+\alpha_{11}\bar{x}_0^6\bar{x}_1^2+\alpha_{12}\bar{x}_0^4\bar{x}_1^4+\alpha_{13}\bar{x}_0^8+\alpha_{14}\bar{x}_1^8\Big)\Big]\end{aligned} \tag{21}$$

We shall take $\psi_{0,0}(\bar{x}_0,\bar{x}_1)$ as the general target state wavefunction for calculating complexity in the following sections. The coefficients $\alpha_0,\alpha_1,\alpha_2\ldots\alpha_{14}$ involved in the approximate wavefunction Equation (21) are given in the Table 1.

Table 1. Expression for coefficients $\alpha_0, \alpha_1, \alpha_2 \ldots \alpha_{14}$, present in the wavefunction.

α_i	Coefficient of α_i
α_0	$-2\Big[\frac{9\lambda_4}{32\tilde\omega_0^3}+\frac{9\lambda_4}{32\tilde\omega_1^3}+\frac{3\lambda_4}{8\tilde\omega_0\tilde\omega_1^2}+\frac{3\lambda_4}{8\tilde\omega_0^2\tilde\omega_1}+\frac{3\lambda_4}{4\tilde\omega_0(-2\tilde\omega_0-2\tilde\omega_1)\tilde\omega_1}+\frac{55\lambda_6}{128\tilde\omega_0^4}+\frac{55\lambda_6}{128\tilde\omega_1^4}+\frac{135\lambda_6}{128\tilde\omega_0\tilde\omega_1^3}+\frac{45\lambda_6}{32\tilde\omega_0^2\tilde\omega_1^2} -\frac{45\lambda_6}{32\tilde\omega_0(-2\tilde\omega_0-4\tilde\omega_1)\tilde\omega_1^2}+\frac{45\lambda_6}{16\tilde\omega_0(-2\tilde\omega_0-2\tilde\omega_1)\tilde\omega_1^2}+\frac{135\lambda_6}{128\tilde\omega_0^3\tilde\omega_1}-\frac{45\lambda_6}{32\tilde\omega_0^2(-4\tilde\omega_0-2\tilde\omega_1)\tilde\omega_1}+\frac{45\lambda_6}{16\tilde\omega_0^2(-2\tilde\omega_0-2\tilde\omega_1)\tilde\omega_1} +\frac{875\lambda_8}{1024\tilde\omega_0^5}+\frac{875\lambda_8}{1024\tilde\omega_1^5}+\frac{385\lambda_8}{128\tilde\omega_0\tilde\omega_1^4}+\frac{105\lambda_8}{256\tilde\omega_0^2\tilde\omega_1^3}+\frac{2625\lambda_8}{256\tilde\omega_0^3\tilde\omega_1^2}+\frac{385\lambda_8}{128\tilde\omega_0^4\tilde\omega_1}-\frac{315\lambda_8}{64\tilde\omega_0\tilde\omega_1^3(\tilde\omega_0+\tilde\omega_1)} -\frac{2835\lambda_8}{256\tilde\omega_0^2\tilde\omega_1^2(\tilde\omega_0+\tilde\omega_1)}-\frac{315\lambda_8}{64\tilde\omega_0^3\tilde\omega_1(\tilde\omega_0+\tilde\omega_1)}+\frac{315\lambda_8}{64\tilde\omega_0^2\tilde\omega_1^2(2\tilde\omega_0+\tilde\omega_1)}+\frac{315\lambda_8}{64\tilde\omega_0^3\tilde\omega_1(2\tilde\omega_0+\tilde\omega_1)}-\frac{105\lambda_8}{64\tilde\omega_0^3\tilde\omega_1(3\tilde\omega_0+\tilde\omega_1)} +\frac{315\lambda_8}{64\tilde\omega_0\tilde\omega_1^3(\tilde\omega_0+2\tilde\omega_1)}+\frac{315\lambda_8}{64\tilde\omega_0^2\tilde\omega_1^2(\tilde\omega_0+2\tilde\omega_1)}-\frac{105\lambda_8}{64\tilde\omega_0\tilde\omega_1^3(\tilde\omega_0+3\tilde\omega_1)}\Big]$
α_1	$\omega_0-2\Big[\frac{-3\lambda_4}{8\tilde\omega_0^2}-\frac{3\lambda_4}{4\tilde\omega_0\tilde\omega_1}-\frac{3\lambda_4}{2(-2\tilde\omega_0-2\tilde\omega_1)\tilde\omega_1}-\frac{15\lambda_6}{32\tilde\omega_0^3}-\frac{45\lambda_6}{32\tilde\omega_0\tilde\omega_1^2}+\frac{45\lambda_6}{16(-2\tilde\omega_0-4\tilde\omega_1)\tilde\omega_1^2}-\frac{45\lambda_6}{8(-2\tilde\omega_0-2\tilde\omega_1)\tilde\omega_1^2} -\frac{45\lambda_6}{32\tilde\omega_0^2\tilde\omega_1}+\frac{45\lambda_6}{8\tilde\omega_0(-4\tilde\omega_0-2\tilde\omega_1)\tilde\omega_1}-\frac{45\lambda_6}{8\tilde\omega_0(-2\tilde\omega_0-2\tilde\omega_1)\tilde\omega_1}-\frac{105\lambda_8}{128\tilde\omega_0^4}-\frac{105\lambda_8}{32\tilde\omega_0\tilde\omega_1^3}-\frac{315\lambda_8}{64\tilde\omega_0^2\tilde\omega_1^2}-\frac{105\lambda_8}{32\tilde\omega_0^3\tilde\omega_1} +\frac{315\lambda_8}{32\tilde\omega_1^3(\tilde\omega_0+\tilde\omega_1)}+\frac{1575\lambda_8}{64\tilde\omega_0\tilde\omega_1^2(\tilde\omega_0+\tilde\omega_1)}+\frac{315\lambda_8}{32\tilde\omega_0^2\tilde\omega_1(\tilde\omega_0+\tilde\omega_1)}-\frac{315\lambda_8}{16\tilde\omega_0\tilde\omega_1^2(2\tilde\omega_0+\tilde\omega_1)}-\frac{315\lambda_8}{16\tilde\omega_0^2\tilde\omega_1(2\tilde\omega_0+\tilde\omega_1)} +\frac{315\lambda_8}{32\tilde\omega_0^2\tilde\omega_1(3\tilde\omega_0+\tilde\omega_1)}-\frac{315\lambda_8}{32\tilde\omega_1^3(\tilde\omega_0+2\tilde\omega_1)}-\frac{315\lambda_8}{32\tilde\omega_0\tilde\omega_1^2(\tilde\omega_0+2\tilde\omega_1)}+\frac{105\lambda_8}{32\tilde\omega_1^3(\tilde\omega_0+3\tilde\omega_1)}\Big]$
α_2	$\omega_1-2\Big[\frac{-3\lambda_4}{8\omega_1^2}-\frac{3\lambda_4}{4\omega_0\omega_1}-\frac{3\lambda_4}{2\omega_0(-2\omega_0-2\omega_1)}-\frac{15\lambda_6}{32\omega_1^3}-\frac{45\lambda_6}{32\omega_0^2\omega_1}+\frac{45\lambda_6}{16\omega_0^2(-4\omega_0-2\omega_1)}-\frac{45\lambda_6}{8\omega_0^2(-2\omega_0-2\omega_1)} -\frac{45\lambda_6}{32\omega_0\omega_1^2}+\frac{45\lambda_6}{8\omega_0(-2\omega_0-4\omega_1)\omega_1}-\frac{45\lambda_6}{8\omega 0(-2\omega_0-2\omega_1)\omega_1}-\frac{105\lambda_8}{128\omega_1^4}-\frac{105\lambda_8}{8\omega_0^3\omega_1}+\frac{315\lambda_8}{64\omega_0^2\omega_1^2}-\frac{105\lambda_8}{32\omega_0\omega_1^3} +\frac{315\lambda_8}{32\omega_0^3(\omega_0+\omega 1)}+\frac{1575\lambda_8}{64\omega_0^2\omega 1(\omega_0+\omega_1)}+\frac{315\lambda_8}{32\omega_0\omega 1^2(\omega_0+\omega 1)}-\frac{315\lambda_8}{32\omega_0^3(2\omega_0+\omega_1)}-\frac{315\lambda_8}{32\omega_0^2\omega_1(2\omega_0+\omega_1)}+\frac{105\lambda_8}{32\omega_0^3(3\omega_0+\omega_1)} -\frac{315\lambda_8}{16\omega_0\omega_1^2(\omega_0+2\omega_1)}-\frac{315\lambda_8}{16\omega_0^2\omega_1(\omega_0+2\omega_1)}+\frac{315\lambda_8}{32\omega 0\omega_1^2(\omega_0+3\omega_1)}\Big]$
α_3	$-2\Big[\frac{3\lambda_4}{-2\tilde\omega_0-2\tilde\omega_1}-\frac{45\lambda_6}{4\tilde\omega_0(-4\tilde\omega_0-2\tilde\omega_1)}+\frac{45\lambda_6}{4\tilde\omega_0(-2\tilde\omega_0-2\tilde\omega_1)}-\frac{45\lambda_6}{4(-2\tilde\omega_0-4\tilde\omega_1)\tilde\omega_1}+\frac{45\lambda_6}{4(-2\tilde\omega_0-2\tilde\omega_1)\tilde\omega_1} -\frac{315\lambda_8}{16\tilde\omega_0^2(\tilde\omega_0+\tilde\omega_1)}-\frac{315\lambda_8}{16\tilde\omega_1^2(\tilde\omega_0+\tilde\omega_1)}-\frac{945\lambda_8}{16\tilde\omega_0\tilde\omega_1(\tilde\omega_0+\tilde\omega_1)}+\frac{315\lambda_8}{8\tilde\omega_0^2(2\tilde\omega_0+\tilde\omega_1)}+\frac{315\lambda_8}{8\tilde\omega_0\tilde\omega_1(2\tilde\omega_0+\tilde\omega_1)}-\frac{315\lambda_8}{16\tilde\omega_0^2(3\tilde\omega_0+\tilde\omega_1)} +\frac{315\lambda_8}{8\tilde\omega_1^2(\tilde\omega_0+2\tilde\omega_1)}+\frac{315\lambda_8}{8\tilde\omega_0\tilde\omega_1(\tilde\omega_0+2\tilde\omega_1)}-\frac{315\lambda_8}{16\tilde\omega_1^2(\tilde\omega_0+3\tilde\omega_1)}\Big]$
α_4	$-2\Big[\frac{-\lambda_4}{8\tilde\omega_0}-\frac{5\lambda_6}{32\tilde\omega_0^2}-\frac{15\lambda_6}{32\tilde\omega_0\tilde\omega_1}-\frac{15\lambda_6}{8(-4\tilde\omega_0-2\tilde\omega_1)\tilde\omega_1}-\frac{35\lambda_8}{128\tilde\omega_0^3}-\frac{105\lambda_8}{64\tilde\omega_0\tilde\omega_1^2}-\frac{35\lambda_8}{32\tilde\omega_0^2\tilde\omega_1}-\frac{105\lambda_8}{64\tilde\omega_1^2(\tilde\omega_0+\tilde\omega_1)} +\frac{105\lambda_8}{16\tilde\omega_1^2(2\tilde\omega_0+\tilde\omega_1)}+\frac{105\lambda_8}{16\tilde\omega_0\tilde\omega_1(2\tilde\omega_0+\tilde\omega_1)}-\frac{105\lambda_8}{16\tilde\omega_0\tilde\omega_1(3\tilde\omega_0+\tilde\omega_1)}\Big]$
α_5	$-2\Big[-\frac{\lambda_4}{8\tilde\omega_1}-\frac{15\lambda_6}{8\tilde\omega_0(-2\tilde\omega_0-4\tilde\omega_1)}-\frac{5\lambda_6}{32\tilde\omega_1^2}-\frac{15\lambda_6}{32\tilde\omega_0\tilde\omega_1}-\frac{35\lambda_8}{128\tilde\omega_1^3}-\frac{35\lambda_8}{32\tilde\omega_0\tilde\omega_1^2}-\frac{105\lambda_8}{64\tilde\omega_0^2\tilde\omega_1}-\frac{105\lambda_8}{64\tilde\omega_0^2(\tilde\omega_0+\tilde\omega_1)}+ \frac{105\lambda_8}{16\tilde\omega_0^2(\tilde\omega_0+2\tilde\omega_1)}+\frac{105\lambda_8}{16\tilde\omega_0\tilde\omega_1(\tilde\omega_0+2\tilde\omega_1)}-\frac{105\lambda_8}{16\tilde\omega_0\tilde\omega_1(\tilde\omega_0+3\tilde\omega_1)}\Big]$

Table 1. *Cont.*

α_i	Coefficient of α_i
α_6	$-2\left[\frac{15\lambda_6}{4(-4\tilde{\omega}_0-2\tilde{\omega}_1)}+\frac{105\lambda_8}{16\tilde{\omega}_1(\tilde{\omega}_0+\tilde{\omega}_1)}-\frac{105\lambda_8}{8\tilde{\omega}_0(2\tilde{\omega}_0+\tilde{\omega}_1)}-\frac{105\lambda_8}{8\tilde{\omega}_1(2\tilde{\omega}_0+\tilde{\omega}_1)}+\frac{105\lambda_8}{8\tilde{\omega}_0(3\tilde{\omega}_0+\tilde{\omega}_1)}\right]$
α_7	$-2\left[\frac{15\lambda_6}{4(-2\tilde{\omega}_0-4\tilde{\omega}_1)}+\frac{105\lambda_8}{16\tilde{\omega}_0(\tilde{\omega}_0+\tilde{\omega}_1)}-\frac{105\lambda_8}{8\tilde{\omega}_0(\tilde{\omega}_0+2\tilde{\omega}_1)}-\frac{105\lambda_8}{8\tilde{\omega}_1(\tilde{\omega}_0+2\tilde{\omega}_1)}+\frac{105\lambda_8}{8\tilde{\omega}_1(\tilde{\omega}_0+3\tilde{\omega}_1)}\right]$
α_8	$-2\left[\frac{\lambda_6}{24\tilde{\omega}_0}-\frac{7\lambda_8}{96\tilde{\omega}_0^2}-\frac{7\lambda_8}{24\tilde{\omega}_0\tilde{\omega}_1}+\frac{7\lambda_8}{8\tilde{\omega}_1(3\tilde{\omega}_0+\tilde{\omega}_1)}\right]$
α_9	$-2\left[\frac{-\lambda_6}{24\tilde{\omega}_1}-\frac{7\lambda_8}{96\tilde{\omega}_1^2}-\frac{7\lambda_8}{24\tilde{\omega}_0\tilde{\omega}_1}+\frac{7\lambda_8}{8\tilde{\omega}_0(\tilde{\omega}_0+3\tilde{\omega}_1)}\right]$
α_{10}	$\frac{7\lambda_8}{2(\tilde{\omega}_0+3\tilde{\omega}_1)}$
α_{11}	$\frac{7\lambda_8}{2(3\tilde{\omega}_0+\tilde{\omega}_1)}$
α_{12}	$\frac{35\lambda_8}{8(\tilde{\omega}_0+\tilde{\omega}_1)}$
α_{13}	$\frac{\lambda_8}{32\tilde{\omega}_0}$
α_{14}	$\frac{\lambda_8}{32\tilde{\omega}_1}$

4.1. Circuit Complexity

We will describe complexity in terms of a quantum circuit model. To calculate the circuit complexity for the two-oscillator system with even interactions up to ϕ^8, we need to fix our reference state, target state, and a set of elementary gates. We will construct the unitary transformation using these gates. This unitary transformation will take the system from the reference state ($|\psi\rangle_R$) to the target state ($|\psi\rangle_T$) (i.e., $|\psi\rangle_T = U\,|\psi\rangle_R$). The minimum number of gates needed to construct such a unitary transformation is the complexity of the target state. Since our wave functions are nearly Gaussian, we can consider our space of states as the space of positive quadratic forms. This space can be parameterized as a function of a smooth parameter s as follows:

$$\psi^s(\bar{x}_0,\bar{x}_1) = \mathcal{N}^s \exp\left[-\frac{1}{2}\Big(v_a A(s)_{ab}\, v_b\Big)\right] \tag{22}$$

Here, $\mathcal{N}^s$ is the normalization constant, and the parameter s runs from 0 to 1. If $s=1$, then the circuit represents the target state in Equation (21) with $\mathcal{N}^{s=1} = \frac{(\bar{\omega}_0\bar{\omega}_1)^{1/4}}{\sqrt{\pi}}\exp[\alpha_0]$, and at $s=0$, the circuit is in the reference state. The continuous unitary transformation, specified by the s parameter, gives us the target state from the reference state. Writing the states in the form of Equation (22) helps us formulate the matrix version of our problem.

Now, we want to represent the exponent of the wavefunction, which is a polynomial in the matrix form $A(s)$:

$$\psi^{s=0}(x_1,x_2) = \mathcal{N}^{s=0}\exp\Big[-\frac{\omega_{ref}}{2}(x_1^2+x_2^2+\lambda_0^4(x_1^4+x_2^4)+\lambda_0^6(x_1^6+x_2^6)+\lambda_0^8(x_1^8+x_2^8))\Big] \tag{23}$$

Here λ_0^4, λ_0^6, and λ_0^8 are the initial coupling constants for ϕ^4, ϕ^6, and ϕ^8 respectively. By transforming them into the normal coordinates, we obtain

$$\begin{aligned}\psi^{s=0}(\bar{x}_0,\bar{x}_1) =& \mathcal{N}^{s=0}\exp\Big[-\frac{\tilde{\omega}_{ref}}{2}(\bar{x}_0^2+\bar{x}_1^2+\frac{\lambda_4}{2}(\bar{x}_0^4+\bar{x}_1^4+6\bar{x}_0^2\bar{x}_1^2)+\frac{\lambda_6}{4}(\bar{x}_0^6+\bar{x}_1^6+15\bar{x}_0^4\bar{x}_1^2 \\ &+15\bar{x}_1^4\bar{x}_0^2)+\frac{\lambda_8}{8}(\bar{x}_0^8+\bar{x}_1^8+28\bar{x}_0^6\bar{x}_1^2+28\bar{x}_0^2\bar{x}_1^6+28\bar{x}_0{}^4\bar{x}_1{}^4))\Big]\end{aligned} \tag{24}$$

We represent the exponent of the reference state shown above in a block diagonal matrix form as follows:

$$A(s=0) = \begin{pmatrix} A_1^0 & 0 & 0 & 0 \\ 0 & A_2^0 & 0 & 0 \\ 0 & 0 & A_3^0 & 0 \\ 0 & 0 & 0 & A_4^0 \end{pmatrix}_{14\times 14} \tag{25}$$

The basis chosen for this representation is

$$\vec{v} = \Big\{\bar{x}_0,\bar{x}_1,\bar{x}_0\bar{x}_1,\bar{x}_0^2,\bar{x}_1^2,\bar{x}_0^2\bar{x}_1,\bar{x}_0\bar{x}_1^2,\bar{x}_0^3,\bar{x}_1^3,\bar{x}_0\bar{x}_1^3,\bar{x}_0^3\bar{x}_1,\bar{x}_0^2\bar{x}_1,\bar{x}_0^4,\bar{x}_1^4\Big\} \tag{26}$$

We need to ensure that the determinants of the $A(s=0)$ and $A(s=1)$ matrices are positive so that the wavefunction remains square-integrable everywhere. It should be noted that the matrix elements of A (i.e., $A_1^0 - A_4^0$) are matrices themselves as shown below:

$$A_1^0 = \begin{pmatrix} \tilde{\omega}_{ref} & 0 \\ 0 & \tilde{\omega}_{ref} \end{pmatrix} \qquad A_2^0 = \lambda_0^4\tilde{\omega}_{ref}\begin{pmatrix} b & 0 & 0 \\ 0 & \frac{1}{2} & \frac{1}{2}(3-b) \\ 0 & \frac{1}{2}(3-b) & \frac{1}{2} \end{pmatrix}$$

$$A_3^0 = \tilde{\omega}_{ref}\lambda_0^6\begin{pmatrix} \frac{p}{2} & 0 & 0 & \frac{1}{8}(15-2k) \\ 0 & k & \frac{1}{8}(15-2p) & 0 \\ 0 & \frac{1}{8}(15-2p) & \frac{1}{4} & 0 \\ \frac{1}{8}(15-2k) & 0 & 0 & \frac{1}{4} \end{pmatrix}$$

$$A_4^0 = \tilde{\omega}_{ref}\lambda_0^8 \begin{pmatrix} \frac{1}{8} & \frac{1}{4}(\frac{35}{4}-e) & 0 & 0 & 0 \\ \frac{1}{4}(\frac{35}{4}-e) & \frac{1}{8} & 0 & 0 & 0 \\ 0 & 0 & e & \frac{1}{16}(1-c) & \frac{1}{16}(1-d) \\ 0 & 0 & \frac{1}{16}(1-c) & \frac{7}{2} & \frac{1}{4}(\frac{35}{4}-e) \\ 0 & 0 & \frac{1}{16}(1-d) & \frac{1}{4}(\frac{35}{4}-e) & \frac{7}{2} \end{pmatrix}$$

We have introduced a few parameters (b, p, k, c, d, and e) to ensure that the determinant of each block diagonal matrix is positive definite. Because we are considering higher even interactions, it is necessary to consider various quadratic and other higher-order terms. To find the positive determinant of the A_2^0 block, the value of b must be in the range $2 < b < 4$. To eliminate the off-diagonal components, we set $b = 3$, as it would give the minimum line element. In the A_3^0 block, we fix $k = \frac{15}{2}$, and the determinant becomes

$$\mathrm{Det}(A_0^3) = -\frac{1}{512} p\Big(221 + 4(-15+p)p\ \omega_{ref}^4 \lambda_6^4\Big)$$

We set p as $15/2$ in the range $\frac{13}{2} < p < \frac{17}{2}$ to satisfy the condition $\mathrm{Det}(A_3^0) > 0$. Similarly, to ensure that the determinant of the A_0^4 block is positive and the line element is at its minimum, we set $c = d = 1$ and $e = 35/4$.

Using the same basis as that mentioned in Equation (26), the target state matrix $A(s=1)$ can be written as another 14×14 matrix:

$$A(s=1) = \begin{pmatrix} A_1^1 & 0 & 0 & 0 \\ 0 & A_2^1 & 0 & 0 \\ 0 & 0 & A_3^1 & 0 \\ 0 & 0 & 0 & A_4^1 \end{pmatrix}_{14\times 14} \tag{27}$$

where we have the following block diagonal entries:

$$A_1^1 = \begin{pmatrix} \alpha_1 & 0 \\ 0 & \alpha_2 \end{pmatrix} \qquad A_2^1 = \begin{pmatrix} \tilde{b}\alpha_5 & 0 & 0 \\ 0 & \alpha_3 & \frac{1}{2}(1-\tilde{b})\alpha_5 \\ 0 & \frac{1}{2}(1-\tilde{b})\alpha_5 & \alpha_4 \end{pmatrix}$$

$$A_3^1 = \begin{pmatrix} \tilde{p}\alpha_6 & 0 & 0 & \frac{1}{2}(1-\tilde{k})\alpha_7 \\ 0 & \tilde{k}\alpha_7 & \frac{1}{2}(1-\tilde{p})\alpha_6 & \\ 0 & \frac{1}{2}(1-\tilde{p})\alpha_6 & \alpha_8 & 0 \\ \frac{1}{2}(1-\tilde{k})\alpha_7 & 0 & 0 & \alpha_9 \end{pmatrix}$$

$$A_4^1 = \begin{pmatrix} \tilde{d}\alpha_{10} & \frac{1}{4}(1-\tilde{e})\alpha_{12} & 0 & 0 & 0 \\ \frac{1}{4}(1-\tilde{e})\alpha_{12} & \tilde{c}\alpha_{11} & 0 & 0 & 0 \\ 0 & 0 & \tilde{e}\alpha_{12} & \frac{1}{2}(1-\tilde{c})\alpha_{11} & \frac{1}{2}(1-\tilde{d})\alpha_{10} \\ 0 & 0 & \frac{1}{2}(1-\tilde{c})\alpha_{11} & \alpha_{13} & \frac{1}{4}(1-\tilde{e})\alpha_{12} \\ 0 & 0 & \frac{1}{2}(1-\tilde{d})\alpha_{10} & \frac{1}{4}(1-\tilde{e})\alpha_{12} & \alpha_{14} \end{pmatrix}$$

Here as well, we fix $\tilde{k}$, $\tilde{c}$, and $\tilde{d}$ to be one to make the off-diagonal terms zero and keep $\tilde{b}$, $\tilde{p}$, and $\tilde{e}$ for the positivity of all the block matrices.

As we are considering a closed quantum system, the reference state evolves into the target state via a certain unitary operator. Now, we represent this as

$$\psi^{s=1}(\bar{x}_0, \bar{x}_1) = \mathbb{U}(s=1)\psi^{s=0}(\bar{x}_0, \bar{x}_1) \tag{28}$$

We represent the unitary matrix in the following form:

$$\mathbb{U} = \overleftarrow{\mathcal{P}} \exp\left[\int_0^s ds Y^I(s)\mathcal{O}_I\right] \tag{29}$$

We have to enact the operators $\mathcal{O}_I$ in a particular order. The Y_I's depend on the specific order in which the $\mathcal{O}_I$s are acting on the reference state. To find the minimum complexity, we try to have a geometric understanding of this unitary evolution process. Then, we can write the expression in Equation (29) as follows:

$$\mathbb{U} = \overleftarrow{\mathcal{P}} \exp\left[\int_0^s Y^I(s)M_I ds\right] \tag{30}$$

where $(M_I)_{jk}'s$ represents the $\mathrm{GL}(14,\mathbb{R})$ generators satisfying

$$\mathrm{Tr}\left[M_I M_J^T\right] = \delta_{IJ} \tag{31}$$

Here, I, J runs from 1 to 196. As mentioned above, $A(s=0)$ is the reference state which undergoes a unitary transformation to find the target state $A(s=1)$. It enables us to calculate the boundary conditions that lead us to calculate the complexity functional. Thus, we have

$$A(s=1) = \mathbb{U}(s=1)A(s=0)\mathbb{U}^T(s=1) \tag{32}$$

This leads to the expression

$$Y^I M_I = \partial_s \mathbb{U}(s)\mathbb{U}(s)^{-1} \tag{33}$$

Hence, we obtain

$$Y^I = \frac{1}{\mathrm{Tr}\left[M^I (M^I)^T\right]} \mathrm{Tr}\left[\partial_s \mathbb{U}(s)\mathbb{U}^{-1}\left(M^I\right)^T\right] \tag{34}$$

Now, the line element can be defined in terms of Y^I's as follows:

$$
\begin{aligned}
ds^2 &= G_{IJ} dY^I dY^J \\
&= G_{IJ} \left[\frac{1}{\mathrm{Tr}\left[M^I \left(M^I\right)^T\right]} \mathrm{Tr}\left[d_s \mathbb{U}(s) \mathbb{U}^{-1} \left(M^I\right)^T \right] \right] \left[\frac{1}{\mathrm{Tr}\left[M^J \left(M^J\right)^T\right]} \mathrm{Tr}\left[d_s \mathbb{U}(s) \mathbb{U}^{-1} \left(M^J\right)^T \right] \right]
\end{aligned}
\tag{35}
$$

Here, we should mention that dY^I does not denote the total differential for Y^I. When observing the structure of the matrix A, we find that $\mathbb{U}(s)$ can be considered an element of $\mathrm{GL}(14, \mathbb{R})$ with a positive determinant. Now, we will express the $\mathbb{U}$ matrix with a similar structure to that in the target state matrix, and the unitary matrix contains four block diagonal matrices:

$$
\mathbb{U} = \begin{pmatrix} \mathbb{U}_1 & 0 & 0 & 0 \\ 0 & \mathbb{U}_2 & 0 & 0 \\ 0 & 0 & \mathbb{U}_3 & 0 \\ 0 & 0 & 0 & \mathbb{U}_4 \end{pmatrix}_{14\times 14} \tag{36}
$$

where

$$
\mathbb{U}_1 = \begin{pmatrix} x_0 - x_1 & x_3 - x_2 \\ x_3 + x_2 & x_0 + x_1 \end{pmatrix} \qquad \mathbb{U}_2 = \begin{pmatrix} \tilde{x}_4 & 0 & 0 \\ 0 & \tilde{x}_5 - \tilde{x}_6 & \tilde{x}_8 - \tilde{x}_7 \\ 0 & \tilde{x}_8 + \tilde{x}_7 & \tilde{x}_5 + \tilde{x}_6 \end{pmatrix}
$$

$$
\mathbb{U}_3 = \begin{pmatrix} \tilde{x}_9 & 0 & 0 & 0 \\ 0 & \tilde{x}_{10} - \tilde{x}_{11} & \tilde{x}_{13} - \tilde{x}_{12} & 0 \\ 0 & \tilde{x}_{13} + \tilde{x}_{12} & \tilde{x}_{10} + \tilde{x}_{11} & 0 \\ 0 & 0 & 0 & \tilde{x}_{14} \end{pmatrix} \quad \mathbb{U}_4 = \begin{pmatrix} \tilde{x}_{15} - \tilde{x}_{16} & \tilde{x}_{18} - \tilde{x}_{17} & 0 & 0 & 0 \\ x_{18} + x_{17} & x_{15} + x_{16} & 0 & 0 & 0 \\ 0 & 0 & \tilde{x}_{19} & 0 & 0 \\ 0 & 0 & 0 & \tilde{x}_{20} - \tilde{x}_{21} & \tilde{x}_{23} - \tilde{x}_{22} \\ 0 & 0 & 0 & \tilde{x}_{23} + \tilde{x}_{22} & \tilde{x}_{20} + \tilde{x}_{21} \end{pmatrix}
$$

We have decomposed $\mathbb{U}(s)$ in terms of four block diagonal matrices. First, we note that the quadratic part of the first block is always diagonal, which induces a flat space, and thus we have $x_3 = x_2 = 0$. In the unitary operator $\mathbb{U}$, we do not allow the off-diagonal terms as in the final state, and only the block diagonal form remains. Thus, if we allow off-diagonal terms, we will have an increased line element, which we do not want. Now, $\mathrm{GL}(2, \mathbb{R})$ can be expressed as $\mathbb{R} \times \mathrm{SL}(2, \mathbb{R})$, and so we observe that our $\mathbb{U}$ has an $\mathbb{R}^{10} \times \mathrm{SL}(2, \mathbb{R})^4$ group structure. We will parameterize each 2×2 block matrix in $\mathbb{U}$ as performed in [18] (i.e., we will parameterize it as an AdS$_3$ space):

$$
\begin{aligned}
&x_0 = \exp[y_1]\cosh(\rho_1) && x_1 = \exp[y_1]\sinh(\rho_1)\\
&\tilde{x}_4 = \exp[y_2] && x_5 = \exp[y_3]\cos(\tau_3)\cosh(\rho_3)\\
&\tilde{x}_6 = \exp[y_3]\sin(\theta_3)\cosh(\rho_3) && \tilde{x}_7 = \exp[y_3]\sin(\tau_3)\cosh(\rho_3)\\
&\tilde{x}_8 = \exp[y_3]\cos(\theta_3)\sinh(\rho_3) && \tilde{x}_9 = \exp[y_4]\\
&\tilde{x}_{10} = \exp[y_5]\cos(\tau_5)\cosh(\rho_5) && \tilde{x}_{11} = \exp[y_5]\sin(\theta_5)\sinh(\rho_5)\\
&\tilde{x}_{12} = \exp[y_5]\sin(\tau_5)\cosh(\rho_5) && \tilde{x}_{13} = \exp[y_5]\cos(\theta_5)\sinh(\rho_5)\\
&\tilde{x}_{14} = \exp[y_6] && \tilde{x}_{15} = \exp[y_7]\cos(\tau_7)\cosh(\rho_7)\\
&\tilde{x}_{16} = \exp[y_7]\sin(\theta_7)\sinh(\rho_7) && \tilde{x}_{17} = \exp[y_7]\sin(\tau_7)\cosh(\rho_7)\\
&\tilde{x}_{18} = \exp[y_7]\cos(\theta_7)\sinh(\rho_7) && \tilde{x}_{19} = \exp[y_8]\\
&\tilde{x}_{20} = \exp[y_9]\cos(\tau_9)\cosh(\rho_9) && \tilde{x}_{21} = \exp[y_7]\sin(\theta_9)\sinh(\rho_9)\\
&\tilde{x}_{22} = \exp[y_9]\sin(\tau_9)\cosh(\rho_9) && \tilde{x}_{23} = \exp[y_9]\cos(\theta_9)\sinh(\rho_9)
\end{aligned}
\tag{37}
$$

Using these parameters for $\mathbb{U}$, we can then calculate the infinitesimal line element in Equation (35), which now becomes

$$
\begin{aligned}
ds^2 = \Bigg[&2y_1^2 + y_2^2 + 2y_3^2 + y_4^2 + 2y_5^2 + y_6^2 + 2y_7^2 + y_8^2 + 2y_9^2 + 2\Bigg(\rho_1^2 + \rho_3^2\\
&+ \rho_5^2 + \rho_7^2 + \rho_9^2 + \cosh(2\rho_3)\Big\{\cosh^2(\rho_3)\tau_3^2 + \sinh^2(\rho_3)\theta_3^2\Big\} - \sinh^2(2\rho_3)\theta_3\tau_3\\
&+ \cosh(2\rho_5)\Big\{\cosh^2(\rho_5)\tau_5^2 + \sinh^2(\rho_5)\theta_5^2\Big\} - \sinh^2(2\rho_5)\theta_5\tau_5\\
&+ \cosh(2\rho_7)\Big\{\cosh^2(\rho_7)\tau_7^2 + \sinh^2(\rho_7)\theta_7^2\Big\} - \sinh^2(2\rho_7)\theta_7\tau_7\\
&+ \cosh(2\rho_9)\Big\{\cosh^2(\rho_9)\tau_9^2 + \sinh^2(\rho_9)\theta_9^2\Big\} - \sinh^2(2\rho_9)\theta_9\tau_9\Bigg)\Bigg]
\end{aligned}
\tag{38}
$$

We need to find the shortest path between the reference and the target state in this geometry, described by metric expressed in Equation (38). This shortest path will be the circuit complexity for our problem. For this purpose, we also need to calculate the proper boundary conditions denoting the reference and target states.

4.2. Boundary Conditions for the Geodesic

As we mentioned before, the minimal geodesic will be equivalent to finding the geodesic in the $GL(14, R)$ group manifold. The geodesic can be found by minimizing the following equation on the distance functional:

$$\mathcal{D}(U) = \int_0^1 \sqrt{g_{ij}\dot{x}^i\dot{x}^j}ds \tag{39}$$

The boundary conditions from Equation (32) are

$$y_i(0) = \rho_j(0) = 0 \tag{40}$$

where $i = 1, 2, \ldots, 9$ and $j = 1, 3, 5, 7, 9$.

For solving the geodesic equations, we have to find conserved charges using the results of [14], as our metric is $\mathbb{R}^{10} \times \mathrm{SL}(2,\mathbb{R})^4$. Using Equations (40) and (42), we obtain

$$y_i(s) = y_i(1)s \qquad \rho_j(s) = \rho_j(1)s \tag{41}$$

where, $i = 1, 2, \ldots, 9$ and $j = 1, 3, 5, 7, 9$:

$$
\begin{aligned}
&2\big(y_1(1)-\rho_1(1)\big)=\ln\left[\frac{\alpha_1}{\tilde{\omega}_{ref}}\right] && 2\big(y_1(1)+\rho_1(1)\big)=\ln\left[\frac{\alpha_2}{\tilde{\omega}_{ref}}\right]\\
&2y_2(1)=\ln\left[\frac{\tilde{b}\alpha_5}{3\tilde{\omega}_{ref}\lambda_4}\right] && 2y_3(1)=\ln\left[\frac{\sqrt{4\alpha_3\alpha_4-(1-\tilde{b})^2\alpha_5^2}}{\tilde{\omega}_{ref}\lambda_4}\right]\\
&2\rho_3(1)=\cosh^{-1}\left[\frac{\alpha_3+\alpha_4}{\sqrt{4\alpha_3\alpha_4-(1-\tilde{b})^2\alpha_5^2}}\right] && 2y_4(1)=\ln\left[\frac{4\tilde{p}\alpha_6}{15\omega_{ref}\lambda_6}\right]\\
&2y_5(1)=\ln\left[\frac{\sqrt{16\alpha_7\alpha_8-4(1-\tilde{p})^2\alpha_6^2}}{\tilde{\omega}_{ref}\lambda_6}\right] && 2y_6(1)=\ln\left[\frac{4\alpha_9}{\tilde{\omega}_{ref}\lambda_6}\right]\\
&2\rho_5(1)=\cosh^{-1}\left[\frac{2(\alpha_7+\alpha_8)}{\sqrt{16\alpha_7\alpha_8-4(1-\tilde{p})^2\alpha_6}}\right] && 2y_7(1)=\ln\left[\frac{\sqrt{64\alpha_{10}\alpha_{11}-4(1-\tilde{e})^2\alpha_{12}^2}}{\tilde{\omega}_{ref}\lambda_8}\right]\\
&2\rho_7(1)=\cosh^{-1}\left[\frac{\alpha_{10}+\alpha_{11}}{\sqrt{64\alpha_{10}\alpha_{11}-4(1-\tilde{e})^2\alpha_{12}^2}}\right] && 2y_8(1)=\ln\left[\frac{4\tilde{e}\alpha_{12}}{35\tilde{\omega}_{ref}\lambda_6}\right]\\
&2\rho_9(1)=\cosh^{-1}\left[\frac{\alpha_{13}+\alpha_{14}}{\sqrt{4\alpha_{13}\alpha_{14}-((1-\tilde{e})^2/4)\alpha_{12}^2}}\right] && 2y_9(1)=\ln\left[\frac{\sqrt{4\alpha_{13}\alpha_{14}-((1-\tilde{e})^2/4)\alpha_{12}^2}}{7\tilde{\omega}_{ref}\lambda_8}\right]
\end{aligned} \tag{42}
$$

With the same arguments in [14], we set

$$\tau_j(s)=0 \qquad \theta_j(s)=\theta_{c_j} \tag{43}$$

where $j=3,5,7,9$ and θ_{c_j} are constants which do not depend on s. Therefore, we have the freedom to choose any constant value of θ_{c_j} here which indicates that it will leave the origin in any direction. (Note: When we are calculating ρ_5, any arbitrary constant value will not provide us an analytical expression, so we choose θ_5 to be zero to find the simple analytical expression in Equation (42)) By taking into account all of these terms and conditions, we find the complexity functional as follows:

$$
\begin{aligned}
\mathcal{D}(U) =& \sqrt{2\left[\sum_{i=1,odd}^{9}[y_i(1)]^2 + \frac{1}{2}\sum_{i=2,even}^{8}[y_i(1)]^2 + \sum_{j=1,odd}^{9}[\rho_i(1)]^2\right]} \\
=& \frac{1}{\sqrt{2}}\left(2\left[\cosh^{-1}\left(\frac{\alpha_3+\alpha_4}{\sqrt{4\alpha_3\alpha_4-\alpha_5^2(-1+\tilde{b})^2}}\right)\right]^2 + 2\left[\cosh^{-1}\left(\frac{\alpha_{10}+\alpha_{11}}{2\sqrt{16\alpha_{10}\alpha_{11}+(1-\tilde{e})^2\alpha_{12}^2}}\right)\right]^2\right. \\
&+ 2\left[\cosh^{-1}\left(\frac{\alpha_{13}+\alpha_{14}}{\sqrt{4\alpha_{13}\alpha_{14}-((1-\tilde{e})^2/4)\alpha_{12}}}\right)\right]^2 + 2\left[\cosh^{-1}\left(\frac{2(\alpha_7+\alpha_8)}{\sqrt{-\alpha_6^2+4\alpha_7\alpha_8+\alpha_6^2\tilde{p}}}\right)\right]^2 \\
&+ \frac{1}{2}\left[\ln\frac{\alpha_2}{\alpha_1}\right]^2 + \frac{1}{2}\left[\ln\left(\frac{\alpha_1\alpha_2}{\tilde{\omega}_{ref}^2}\right)\right]^2 + \left[\ln\left(\frac{4\alpha_9}{\lambda_6\tilde{\omega}_{ref}}\right)\right]^2 + 2\left[\ln\left(\frac{\sqrt{4\alpha_3\alpha_4-(1-\tilde{b})^2\alpha_5^2}}{\tilde{\omega}_{ref}\lambda_4}\right)\right]^2 \\
&+ 2\left[\ln\left(\frac{\tilde{b}\alpha_5}{3\lambda_4\tilde{\omega}_{ref}}\right)\right]^2 + 2\left[\ln\left(\frac{\sqrt{64\alpha_{10}\alpha_{11}-4(-1+\tilde{e})^2\alpha_{12}^2}}{\tilde{\omega}_{ref}\lambda_8}\right)\right]^2 + \left[\ln\left(\frac{4\alpha_{12}\tilde{e}}{35\lambda_8\tilde{\omega}_{ref}}\right)\right]^2 \\
&+ 2\left[\ln\left(\frac{\sqrt{4\alpha_{13}\alpha_{14}-((-1+\tilde{e})^2/16)\alpha_{12}^2}}{7\tilde{\omega}_{ref}\lambda_8}\right)\right]^2 + 2\left[\ln\left(\frac{2\sqrt{-\alpha_6^2+4\alpha_7\alpha_8+\alpha_6\tilde{p}}}{\tilde{\omega}_{ref}\lambda_6}\right)\right]^2 \\
&\left.+ \left[\ln\left(\frac{4\alpha_6\tilde{p}}{15\lambda_6\tilde{\omega}_{ref}}\right)\right]^2\right)^{\frac{1}{2}}
\end{aligned}
\tag{44}
$$

which is a straight line, as there is no off-diagonal term for when we set $\tau_i(s)$ to be 0 and $\theta_j(s)$ to be independent of s, according to Equation (41).

For the particular choice of a cost function that we used (i.e., $\mathcal{F}_2$), the complexity functional is

$$\mathcal{C}_2 = \int_{s=0}^{1} ds\mathcal{F}_2 \tag{45}$$

As was shown in Equation (44), the complexity functional can be written in terms of some boundary values only. It can also be proven that this functional can just involve the eigenvalues of the reference and target matrix:

$$\mathcal{C}_2 = \frac{1}{2}\sqrt{\sum_{i=1}^{14}\log\left[\frac{(\lambda_T)_i}{(\lambda_R)_i}\right]^2} \tag{46}$$

The proof of this expression is explicitly constructed in Appendix B. This result is very crucial, and we exploit this relation to generalize the complexity to N oscillators.

5. Analysis for N Oscillators

To this point, our discussion in this paper has been concerned with two coupled harmonic oscillators involving higher-order interactions. To extend our analysis to effective field theories, we first need to generalize our results to N coupled harmonic oscillators with $(\phi^4+\phi^6+\phi^8)$ interaction terms. Then, we will gradually move toward the continuum limit for this problem. With that in mind, we consider the following Hamiltonian:

$$H = \frac{1}{2}\sum_{a=0}^{N-1}\left[p_a^2+\omega^2x_a^2+\Omega^2(x_a-x_{a+1})^2+2\lambda_4x_a^4+2\lambda_6x_a^6+2\lambda_8x_a^8\right] \tag{47}$$

Now, we will assume that the periodic boundary condition is valid on this lattice of N oscillators such that $x_{a+N} = x_a$ (as it allows us to impose translational symmetry and use a Fourier transform for expression in terms of the normal mode coordinates). Then, we perform discrete a Fourier transform for this lattice using

$$x_a = \frac{1}{\sqrt{N}} \sum_{k=0}^{N-1} \exp\left[i\frac{2\pi a}{N}k\right] \tilde{x}_k \tag{48}$$

$$p_a = \frac{1}{\sqrt{N}} \sum_{k=0}^{N-1} \exp\left[i\frac{2\pi a}{N}k\right] \tilde{p}_k \tag{49}$$

Using the above Equations (48) and (49), we can transform the spatial coordinates into normal mode coordinates. The resultant Hamiltonian is then

$$\begin{aligned} H &= \frac{1}{2} \sum_{a=0}^{N-1} \left[p_a^2 + \omega^2 x_a^2 + \Omega^2 (x_a - x_{a+1})^2 + 2\lambda_4 x_a^4 + 2\lambda_6 x_a^6 + 2\lambda_8 x_a^8\right] \\ &= \frac{1}{2} \sum_{k=0}^{N-1} \left[|\tilde{p}_k|^2 + \left(\omega^2 + 4\Omega^2 \sin^2\left(\frac{\pi k}{N}\right)\right)|\tilde{x}_k|^2\right] + H'_{\phi^4} + H'_{\phi^6} + H'_{\phi^8} \end{aligned} \tag{50}$$

where H'_{ϕ^4} ,H'_{ϕ^6}, and H'_{ϕ^8} are the contributions from the ϕ^4, ϕ^6, and ϕ^8 interaction terms, respectively. Now, we have

$$H'_{\phi^4} = \frac{\lambda_4}{N} \sum_{k_1,k_2,k_3=0}^{N-1} \tilde{x}_\alpha \tilde{x}_{k_1} \tilde{x}_{k_2} \tilde{x}_{k_3} \ ; \ \alpha = N - k_1 - k_2 - k_3 \bmod N \tag{51}$$

$$H'_{\phi^6} = \frac{\lambda_6}{N^2} \sum_{k_1,k_2,k_3,k_4,k_5=0}^{N-1} \tilde{x}_\alpha \tilde{x}_{k_1} \tilde{x}_{k_2} \tilde{x}_{k_3} \tilde{x}_{k_4} \tilde{x}_{k_5} \ ; \ \alpha = \left(N - \sum_{i=1}^{5} k_i\right) \bmod N \tag{52}$$

$$H'_{\phi^8} = \frac{\lambda_8}{N^3} \sum_{k_1,k_2,k_3,k_4,k_5,k_6,k_7=0}^{N-1} \tilde{x}_\alpha \tilde{x}_{k_1} \tilde{x}_{k_2} \tilde{x}_{k_3} \tilde{x}_{k_4} \tilde{x}_{k_5} \tilde{x}_{k_6} \tilde{x}_{k_7} \ ; \ \alpha = \left(N - \sum_{i=1}^{7} k_i\right) \bmod N \tag{53}$$

The proof of transformation of the interaction Hamiltonian in a Fourier space is given in Appendix A.

The target state wavefunction is given by

$$\psi_{0,0,\cdots 0}(\bar{x}_0, \cdots \tilde{x}_{N-1}) = \left(\frac{\tilde{\omega}_0 \tilde{\omega}_1 \ldots \tilde{\omega}_{N-1}}{\pi^N}\right)^{\frac{1}{4}} \exp\left[-\frac{1}{2} \sum_{k=0}^{N-1} \tilde{\omega}_k \tilde{x}_k^2 + \lambda_4 \psi_4^1 + \lambda_6 \psi_6^1 + \lambda_8 \psi_8^1\right] \tag{54}$$

where the total perturbation wavefunction ψ^1 is

$$\psi^1 = \lambda_4 \psi_4^1 + \lambda_6 \psi_6^1 + \lambda_8 \psi_8^1 \tag{55}$$

where $\lambda_4 \psi_4^1$, $\lambda_6 \psi_6^1$, and $\lambda_8 \psi_8^1$ are first-order perturbation corrections for the self-interaction terms ϕ^4, ϕ^6, and ϕ^8, respectively.

The expression of ψ_4^1 along with the B terms was taken from [18].

The expression for ψ_4^1 is

$$\psi_4^1 = \sum_{\substack{a=0 \\ 4a \bmod N \equiv 0}}^{N-1} B_1(a) + \sum_{\substack{a,b=0 \\ (2a+2b) \bmod N \equiv 0 \\ a \neq b}}^{N-1} \frac{B_2(a,b)}{2} + \sum_{\substack{a,b=0 \\ (3b+a) \bmod N \equiv 0 \\ a \neq b}}^{N-1} B_3(a,b)$$
$$+ \sum_{\substack{a,b,c=0 \\ (a+2b+c) \bmod N \equiv 0 \\ a \neq b \neq c}}^{N-1} \frac{B_4(a,b,c)}{2} + \sum_{\substack{a,b,c,d=0 \\ (a+b+k+d) \bmod N \equiv 0 \\ a \neq b \neq c \neq d}}^{N-1} \frac{B_5(a,b,c,d)}{24} \tag{56}$$

The expression for ψ_6^1 is

$$\psi_6^1 = \frac{1}{N^2}\Bigg[\sum_{\substack{a=0 \\ 6a \bmod N \equiv 0}}^{N-1} C_1(a) + \sum_{\substack{a,b=0 \\ (a+5b) \bmod N \equiv 0 \\ a \neq b}}^{N-1} C_2(a,b)$$
$$+ \sum_{\substack{a,b=0 \\ (3b+3a) \bmod N \equiv 0 \\ a \neq b}}^{N-1} \frac{1}{2} C_3(a,b) + \sum_{\substack{a,b=0 \\ (2a+4b) \bmod N \equiv 0 \\ a \neq b}}^{N-1} C_4(a,b)$$
$$+ \sum_{\substack{a,b,c=0 \\ (a+b+4c) \bmod N \equiv 0 \\ a \neq b \neq c}}^{N-1} \frac{1}{2} C_5(a,b,c) + \sum_{\substack{a,b,c=0 \\ (2a+b+3c) \bmod N \equiv 0 \\ a \neq b \neq c}}^{N-1} C_6(a,b,c)$$
$$+ \sum_{\substack{a,b,c=0 \\ (2a+2b+2c) \bmod N \equiv 0 \\ a \neq b \neq c}}^{N-1} \frac{1}{6} C_7(a,b,c) + \sum_{\substack{a,b,c,d=0 \\ (a+b+c+3d) \bmod N \equiv 0 \\ a \neq b \neq c \neq d}}^{N-1} \frac{1}{6} C_8(a,b,c,d)$$
$$+ \sum_{\substack{a,b,c,d=0 \\ (a+b+2c+2d) \bmod N \equiv 0 \\ a \neq b \neq c \neq d}}^{N-1} \frac{1}{4} C_9(a,b,c,d) + \sum_{\substack{a,b,c,d,e=0 \\ (a+b+c+d+2e) \bmod N \equiv 0 \\ a \neq b \neq c \neq d \neq e}}^{N-1} \frac{1}{4!} C_{10}(a,b,c,d,e)$$
$$+ \sum_{\substack{a,b,c,d,e,f=0 \\ (a+b+c+d+e+f) \bmod N \equiv 0 \\ a \neq b \neq c \neq d \neq e \neq f}}^{N-1} \frac{1}{6!} C_{11}(a,b,c,d,e,f) \Bigg] \tag{57}$$

where the terms $C_1, C_2, \dots, C_{11}$ are given according to the Table 2.

Table 2. Expression for the terms C_1, $C_2 \ldots C_{11}$.

	Expression for C_i Coefficients
C_1	$\left[\frac{55}{32\tilde{\omega}_a^4}-\frac{15\tilde{x}_a^2}{8\tilde{\omega}_a^3}-\frac{5\tilde{x}_a^4}{8\tilde{\omega}_a^2}-\frac{\tilde{x}_a^6}{6\tilde{\omega}_a}\right]$
C_2	$\left[\frac{-180\tilde{x}_a\tilde{x}_b}{(\tilde{\omega}_a+\tilde{\omega}_b)(\tilde{\omega}_a+3\tilde{\omega}_b)(\tilde{\omega}_a+5\tilde{\omega}_b)}-\frac{60\tilde{x}_a\tilde{x}_b^3}{(\tilde{\omega}_a+3\tilde{\omega}_b)(\tilde{\omega}_a+5\tilde{\omega}_b)}-\frac{6\tilde{x}_a\tilde{x}_b^5}{\tilde{\omega}_a+5\tilde{\omega}_b}\right]$
C_3	$\left[\frac{-120\tilde{x}_a\tilde{x}_b}{(\tilde{\omega}_a+\tilde{\omega}_b)(3\tilde{\omega}_a+\tilde{\omega}_b)(\tilde{\omega}_a+3\tilde{\omega}_b)}-\frac{10\tilde{x}_a^3\tilde{x}_b}{(\tilde{\omega}_a+\tilde{\omega}_b)(3\tilde{\omega}_a+\tilde{\omega}_b)}-\frac{10\tilde{x}_a\tilde{x}_b^3}{(\tilde{\omega}_a+\tilde{\omega}_b)(\tilde{\omega}_a+3\tilde{\omega}_b)}-\frac{10\tilde{x}_a^3\tilde{x}_b^3}{3(\tilde{\omega}_a+\tilde{\omega}_b)}\right]$
C_4	$\Big[\frac{135}{32\tilde{\omega}_a\tilde{\omega}_b^3}+\frac{45}{8\tilde{\omega}_a^2(\tilde{\omega}_a+\tilde{\omega}_b)(\tilde{\omega}_a+2\tilde{\omega}_b)}-\frac{45\tilde{x}_a^2}{4\tilde{\omega}_a(\tilde{\omega}_a+\tilde{\omega}_b)(\tilde{\omega}_a+2\tilde{\omega}_b)}-\frac{45(\tilde{\omega}_a+3\tilde{\omega}_b)\tilde{x}_b^2}{8\tilde{\omega}_b^2(\tilde{\omega}_a+\tilde{\omega}_b)(\tilde{\omega}_a+2\tilde{\omega}_b)}-\frac{45\tilde{x}_a^2\tilde{x}_b^2}{2(\tilde{\omega}_a+\tilde{\omega}_b)(\tilde{\omega}_a+2\tilde{\omega}_b)}$ $-\frac{15\tilde{x}_b^4}{8\tilde{\omega}_a\tilde{\omega}_b+16\tilde{\omega}_b^2}-\frac{15\tilde{x}_a^2\tilde{x}_b^4}{2\tilde{\omega}_a+4\tilde{\omega}_b}\Big]$
C_5	$\left[-\frac{180\tilde{x}_a\tilde{x}_b}{(\tilde{\omega}_a+\tilde{\omega}_b)(\tilde{\omega}_a+\tilde{\omega}_b+2\tilde{\omega}_c)(\tilde{\omega}_a+\tilde{\omega}_b+4\tilde{\omega}_c)}-\frac{180\tilde{x}_a\tilde{x}_b\tilde{x}_c^2}{(\tilde{\omega}_a+\tilde{\omega}_b+2\tilde{\omega}_c)(\tilde{\omega}_a+\tilde{\omega}_b+4\tilde{\omega}_c)}-\frac{30\tilde{x}_a\tilde{x}_b\tilde{x}_c^4}{\tilde{\omega}_a+\tilde{\omega}_b+4\tilde{\omega}_c}\right]$
C_6	$\Big[\frac{-360(\tilde{\omega}_a+\tilde{\omega}_b+2\tilde{\omega}_c)\tilde{x}_b\tilde{x}_c}{(\tilde{\omega}_b+\tilde{\omega}_c)(2\tilde{\omega}_a+\tilde{\omega}_b+\tilde{\omega}_c)(\tilde{\omega}_b+3\tilde{\omega}_c)(2\tilde{\omega}_a+\tilde{\omega}_b+3\tilde{\omega}_c)}-\frac{180\tilde{x}_a^2\tilde{x}_b\tilde{x}_c}{(2\tilde{\omega}_a+\tilde{\omega}_b+\tilde{\omega}_c)(2\tilde{\omega}_a+\tilde{\omega}_b+3\tilde{\omega}_c)}-\frac{60\tilde{x}_b\tilde{x}_c^3}{(\tilde{\omega}_b+3\tilde{\omega}_c)(2\tilde{\omega}_a+\tilde{\omega}_b+3\tilde{\omega}_c)}$ $-\frac{60\tilde{x}_a^2\tilde{x}_b\tilde{x}_c^3}{2\tilde{\omega}_a+\tilde{\omega}_b+3\tilde{\omega}_c}\Big]$
C_7	$\Big[\frac{45}{8\tilde{\omega}_a\tilde{\omega}_b\tilde{\omega}_c^2}+\frac{45}{8\tilde{\omega}_a\tilde{\omega}_b^2\tilde{\omega}_c}+\frac{45}{8\tilde{\omega}_a^2\tilde{\omega}_b\tilde{\omega}_c}-\frac{45}{8\tilde{\omega}_a\tilde{\omega}_b(\tilde{\omega}_a+\tilde{\omega}_b)\tilde{\omega}_c}-\frac{45}{8\tilde{\omega}_a\tilde{\omega}_b\tilde{\omega}_c(\tilde{\omega}_a+\tilde{\omega}_c)}-\frac{45}{8\tilde{\omega}_a\tilde{\omega}_b\tilde{\omega}_c(\tilde{\omega}_b+\tilde{\omega}_c)}$ $+\frac{45}{8\tilde{\omega}_a\tilde{\omega}_b\tilde{\omega}_c(\tilde{\omega}_a+\tilde{\omega}_b+\tilde{\omega}_c)}-\frac{45(2\tilde{\omega}_a+\tilde{\omega}_b+\tilde{\omega}_c)\tilde{x}_a^2}{4\tilde{\omega}_a(\tilde{\omega}_a+\tilde{\omega}_b)(\tilde{\omega}_a+\tilde{\omega}_c)(\tilde{\omega}_a+\tilde{\omega}_b+\tilde{\omega}_c)}-\frac{45\tilde{x}_a^2\tilde{x}_a^2\tilde{x}_c^2}{\tilde{\omega}_a+\tilde{\omega}_b+\tilde{\omega}_c}-\frac{45\tilde{x}_a^2\tilde{x}_b^2}{2(\tilde{\omega}_a+\tilde{\omega}_b)(\tilde{\omega}_a+\tilde{\omega}_b+\tilde{\omega}_c)}$ $-\frac{45(\tilde{\omega}_a+\tilde{\omega}_b+2\tilde{\omega}_c)\tilde{x}_c^2}{4\tilde{\omega}_c(\tilde{\omega}_a+\tilde{\omega}_c)(\tilde{\omega}_b+\tilde{\omega}_c)(\tilde{\omega}_a+\tilde{\omega}_b+\tilde{\omega}_c)}-\frac{45\tilde{x}_a^2\tilde{x}_c^2}{2(\tilde{\omega}_a+\tilde{\omega}_c)(\tilde{\omega}_a+\tilde{\omega}_b+\tilde{\omega}_c)}-\frac{45\tilde{x}_a^2\tilde{x}_c^2}{2(\tilde{\omega}_b+\tilde{\omega}_c)(\tilde{\omega}_a+\tilde{\omega}_b+\tilde{\omega}_c)}$ $-\frac{45(\tilde{\omega}_a+2\tilde{\omega}_b+\tilde{\omega}_c)\tilde{x}_a^2}{4\tilde{\omega}_b(\tilde{\omega}_a+\tilde{\omega}_b)(\tilde{\omega}_b+\tilde{\omega}_c)(\tilde{\omega}_a+\tilde{\omega}_b+\tilde{\omega}_c)}\Big]$
C_8	$\left[\frac{-360\tilde{x}_a\tilde{x}_b\tilde{x}_c\tilde{x}_d}{(\tilde{\omega}_a+\tilde{\omega}_b+\tilde{\omega}_c+\tilde{\omega}_d)(\tilde{\omega}_a+\tilde{\omega}_b+\tilde{\omega}_c+3\tilde{\omega}_d)}-\frac{120\tilde{x}_a\tilde{x}_b\tilde{x}_c\tilde{x}_d^3}{\tilde{\omega}_a+\tilde{\omega}_b+\tilde{\omega}_c+3\tilde{\omega}_d}\right]$
C_9	$\Big[\frac{-360(\tilde{\omega}_a+\tilde{\omega}_b+\tilde{\omega}_c+\tilde{\omega}_d)\tilde{x}_a\tilde{x}_b}{(\tilde{\omega}_a+\tilde{\omega}_b)(\tilde{\omega}_a+\tilde{\omega}_b+2\tilde{\omega}_c)(\tilde{\omega}_a+\tilde{\omega}_b+2\tilde{\omega}_d)(\tilde{\omega}_a+\tilde{\omega}_b+2(\tilde{\omega}_c+\tilde{\omega}_d))}-\frac{180\tilde{x}_a\tilde{x}_b\left((\tilde{\omega}_a+\tilde{\omega}_b+2\tilde{\omega}_d)\tilde{x}_x^2+(\tilde{\omega}_a+\tilde{\omega}_b+2\tilde{\omega}_c)\tilde{x}_d^2\right)}{(\tilde{\omega}_a+\tilde{\omega}_b+2\tilde{\omega}_c)(\tilde{\omega}_a+\tilde{\omega}_b+2\tilde{\omega}_d)(\tilde{\omega}_a+\tilde{\omega}_b+2(\tilde{\omega}_c+\tilde{\omega}_d))}$ $-\frac{180\tilde{x}_a\tilde{x}_b\tilde{x}_x^2\tilde{x}_d^2}{\tilde{\omega}_a+\tilde{\omega}_b+2(\tilde{\omega}_c+\tilde{\omega}_d)}\Big]$

Table 2. *Cont.*

	Expression for C_i Coefficients
C_{10}	$\left[\frac{-360\tilde{x}_a\tilde{x}_b\tilde{x}_c\tilde{x}_d}{(\tilde{\omega}_a+\tilde{\omega}_b+\tilde{\omega}_c+\tilde{\omega}_d)(\tilde{\omega}_a+\tilde{\omega}_b+\tilde{\omega}_c+\tilde{\omega}_d+2\tilde{\omega}_e)} - \frac{360\tilde{x}_a\tilde{x}_b\tilde{x}_c\tilde{x}_d\tilde{x}_e^2}{(\tilde{\omega}_a+\tilde{\omega}_b+\tilde{\omega}_c+\tilde{\omega}_d+2\tilde{\omega}_e)}\right]$
C_{11}	$\left[\frac{-720\tilde{x}_a\tilde{x}_b\tilde{x}_c\tilde{x}_d\tilde{x}_e\tilde{x}_f}{(\tilde{\omega}_a+\tilde{\omega}_b+\tilde{\omega}_c+\tilde{\omega}_d+\tilde{\omega}_e+\tilde{\omega}_f)}\right]$

The expression for ψ_8^1 is

$$
\begin{aligned}
\psi_8^1 = {} & \\
& \frac{1}{N^3}\Bigg[\sum_{\substack{a=0 \\ 8a \bmod N\equiv 0}}^{N-1} D_1(a) + \sum_{\substack{a,b=0 \\ (6a+2b) \bmod N\equiv 0 \\ a\neq b}}^{N-1} D_2(a,b) \\
& + \sum_{\substack{a,b=0 \\ (5a+3b) \bmod N\equiv 0 \\ a\neq b}}^{N-1} D_3(a,b) + \sum_{\substack{a,b=0 \\ (4a+4b) \bmod N\equiv 0 \\ a\neq b}}^{N-1} \frac{1}{2} D_4(a,b) \\
& + \sum_{\substack{a,b=0 \\ (a+7b) \bmod N\equiv 0 \\ a\neq b}}^{N-1} D_5(a,b) + \sum_{\substack{a,b,c=0 \\ (a+b+6c) \bmod N\equiv 0}}^{N-1} \frac{1}{2} D_6(a,b,c) \\
& + \sum_{\substack{a,b,c=0 \\ (a+2b+5c) \bmod N\equiv 0 \\ a\neq b\neq c}}^{N-1} D_7(a,b,c) + \sum_{\substack{a,b,c=0 \\ (a+4b+3c) \bmod N\equiv 0 \\ a\neq b\neq c}}^{N-1} D_8(a,b,c) \\
& + \sum_{\substack{a,b,c=0 \\ (2a+2b+4c) \bmod N\equiv 0 \\ a\neq b\neq c}}^{N-1} \frac{D_9(a,b,c)}{2} + \sum_{\substack{a,b,c=0 \\ (3a+2b+3c) \bmod N\equiv 0 \\ a\neq b\neq c}}^{N-1} \frac{D_{10}(a,b,c)}{2} \\
& + \sum_{\substack{a,b,c,d=0 \\ (a+b+2c+4d) \bmod N\equiv 0 \\ a\neq b\neq c\neq d}}^{N-1} \frac{D_{11}(a,b,c,d)}{2} + \sum_{\substack{a,b,c,d=0 \\ 2(a+b+c+d) \bmod N\equiv 0 \\ a\neq b\neq c\neq d}}^{N-1} \frac{D_{12}(a,b,c,d)}{24} \\
& + \sum_{\substack{a,b,c,d=0 \\ (a+2b+2c+3d) \bmod N\equiv 0 \\ a\neq b\neq c\neq d}}^{N-1} \frac{D_{13}(a,b,c,d)}{2} + \sum_{\substack{a,b,c,d=0 \\ (a+b+c+5d) \bmod N\equiv 0 \\ a\neq b\neq c\neq d}}^{N-1} \frac{D_{14}(a,b,c,d)}{6} \\
& + \sum_{\substack{a,b,c,d=0 \\ (a+b+3c+3d) \bmod N\equiv 0 \\ a\neq b\neq c\neq d}}^{N-1} \frac{D_{15}(a,b,c,d)}{4} + \sum_{\substack{a,b,c,d,e=0 \\ a+b+2(c+d+e) \bmod N\equiv 0 \\ a\neq b\neq c\neq d\neq e}}^{N-1} \frac{D_{16}(a,b,c,d,e)}{12} \\
& + \sum_{\substack{a,b,c,d,e=0 \\ (a+b+c+2d+3e) \bmod N\equiv 0 \\ a\neq b\neq c\neq d\neq e}}^{N-1} \frac{D_{17}(a,b,c,d,e)}{6} + \sum_{\substack{a,b,c,d,e=0 \\ (a+b+c+d+4e) \bmod N\equiv 0 \\ a\neq b\neq c\neq d\neq e}}^{N-1} \frac{D_{18}(a,b,c,d,e)}{24} \\
& + \sum_{\substack{a,b,c,d,e,f=0 \\ (a+b+c+d+e \\ +3f) \bmod N\equiv 0 \\ a\neq b\neq c\neq d\neq e\neq f}}^{N-1} \frac{D_{19}(a,b,c,d,e,f)}{5!} + \sum_{\substack{a,b,c,d,e,f=0 \\ (a+b+c+d+2e \\ +2f) \bmod N\equiv 0 \\ a\neq b\neq c\neq d\neq e\neq f}}^{N-1} \frac{D_{20}(a,b,c,d,e,f)}{48} \\
& + \sum_{\substack{a,b,c,d,e,f,g=0 \\ (a+b+c+d+e+f \\ +2g) \bmod N\equiv 0 \\ a\neq b\neq c\neq d\neq e\neq f\neq g}}^{N-1} \frac{D_{21}(a,b,c,d,e,f,g)}{6!} + \sum_{\substack{a,b,c,d,e, \\ f,g,h=0 \\ (a+b+c+d+e+f \\ +g+h) \bmod N\equiv 0 \\ a\neq b\neq c\neq d\neq e \\ \neq f\neq g\neq h}}^{N-1} \frac{D_{22}(a,b,c,d,e,f,g,h)}{8!}\Bigg]
\end{aligned} \tag{58}
$$

The terms $D_1, D_2, D_3 \ldots D_{22}$ are given in the Table 3.

Table 3. Expression for the terms $D_1, D_2, D_3 \ldots D_{22}$.

	Expression for D_i Coefficients
D_1	$\left[\frac{875}{128\tilde{\omega}_a^5} - \frac{105x_b^2}{16\tilde{\omega}_a^4} - \frac{35x_a^4}{16\tilde{\omega}_a^3} - \frac{7x_a^6}{12\tilde{\omega}_a^2} - \frac{x_a^8}{8\tilde{\omega}_a}\right]$
D_2	$\frac{8!}{2!6!}\left[\frac{5\left(36\tilde{\omega}_a^4+66\tilde{\omega}_a^3\tilde{\omega}_b+121\tilde{\omega}_a^2\tilde{\omega}_b^2+66\tilde{\omega}_a\tilde{\omega}_b^3+11\tilde{\omega}_b^4\right)}{64\tilde{\omega}_a^4\tilde{\omega}_b^2(\tilde{\omega}_a+\tilde{\omega}_b)(2\tilde{\omega}_a+\tilde{\omega}_b)(3\tilde{\omega}_a+\tilde{\omega}_b)} - \frac{15\left(11\tilde{\omega}_a^2+6\tilde{\omega}_a\tilde{\omega}_b+\tilde{\omega}_b^2\right)x_a^2}{16\tilde{\omega}_a^3(\tilde{\omega}_a+\tilde{\omega}_b)(2\tilde{\omega}_a+\tilde{\omega}_b)(3\tilde{\omega}_a+\tilde{\omega}_b)} - \frac{45x_b^2}{8\tilde{\omega}_b(\tilde{\omega}_a+\tilde{\omega}_b)(2\tilde{\omega}_a+\tilde{\omega}_b)(3\tilde{\omega}_a+\tilde{\omega}_b)} - \frac{5(5\tilde{\omega}_a+\tilde{\omega}_b)x_a^4}{16\tilde{\omega}_a^2(2\tilde{\omega}_a+\tilde{\omega}_b)(3\tilde{\omega}_a+\tilde{\omega}_b)} - \frac{45x_a^2x_b^2}{4(\tilde{\omega}_a+\tilde{\omega}_b)(2\tilde{\omega}_a+\tilde{\omega}_b)(3\tilde{\omega}_a+\tilde{\omega}_b)} - \frac{x_b^6}{12\tilde{\omega}_a(3\tilde{\omega}_a+\tilde{\omega}_b)} - \frac{15x_b^4x_b^2}{4(2\tilde{\omega}_a+\tilde{\omega}_b)(3\tilde{\omega}_a+\tilde{\omega}_b)} - \frac{x_a^6x_b^2}{2(3\tilde{\omega}_b+\tilde{\omega}_a)}\right]$
D_3	$\frac{8!}{3!5!}\left[\frac{-30(23\tilde{\omega}_a+13\tilde{\omega}_b)x_ax_b}{(\tilde{\omega}_a+\tilde{\omega}_b)(3\tilde{\omega}_a+\tilde{\omega}_b)(5\tilde{\omega}_a+\tilde{\omega}_b)(\tilde{\omega}_a+3\tilde{\omega}_b)(5\tilde{\omega}_a+3\tilde{\omega}_b)} - \frac{10x_ax_b^3}{(\tilde{\omega}_a+\tilde{\omega}_b)(\tilde{\omega}_a+3\tilde{\omega}_b)(5\tilde{\omega}_a+3\tilde{\omega}_b)} - \frac{40(2\tilde{\omega}_a+\tilde{\omega}_b)x_a^3x_b}{(\tilde{\omega}_a+\tilde{\omega}_b)(3\tilde{\omega}_a+\tilde{\omega}_b)(5\tilde{\omega}_a+\tilde{\omega}_b)(5\tilde{\omega}_a+3\tilde{\omega}_b)} - \frac{10x_a^3x_b^3}{3(\tilde{\omega}_a+\tilde{\omega}_b)(5\tilde{\omega}_a+3\tilde{\omega}_b)} - \frac{3x_a^5x_b}{(5\tilde{\omega}_a+\tilde{\omega}_b)(5\tilde{\omega}_a+3\tilde{\omega}_b)} - \frac{x_a^5x_b^3}{5\tilde{\omega}_a+3\tilde{\omega}_b}\right]$
D_4	$\frac{8!}{4!4!}\left[\frac{27\left(2\tilde{\omega}_a^4+7\tilde{\omega}_a^3\tilde{\omega}_b+7\tilde{\omega}_a^2\tilde{\omega}_b^2+7\tilde{\omega}_a\tilde{\omega}_b^3+2\tilde{\omega}_b^4\right)}{64\tilde{\omega}_a^3\tilde{\omega}_b^3(\tilde{\omega}_a+\tilde{\omega}_b)(2\tilde{\omega}_a+\tilde{\omega}_b)(\tilde{\omega}_a+2\tilde{\omega}_b)} - \frac{9(7\tilde{\omega}_a+2\tilde{\omega}_b)x_a^2}{16\tilde{\omega}_a^2(\tilde{\omega}_a+\tilde{\omega}_b)(2\tilde{\omega}_a+\tilde{\omega}_b)(\tilde{\omega}_a+2\tilde{\omega}_b)} - \frac{9(2\tilde{\omega}_a+7\tilde{\omega}_b)x_b^2}{16\tilde{\omega}_b^2(\tilde{\omega}_a+\tilde{\omega}_b)(2\tilde{\omega}_a+\tilde{\omega}_b)(\tilde{\omega}_a+2\tilde{\omega}_b)} - \frac{3x_b^4}{16\tilde{\omega}_b(\tilde{\omega}_a+\tilde{\omega}_b)(\tilde{\omega}_a+2\tilde{\omega}_b)} - \frac{3x_b^4}{16\tilde{\omega}_b(\tilde{\omega}_b+\tilde{\omega}_b)(\tilde{\omega}_a+2\tilde{\omega}_b)} - \frac{27x_a^2x_b^2}{4(\tilde{\omega}_a+\tilde{\omega}_b)(2\tilde{\omega}_a+\tilde{\omega}_b)(\tilde{\omega}_a+2\tilde{\omega}_b)} - \frac{3x_a^2x_b^4}{4(\tilde{\omega}_a+\tilde{\omega}_b)(\tilde{\omega}_a+2\tilde{\omega}_b)} - \frac{3x_a^4x_b^2}{4(\tilde{\omega}_a+\tilde{\omega}_b)(2\tilde{\omega}_a+\tilde{\omega}_b)} - \frac{x_b^4x_b^4}{4(\tilde{\omega}_a+\tilde{\omega}_b)}\right]$
D_5	$\frac{8!}{7!}\left[\frac{-630x_ax_b}{(\tilde{\omega}_a+\tilde{\omega}_b)(\tilde{\omega}_a+3\tilde{\omega}_b)(\tilde{\omega}_a+5\tilde{\omega}_b)(\tilde{\omega}_a+7\tilde{\omega}_b)} - \frac{210x_ax_b^3}{(\tilde{\omega}_a+3\tilde{\omega}_b)(\tilde{\omega}_a+5\tilde{\omega}_b)(\tilde{\omega}_a+7\tilde{\omega}_b)} - \frac{21x_ax_b^5}{(\tilde{\omega}_a+5\tilde{\omega}_b)(\tilde{\omega}_a+7\tilde{\omega}_b)} - \frac{x_ax_b^7}{\tilde{\omega}_a+7\tilde{\omega}_b}\right]$
D_6	$\frac{8!}{6!}\left[\frac{-90x_ax_b}{(\tilde{\omega}_a+\tilde{\omega}_b)(\tilde{\omega}_a+\tilde{\omega}_b+2\tilde{\omega}_c)(\tilde{\omega}_a+\tilde{\omega}_b+4\tilde{\omega}_c)(\tilde{\omega}_a+\tilde{\omega}_b+6\tilde{\omega}_c)} - \frac{90x_ax_bx_c^2}{(\tilde{\omega}_c+\tilde{\omega}_b+2\tilde{\omega}_c)(\tilde{\omega}_a+\tilde{\omega}_b+4\tilde{\omega}_c)(\tilde{\omega}_a+\tilde{\omega}_b+6\tilde{\omega}_c)} - \frac{15x_ax_bx_c^4}{(\tilde{\omega}_a+\tilde{\omega}_b+4\tilde{\omega}_c)(\tilde{\omega}_a+\tilde{\omega}_b+6\tilde{\omega}_c)} - \frac{x_ax_bx_c^6}{\tilde{\omega}_a+\tilde{\omega}_b+6\tilde{\omega}_c}\right]$
D_7	$\frac{8!}{2!5!}\left[\frac{-20x_ax_c^3(\tilde{\omega}_a+\tilde{\omega}_b+4\tilde{\omega}_c)}{(\tilde{\omega}_a+3\tilde{\omega}_c)(\tilde{\omega}_a+2\tilde{\omega}_b+3\tilde{\omega}_c)(\tilde{\omega}_a+5\tilde{\omega}_c)(\tilde{\omega}_a+2\tilde{\omega}_b+5\tilde{\omega}_c)} - \frac{x_ax_b^2x_c}{(\tilde{\omega}_a+2\tilde{\omega}_b+\tilde{\omega}_c)(\tilde{\omega}_a+2\tilde{\omega}_b+3\tilde{\omega}_c)(\tilde{\omega}_a+2\tilde{\omega}_b+5\tilde{\omega}_c)} - \frac{x_ax_c^5}{(\tilde{\omega}_a+5\tilde{\omega}_c)(\tilde{\omega}_a+2\tilde{\omega}_b+5\tilde{\omega}_c)} - \frac{10x_ax_b^3x_c^3}{(\tilde{\omega}_a+2\tilde{\omega}_b+3\tilde{\omega}_c)(\tilde{\omega}_a+2\tilde{\omega}_b+5\tilde{\omega}_c)} - \frac{x_ax_b^2x_c^5}{\tilde{\omega}_a+2\tilde{\omega}_b+5\tilde{\omega}_c} - \frac{30x_ax_c\left(3\tilde{\omega}_a^2+6\tilde{\omega}_a\tilde{\omega}_b+4\tilde{\omega}_b^2+18\tilde{\omega}_a\tilde{\omega}_c+18\tilde{\omega}_b\tilde{\omega}_c+23\tilde{\omega}_c^2\right)}{(\tilde{\omega}_a+\tilde{\omega}_c)(\tilde{\omega}_a+2\tilde{\omega}_b+\tilde{\omega}_c)(\tilde{\omega}_a+3\tilde{\omega}_c)(\tilde{\omega}_a+2\tilde{\omega}_b+3\tilde{\omega}_c)(\tilde{\omega}_a+5\tilde{\omega}_c)(\tilde{\omega}_a+2\tilde{\omega}_b+5\tilde{\omega}_c)}\right]$

Table 3. *Cont.*

	Expression for D_i Coefficients
D_8	$\frac{8!}{3!4!}\left[\frac{-6x_ax_b^3}{(\tilde{\omega}_a+3\tilde{\omega}_b)(\tilde{\omega}_a+3\tilde{\omega}_b+2\tilde{\omega}_c)(\tilde{\omega}_a+3\tilde{\omega}_b+4\tilde{\omega}_c)}-\frac{36x_ax_bx_c^2(\tilde{\omega}_a+2\tilde{\omega}_b+3\tilde{\omega}_c)}{(\tilde{\omega}_a+\tilde{\omega}_b+2\tilde{\omega}_c)(\tilde{\omega}_a+3\tilde{\omega}_b+2\tilde{\omega}_c)(\tilde{\omega}_a+\tilde{\omega}_b+4\tilde{\omega}_c)(\tilde{\omega}_a+3\tilde{\omega}_b+4\tilde{\omega}_c)}-\frac{3x_ax_bx_c^4}{(\tilde{\omega}_a+\tilde{\omega}_b+4\tilde{\omega}_c)(\tilde{\omega}_a+3\tilde{\omega}_b+4\tilde{\omega}_c)}-\frac{6x_ax_b^3x_c^2}{(\tilde{\omega}_a+3\tilde{\omega}_b+2\tilde{\omega}_c)(\tilde{\omega}_a+3\tilde{\omega}_b+4\tilde{\omega}_c)}-\frac{x_ax_b^3x_c^4}{\tilde{\omega}_a+3\tilde{\omega}_b+4\tilde{\omega}_c}-\frac{18x_ax_b\left(3\tilde{\omega}_a^2+13\tilde{\omega}_b^2+24\tilde{\omega}_b\tilde{\omega}_c+8\tilde{\omega}_c^2+12\tilde{\omega}_a(\tilde{\omega}_b+\tilde{\omega}_c)\right)}{(\tilde{\omega}_a+\tilde{\omega}_b)(\tilde{\omega}_a+3\tilde{\omega}_b)(\tilde{\omega}_a+\tilde{\omega}_b+2\tilde{\omega}_c)(\tilde{\omega}_a+3\tilde{\omega}_b+2\tilde{\omega}_c)(\tilde{\omega}_a+\tilde{\omega}_b+4\tilde{\omega}_c)(\tilde{\omega}_a+3\tilde{\omega}_b+4\tilde{\omega}_c)}\right]$
D_9	$\frac{8!}{2!2!4!}\left[\frac{9}{64\tilde{\omega}_a\tilde{\omega}_b\tilde{\omega}_c^3}+\frac{3}{32\tilde{\omega}_a\tilde{\omega}_b^2\tilde{\omega}_c^2}+\frac{3}{32\tilde{\omega}_a^2\tilde{\omega}_b\tilde{\omega}_c^2}-\frac{3}{32\tilde{\omega}_a\tilde{\omega}_b(\tilde{\omega}_a+\tilde{\omega}_b)\tilde{\omega}_c^2}-\frac{3}{16\tilde{\omega}_a\tilde{\omega}_b\tilde{\omega}_c^2(\tilde{\omega}_a+\tilde{\omega}_c)}-\frac{3}{16\tilde{\omega}_a\tilde{\omega}_b\tilde{\omega}_c^2(\tilde{\omega}_b+\tilde{\omega}_c)}+\frac{3}{16\tilde{\omega}_a\tilde{\omega}_b\tilde{\omega}_c^2(\tilde{\omega}_a+\tilde{\omega}_b+\tilde{\omega}_c)}+\frac{3}{32\tilde{\omega}_a\tilde{\omega}_b\tilde{\omega}_c^2(\tilde{\omega}_a+2\tilde{\omega}_c)}+\frac{3}{32\tilde{\omega}_a\tilde{\omega}_b\tilde{\omega}_c^2(\tilde{\omega}_b+2\tilde{\omega}_c)}-\frac{3}{32\tilde{\omega}_a\tilde{\omega}_b\tilde{\omega}_c^2(\tilde{\omega}_a+\tilde{\omega}_b+2\tilde{\omega}_c)}-\frac{3x_a^2}{16\tilde{\omega}_a\tilde{\omega}_b\tilde{\omega}_c^2}-\frac{3x_a^2\left(3\tilde{\omega}_a^2+\tilde{\omega}_b^2+3\tilde{\omega}_b\tilde{\omega}_c+2\tilde{\omega}_c^2+3\tilde{\omega}_a(\tilde{\omega}_b+2\tilde{\omega}_c)\right)}{8\tilde{\omega}_a(\tilde{\omega}_a+\tilde{\omega}_b)(\tilde{\omega}_a+\tilde{\omega}_c)(\tilde{\omega}_a+\tilde{\omega}_b+\tilde{\omega}_c)(\tilde{\omega}_a+2\tilde{\omega}_c)(\tilde{\omega}_a+\tilde{\omega}_b+2\tilde{\omega}_c)}-\frac{3x_b^2\left(\tilde{\omega}_a^2+3\tilde{\omega}_b^2+6\tilde{\omega}_b\tilde{\omega}_c+2\tilde{\omega}_c^2+3\tilde{\omega}_a(\tilde{\omega}_b+\tilde{\omega}_c)\right)}{8\tilde{\omega}_b(\tilde{\omega}_a+\tilde{\omega}_b)(\tilde{\omega}_b+\tilde{\omega}_c)(\tilde{\omega}_a+\tilde{\omega}_b+\tilde{\omega}_c)(\tilde{\omega}_b+2\tilde{\omega}_c)(\tilde{\omega}_a+\tilde{\omega}_b+2\tilde{\omega}_c)}-\frac{3x_c^2}{16\tilde{\omega}_a\tilde{\omega}_b\tilde{\omega}_c^2}+\frac{3x_c^2}{8\tilde{\omega}_a\tilde{\omega}_b(\tilde{\omega}_b+\tilde{\omega}_c)(\tilde{\omega}_b+2\tilde{\omega}_c)}+\frac{3x_c^2}{8\tilde{\omega}_a\tilde{\omega}_b(\tilde{\omega}_a+\tilde{\omega}_c)(\tilde{\omega}_a+2\tilde{\omega}_c)}-\frac{x_c^4(\tilde{\omega}_a+\tilde{\omega}_b+4\tilde{\omega}_c)}{16\tilde{\omega}_c(\tilde{\omega}_a+2\tilde{\omega}_c)(\tilde{\omega}_b+2\tilde{\omega}_c)(\tilde{\omega}_a+\tilde{\omega}_b+2\tilde{\omega}_c)}-\frac{3x_a^2x_b^2}{4(\tilde{\omega}_a+\tilde{\omega}_b)(\tilde{\omega}_a+\tilde{\omega}_b+\tilde{\omega}_c)(\tilde{\omega}_a+\tilde{\omega}_b+2\tilde{\omega}_c)}-\frac{x_a^2x_c^2(2\tilde{\omega}_a+\tilde{\omega}_b+3\tilde{\omega}_c)}{4(\tilde{\omega}_a+\tilde{\omega}_c)(\tilde{\omega}_a+\tilde{\omega}_b+\tilde{\omega}_c)(\tilde{\omega}_a+2\tilde{\omega}_c)(\tilde{\omega}_a+\tilde{\omega}_b+2\tilde{\omega}_c)}-\frac{3x_b^2x_c^2(\tilde{\omega}_a+2\tilde{\omega}_b+3\tilde{\omega}_c)}{4(\tilde{\omega}_b+\tilde{\omega}_c)(\tilde{\omega}_a+\tilde{\omega}_b+\tilde{\omega}_c)(\tilde{\omega}_b+2\tilde{\omega}_c)(\tilde{\omega}_a+\tilde{\omega}_b+2\tilde{\omega}_c)}-\frac{x_a^2x_c^4}{4(\tilde{\omega}_a+2\tilde{\omega}_c)(\tilde{\omega}_a+\tilde{\omega}_b+2\tilde{\omega}_c)}-\frac{x_b^2x_c^4}{4(\tilde{\omega}_b+2\tilde{\omega}_c)(\tilde{\omega}_a+\tilde{\omega}_b+2\tilde{\omega}_c)}-\frac{3x_a^2x_b^2x_c^2}{2(\tilde{\omega}_a+\tilde{\omega}_b+\tilde{\omega}_c)(\tilde{\omega}_a+\tilde{\omega}_b+2\tilde{\omega}_c)}-\frac{x_a^2x_b^2x_c^4}{2(\tilde{\omega}_a+\tilde{\omega}_b+2\tilde{\omega}_c)}\right]$
D_{10}	$\frac{8!}{2!3!3!}\left[\frac{9x_ax_c}{4\tilde{\omega}_b\tilde{\omega}_c(\tilde{\omega}_a+2\tilde{\omega}_b+\tilde{\omega}_c)(3\tilde{\omega}_a+2\tilde{\omega}_b+\tilde{\omega}_c)}-\frac{6x_ax_c}{\tilde{\omega}_b(\tilde{\omega}_a+\tilde{\omega}_c)(3\tilde{\omega}_a+\tilde{\omega}_c)(\tilde{\omega}_a+3\tilde{\omega}_c)}-\frac{x_a^3x_b^2x_c^3}{3\tilde{\omega}_a+2\tilde{\omega}_b+3\tilde{\omega}_c}+\frac{9x_ax_c}{4\sqrt{2}\tilde{\omega}_a\tilde{\omega}_b\tilde{\omega}_c(\tilde{\omega}_a+2\tilde{\omega}_b+3\tilde{\omega}_c)}+\frac{9x_ax_c}{8\tilde{\omega}_a\tilde{\omega}_b\tilde{\omega}_c(3\tilde{\omega}_a+2\tilde{\omega}_b+3\tilde{\omega}_c)}-\frac{x_a^3x_c}{2\tilde{\omega}_b(\tilde{\omega}_a+\tilde{\omega}_c)(3\tilde{\omega}_c+\tilde{\omega}_c)}+\frac{3x_a^3x_c}{2\tilde{\omega}_b(3\tilde{\omega}_a+2\tilde{\omega}_b+\tilde{\omega}_c)(3\tilde{\omega}_a+2\tilde{\omega}_b+3\tilde{\omega}_c)}-\frac{9x_ax_b^2x_c\left((3\tilde{\omega}_a+2\tilde{\omega}_b)^2+10\tilde{\omega}_a\tilde{\omega}_c+4\tilde{\omega}_b\tilde{\omega}_c+\tilde{\omega}_c^2\right)}{4\tilde{\omega}_a\tilde{\omega}_c(\tilde{\omega}_a+2\tilde{\omega}_b+\tilde{\omega}_c)(3\tilde{\omega}_a+2\tilde{\omega}_b+\tilde{\omega}_c)(3\tilde{\omega}_a+2\tilde{\omega}_b+3\tilde{\omega}_c)}-\frac{3x_c^3x_b^2x_c}{(3\tilde{\omega}_a+2\tilde{\omega}_b+\tilde{\omega}_c)(3\tilde{\omega}_c+2\tilde{\omega}_b+3\tilde{\omega}_c)}-\frac{x_ax_c^3}{2\tilde{\omega}_b(\tilde{\omega}_a+\tilde{\omega}_c)(\tilde{\omega}_a+3\tilde{\omega}_c)}+\frac{3x_ax_b^2x_c^3}{2\tilde{\omega}_a(3\tilde{\omega}_a+2\tilde{\omega}_b+3\tilde{\omega}_c)}-\frac{3x_ax_c^3\left(\tilde{\omega}_a+3\sqrt{2}\tilde{\omega}_a+2\tilde{\omega}_b+2\sqrt{2}\tilde{\omega}_b+3\tilde{\omega}_c+3\sqrt{2}\tilde{\omega}_c\right)}{4\tilde{\omega}_a\tilde{\omega}_b(\tilde{\omega}_a+2\tilde{\omega}_b+3\tilde{\omega}_c)(3\tilde{\omega}_a+2\tilde{\omega}_b+3\tilde{\omega}_c)}-\frac{x_c^3x_c^3}{3(\tilde{\omega}_a+\tilde{\omega}_c)(3\tilde{\omega}_a+2\tilde{\omega}_b+3\tilde{\omega}_c)}\right]$
D_{11}	$\frac{8!}{2!4!}\left[\frac{6\left(-3(\tilde{\omega}_a+\tilde{\omega}_b)^2-6(\tilde{\omega}_a+\tilde{\omega}_b)\tilde{\omega}_c-4\tilde{\omega}_c^2-12(\tilde{\omega}_a+\tilde{\omega}_b+\tilde{\omega}_c)\tilde{\omega}_d-8\tilde{\omega}_d^2\right)x_ax_b}{(\tilde{\omega}_a+\tilde{\omega}_b)(\tilde{\omega}_a+\tilde{\omega}_b+2\tilde{\omega}_c)(\tilde{\omega}_a+\tilde{\omega}_b+2\tilde{\omega}_d)(\tilde{\omega}_a+\tilde{\omega}_b+4\tilde{\omega}_d)(\tilde{\omega}_a+\tilde{\omega}_b+2\tilde{\omega}_c+4\tilde{\omega}_d)(\tilde{\omega}_a+\tilde{\omega}_b+2(\tilde{\omega}_c+\tilde{\omega}_d))}-\frac{6x_ax_bx_c^2}{(\tilde{\omega}_a+\tilde{\omega}_b+2\tilde{\omega}_c)(\tilde{\omega}_a+\tilde{\omega}_b+2\tilde{\omega}_c+4\tilde{\omega}_d)(\tilde{\omega}_a+\tilde{\omega}_b+2(\tilde{\omega}_c+\tilde{\omega}_d))}-\frac{x_ax_bx_d^4}{(\tilde{\omega}_a+\tilde{\omega}_b+4\tilde{\omega}_d)(\tilde{\omega}_a+\tilde{\omega}_b+2\tilde{\omega}_c+4\tilde{\omega}_d)}-\frac{12(\tilde{\omega}_a+\tilde{\omega}_b+\tilde{\omega}_c+3\tilde{\omega}_d)x_ax_bx_d^2}{(\tilde{\omega}_a+\tilde{\omega}_b+2\tilde{\omega}_d)(\tilde{\omega}_a+\tilde{\omega}_b+4\tilde{\omega}_d)(\tilde{\omega}_a+\tilde{\omega}_b+2\tilde{\omega}_c+4\tilde{\omega}_d)(\tilde{\omega}_a+\tilde{\omega}_b+2(\tilde{\omega}_c+\tilde{\omega}_d))}-\frac{x_ax_bx_c^2x_d^4}{\tilde{\omega}_a+\tilde{\omega}_b+2\tilde{\omega}_c+4\tilde{\omega}_d}-\frac{6x_ax_bx_c^2x_d^2}{(\tilde{\omega}_a+\tilde{\omega}_b+2\tilde{\omega}_c+4\tilde{\omega}_d)(\tilde{\omega}_a+\tilde{\omega}_b+2(\tilde{\omega}_c+\tilde{\omega}_d))}\right]$

Table 3. *Cont.*

	Expression for D_i Coefficients
D_{12}	$\begin{aligned} &\frac{8!}{2!2!2!2!}\Bigg[\frac{1}{32\tilde{\omega}_a\tilde{\omega}_b\tilde{\omega}_c\tilde{\omega}_d{}^2}+\frac{1}{32\tilde{\omega}_a\tilde{\omega}_b\tilde{\omega}_c^2\tilde{\omega}_d}+\frac{1}{32\tilde{\omega}_a\tilde{\omega}_b^2\tilde{\omega}_c\tilde{\omega}_d}+\frac{1}{32\tilde{\omega}_a^2\tilde{\omega}_b\tilde{\omega}_c\tilde{\omega}_d}-\frac{1}{32\tilde{\omega}_a\tilde{\omega}_b(\tilde{\omega}_a+\tilde{\omega}_b)\tilde{\omega}_c\tilde{\omega}_d} \\ &-\frac{1}{32\tilde{\omega}_a\tilde{\omega}_b\tilde{\omega}_c(\tilde{\omega}_a+\tilde{\omega}_c)\tilde{\omega}_d}-\frac{1}{32\tilde{\omega}_d\tilde{\omega}_b\tilde{\omega}_c(\tilde{\omega}_b+\tilde{\omega}_c)\tilde{\omega}_d}+\frac{1}{32\tilde{\omega}_a\tilde{\omega}_b\tilde{\omega}_c(\tilde{\omega}_a+\tilde{\omega}_b+\tilde{\omega}_c)\tilde{\omega}_d}-\frac{1}{32\tilde{\omega}_a\tilde{\omega}_b\tilde{\omega}_c\tilde{\omega}_d(\tilde{\omega}_a+\tilde{\omega}_d)} \\ &-\frac{1}{32\tilde{\omega}_a\tilde{\omega}_b\tilde{\omega}_c\tilde{\omega}_d(\tilde{\omega}_b+\tilde{\omega}_d)}+\frac{1}{32\tilde{\omega}_a\tilde{\omega}_b\tilde{\omega}_c\tilde{\omega}_d(\tilde{\omega}_a+\tilde{\omega}_b+\tilde{\omega}_d)}-\frac{1}{32\tilde{\omega}_a\tilde{\omega}_b\tilde{\omega}_c\tilde{\omega}_d(\tilde{\omega}_c+\tilde{\omega}_d)}+\frac{1}{32\tilde{\omega}_a\tilde{\omega}_b\tilde{\omega}_c\tilde{\omega}_d(\tilde{\omega}_a+\tilde{\omega}_c+\tilde{\omega}_c)} \\ &+\frac{1}{32\tilde{\omega}_a\tilde{\omega}_b\tilde{\omega}_c\tilde{\omega}_d(\tilde{\omega}_b+\tilde{\omega}_c+\tilde{\omega}_c)}-\frac{1}{32\tilde{\omega}_a\tilde{\omega}_b\tilde{\omega}_c\tilde{\omega}_d(\tilde{\omega}_a+\tilde{\omega}_b+\tilde{\omega}_c+\tilde{\omega}_d)}-\frac{x_a^2}{16\tilde{\omega}_a\tilde{\omega}_b\tilde{\omega}_c\tilde{\omega}_d}+\frac{x_a^2}{16\tilde{\omega}_b(\tilde{\omega}_a+\tilde{\omega}_b)\tilde{\omega}_c\tilde{\omega}_d} \\ &+\frac{x_a^2}{16\tilde{\omega}_b\tilde{\omega}_c(\tilde{\omega}_a+\tilde{\omega}_c)\tilde{\omega}_d}-\frac{x_a^2}{16\tilde{\omega}_b\tilde{\omega}_c(\tilde{\omega}_a+\tilde{\omega}_b+\tilde{\omega}_c)\tilde{\omega}_d}+\frac{x_a^2}{16\tilde{\omega}_b\tilde{\omega}_c\tilde{\omega}_d(\tilde{\omega}_a+\tilde{\omega}_d)}-\frac{x_a^2}{16\tilde{\omega}_b\tilde{\omega}_c\tilde{\omega}_d(\tilde{\omega}_a+\tilde{\omega}_b+\tilde{\omega}_d)} \\ &-\frac{x_a^2}{16\tilde{\omega}_b\tilde{\omega}_c\tilde{\omega}_d(\tilde{\omega}_a+\tilde{\omega}_c+\tilde{\omega}_d)}+\frac{x_a^2}{16\tilde{\omega}_b\tilde{\omega}_c\tilde{\omega}_d(\tilde{\omega}_a+\tilde{\omega}_b+\tilde{\omega}_c+\tilde{\omega}_d)}-\frac{x_b^2}{16\tilde{\omega}_a\tilde{\omega}_b\tilde{\omega}_c\tilde{\omega}_d}+\frac{x_b^2}{16\tilde{\omega}_a(\tilde{\omega}_a+\tilde{\omega}_b)\tilde{\omega}_c\tilde{\omega}_d} \\ &+\frac{x_b^2}{16\tilde{\omega}_a\tilde{\omega}_c(\tilde{\omega}_b+\tilde{\omega}_c)\tilde{\omega}_d}-\frac{x_b^2}{16\tilde{\omega}_a\tilde{\omega}_c(\tilde{\omega}_a+\tilde{\omega}_b+\tilde{\omega}_c)\tilde{\omega}_d}+\frac{x_b^2}{16\tilde{\omega}_a\tilde{\omega}_c\tilde{\omega}_d(\tilde{\omega}_b+\tilde{\omega}_d)}-\frac{x_b^2}{16\tilde{\omega}_a\tilde{\omega}_c\tilde{\omega}_d(\tilde{\omega}_a+\tilde{\omega}_b+\tilde{\omega}_d)} \\ &-\frac{x_b^2}{16\tilde{\omega}_a\tilde{\omega}_c\tilde{\omega}_d(\tilde{\omega}_b+\tilde{\omega}_c+\tilde{\omega}_d)}+\frac{x_b^2}{16\tilde{\omega}_a\tilde{\omega}_c\tilde{\omega}_d(\tilde{\omega}_a+\tilde{\omega}_b+\tilde{\omega}_c+\tilde{\omega}_d)}-\frac{x_a^2x_b^2}{8(\tilde{\omega}_a+\tilde{\omega}_b)\tilde{\omega}_c\tilde{\omega}_d}+\frac{x_a^2x_b^2}{8\tilde{\omega}_c(\tilde{\omega}_a+\tilde{\omega}_b+\tilde{\omega}_c)\tilde{\omega}_d} \\ &+\frac{x_a^2x_b^2}{8\tilde{\omega}_c\tilde{\omega}_d(\tilde{\omega}_a+\tilde{\omega}_b+\tilde{\omega}_d)}-\frac{x_a^2x_b^2}{8\tilde{\omega}_c\tilde{\omega}_d(\tilde{\omega}_a+\tilde{\omega}_b+\tilde{\omega}_c+\tilde{\omega}_d)}-\frac{x_c^2}{16\tilde{\omega}_a\tilde{\omega}_b\tilde{\omega}_c\tilde{\omega}_d}+\frac{x_c^2}{16\tilde{\omega}_a\tilde{\omega}_b(\tilde{\omega}_a+\tilde{\omega}_c)\tilde{\omega}_d} \\ &+\frac{x_c^2}{16\tilde{\omega}_a\tilde{\omega}_b(\tilde{\omega}_b+\tilde{\omega}_c)\tilde{\omega}_d}-\frac{x_c^2}{16\tilde{\omega}_a\tilde{\omega}_b(\tilde{\omega}_a+\tilde{\omega}_b+\tilde{\omega}_c)\tilde{\omega}_d}+\frac{x_c^2}{16\tilde{\omega}_a\tilde{\omega}_b\tilde{\omega}_d(\tilde{\omega}_c+\tilde{\omega}_d)}-\frac{x_c^2}{16\tilde{\omega}_a\tilde{\omega}_b\tilde{\omega}_d(\tilde{\omega}_a+\tilde{\omega}_c+\tilde{\omega}_d)} \\ &-\frac{x_c^2}{16\tilde{\omega}_a\tilde{\omega}_b\tilde{\omega}_d(\tilde{\omega}_b+\tilde{\omega}_c+\tilde{\omega}_d)}+\frac{x_c^2}{16\tilde{\omega}_a\tilde{\omega}_b\tilde{\omega}_d(\tilde{\omega}_a+\tilde{\omega}_b+\tilde{\omega}_c+\tilde{\omega}_d)}-\frac{x_a^2x_c^2}{8\tilde{\omega}_b(\tilde{\omega}_a+\tilde{\omega}_c)\tilde{\omega}_d}+\frac{x_a^2x_c^2}{8\tilde{\omega}_b(\tilde{\omega}_a+\tilde{\omega}_b+\tilde{\omega}_c)\tilde{\omega}_d} \\ &+\frac{x_a^2x_c^2}{8\tilde{\omega}_b\tilde{\omega}_d(\tilde{\omega}_a+\tilde{\omega}_c+\tilde{\omega}_d)}-\frac{x_a^2x_c^2}{8\tilde{\omega}_b\tilde{\omega}_d(\tilde{\omega}_a+\tilde{\omega}_b+\tilde{\omega}_c+\tilde{\omega}_d)}-\frac{x_b^2x_c^2}{8\tilde{\omega}_a(\tilde{\omega}_b+\tilde{\omega}_c)\tilde{\omega}_d}+\frac{x_b^2x_c^2}{8\tilde{\omega}_a(\tilde{\omega}_a+\tilde{\omega}_b+\tilde{\omega}_c)\tilde{\omega}_d} \\ &+\frac{x_b^2x_c^2}{8\tilde{\omega}_a\tilde{\omega}_d(\tilde{\omega}_b+\tilde{\omega}_c+\tilde{\omega}_d)}-\frac{x_b^2x_c^2}{8\tilde{\omega}_a\tilde{\omega}_d(\tilde{\omega}_a+\tilde{\omega}_b+\tilde{\omega}_c+\tilde{\omega}_d)}-\frac{x_a^2x_b^2x_c^2}{4(\tilde{\omega}_a+\tilde{\omega}_b+\tilde{\omega}_c)\tilde{\omega}_d}+\frac{x_a^2x_b^2x_c^2}{4\tilde{\omega}_d(\tilde{\omega}_a+\tilde{\omega}_b+\tilde{\omega}_c+\tilde{\omega}_d)}-\frac{x_d^2}{16\tilde{\omega}_a\tilde{\omega}_b\tilde{\omega}_c\tilde{\omega}_d} \\ &+\frac{x_d^2}{16\tilde{\omega}_a\tilde{\omega}_b\tilde{\omega}_c(\tilde{\omega}_a+\tilde{\omega}_d)}+\frac{x_d^2}{16\tilde{\omega}_a\tilde{\omega}_b\tilde{\omega}_c(\tilde{\omega}_b+\tilde{\omega}_d)}-\frac{x_d^2}{16\tilde{\omega}_a\tilde{\omega}_b\tilde{\omega}_c(\tilde{\omega}_a+\tilde{\omega}_b+\tilde{\omega}_d)}+\frac{x_d^2}{16\tilde{\omega}_a\tilde{\omega}_b\tilde{\omega}_c(\tilde{\omega}_c+\tilde{\omega}_d)} \\ &-\frac{x_d^2}{16\tilde{\omega}_a\tilde{\omega}_b\tilde{\omega}_c(\tilde{\omega}_a+\tilde{\omega}_c+\tilde{\omega}_d)}-\frac{x_d^2}{16\tilde{\omega}_a\tilde{\omega}_b\tilde{\omega}_c(\tilde{\omega}_b+\tilde{\omega}_c+\tilde{\omega}_d)}+\frac{x_d^2}{16\tilde{\omega}_a\tilde{\omega}_b\tilde{\omega}_c(\tilde{\omega}_a+\tilde{\omega}_b+\tilde{\omega}_c+\tilde{\omega}_d)}-\frac{x_a^2x_d^2}{8\tilde{\omega}_b\tilde{\omega}_c(\tilde{\omega}_a+\tilde{\omega}_d)} \\ &+\frac{x_a^2x_d^2}{8\tilde{\omega}_b\tilde{\omega}_c(\tilde{\omega}_a+\tilde{\omega}_b+\tilde{\omega}_d)}+\frac{x_a^2x_d^2}{8\tilde{\omega}_b\tilde{\omega}_c(\tilde{\omega}_a+\tilde{\omega}_c+\tilde{\omega}_d)}-\frac{x_a^2x_d^2}{8\tilde{\omega}_b\tilde{\omega}_c(\tilde{\omega}_a+\tilde{\omega}_b+\tilde{\omega}_c+\tilde{\omega}_d)}-\frac{x_b^2x_d^2}{8\tilde{\omega}_a\tilde{\omega}_c(\tilde{\omega}_b+\tilde{\omega}_d)}+\frac{x_b^2x_d^2}{8\tilde{\omega}_a\tilde{\omega}_c(\tilde{\omega}_a+\tilde{\omega}_b+\tilde{\omega}_d)} \\ &+\frac{x_b^2x_d^2}{8\tilde{\omega}_a\tilde{\omega}_c(\tilde{\omega}_b+\tilde{\omega}_c+\tilde{\omega}_d)}-\frac{x_b^2x_d^2}{8\tilde{\omega}_a\tilde{\omega}_c(\tilde{\omega}_a+\tilde{\omega}_b+\tilde{\omega}_c+\tilde{\omega}_d)}-\frac{x_a^2x_b^2x_d^2}{4\tilde{\omega}_c(\tilde{\omega}_a+\tilde{\omega}_b+\tilde{\omega}_d)}+\frac{x_a^2x_b^2x_d^2}{4\tilde{\omega}_c(\tilde{\omega}_a+\tilde{\omega}_b+\tilde{\omega}_c+\tilde{\omega}_d)} \\ &-\frac{x_c^2x_d^2}{8\tilde{\omega}_a\tilde{\omega}_b(\tilde{\omega}_c+\tilde{\omega}_d)}+\frac{x_c^2x_d^2}{8\tilde{\omega}_a\tilde{\omega}_b(\tilde{\omega}_a+\tilde{\omega}_c+\tilde{\omega}_d)}+\frac{x_c^2x_d^2}{8\tilde{\omega}_a\tilde{\omega}_b(\tilde{\omega}_b+\tilde{\omega}_c+\tilde{\omega}_d)}-\frac{x_c^2x_d^2}{8\tilde{\omega}_a\tilde{\omega}_b(\tilde{\omega}_a+\tilde{\omega}_b+\tilde{\omega}_c+\tilde{\omega}_d)}-\frac{x_a^2x_c^2x_d^2}{4\tilde{\omega}_b(\tilde{\omega}_c+\tilde{\omega}_c+\tilde{\omega}_d)} \\ &+\frac{x_a^2x_c^2x_d^2}{4\tilde{\omega}_b(\tilde{\omega}_a+\tilde{\omega}_b+\tilde{\omega}_c+\tilde{\omega}_d)}-\frac{x_b^2x_c^2x_d^2}{4\tilde{\omega}_a(\tilde{\omega}_b+\tilde{\omega}_c+\tilde{\omega}_d)}+\frac{x_b^2x_c^2x_d^2}{4\tilde{\omega}_a(\tilde{\omega}_a+\tilde{\omega}_b+\tilde{\omega}_c+\tilde{\omega}_d)}-\frac{x_a^2x_b^2x_c^2x_d^2}{2(\tilde{\omega}_a+\tilde{\omega}_b+\tilde{\omega}_c+\tilde{\omega}_d)}\Bigg] \end{aligned}$
D_{13}	$\begin{aligned} &\frac{8!}{2!2!3!}\Bigg[\frac{x_ax_d}{8\tilde{\omega}_b\tilde{\omega}_c\tilde{\omega}_d(\tilde{\omega}_a+\tilde{\omega}_d)}+\frac{3x_ax_d}{8\tilde{\omega}_b\tilde{\omega}_c\tilde{\omega}_d(\tilde{\omega}_a+2\tilde{\omega}_b+\tilde{\omega}_d)}+\frac{3x_ax_d}{8\tilde{\omega}_b\tilde{\omega}_c\tilde{\omega}_d(\tilde{\omega}_a+2\tilde{\omega}_c+\tilde{\omega}_d)} \\ &-\frac{3x_ax_d}{8\tilde{\omega}_b\tilde{\omega}_c\tilde{\omega}_d(\tilde{\omega}_a+2(\tilde{\omega}_b+\tilde{\omega}_c)+\tilde{\omega}_d)}+\frac{3x_ax_d}{8\tilde{\omega}_b\tilde{\omega}_c\tilde{\omega}_d(\tilde{\omega}_a+3\tilde{\omega}_d)}-\frac{3x_ax_d}{8\tilde{\omega}_b\tilde{\omega}_c\tilde{\omega}_d(\tilde{\omega}_a+2\tilde{\omega}_b+3\tilde{\omega}_d)}-\frac{3x_ax_d}{8\tilde{\omega}_b\tilde{\omega}_c\tilde{\omega}_d(\tilde{\omega}_a+2\tilde{\omega}_c+3\tilde{\omega}_d)} \\ &+\frac{3x_ax_d}{8\tilde{\omega}_b\tilde{\omega}_c\tilde{\omega}_d(\tilde{\omega}_a+2(\tilde{\omega}_b+\tilde{\omega}_c)+3\tilde{\omega}_d)}-\frac{6(\tilde{\omega}_a+2\tilde{\omega}_b+\tilde{\omega}_c+2\tilde{\omega}_d)_ax_b^2x_d}{(\tilde{\omega}_a+2\tilde{\omega}_b+\tilde{\omega}_d)(\tilde{\omega}_a+2(\tilde{\omega}_b+\tilde{\omega}_c)+\tilde{\omega}_d)(\tilde{\omega}_a+2\tilde{\omega}_b+3\tilde{\omega}_d)(\tilde{\omega}_a+2(\tilde{\omega}_b+\tilde{\omega}_c)+3\tilde{\omega}_d)} \\ &-\frac{6(\tilde{\omega}_a+\tilde{\omega}_b+2(\tilde{\omega}_c+\tilde{\omega}_d))x_ax_c^2x_d}{(\tilde{\omega}_a+2\tilde{\omega}_c+\tilde{\omega}_d)(\tilde{\omega}_a+2(\tilde{\omega}_b+\tilde{\omega}_c)+\tilde{\omega}_d)(\tilde{\omega}_a+2\tilde{\omega}_c+3\tilde{\omega}_d)(\tilde{\omega}_a+2(\tilde{\omega}_b+\tilde{\omega}_c)+3\tilde{\omega}_d)}-\frac{x_ax_b^2x_c^2x_d^3}{\tilde{\omega}_a+2(\tilde{\omega}_b+\tilde{\omega}_c)+3\tilde{\omega}_d} \\ &-\frac{3x_ax_b^2x_c^2x_d}{(\tilde{\omega}_a+2(\tilde{\omega}_b+\tilde{\omega}_c)+\tilde{\omega}_d)(\tilde{\omega}_a+2(\tilde{\omega}_b+\tilde{\omega}_c)+3\tilde{\omega}_d)}-\frac{2(\tilde{\omega}_d+\tilde{\omega}_b+\tilde{\omega}_c+3\tilde{\omega}_d)x_ax_d^3}{(\tilde{\omega}_d+3\tilde{\omega}_d)(\tilde{\omega}_a+2\tilde{\omega}_b+3\tilde{\omega}_d)(\tilde{\omega}_a+2\tilde{\omega}_c+3\tilde{\omega}_d)(\tilde{\omega}_a+2(\tilde{\omega}_b+\tilde{\omega}_c)+3\tilde{\omega}_d)} \\ &-\frac{x_ax_b^2x_d^3}{(\tilde{\omega}_a+2\tilde{\omega}_b+3\tilde{\omega}_d)(\tilde{\omega}_a+2(\tilde{\omega}_b+\tilde{\omega}_c)+3\tilde{\omega}_d)}-\frac{x_ax_c^2x_d^3}{(\tilde{\omega}_a+2\tilde{\omega}_c+3\tilde{\omega}_d)(\tilde{\omega}_a+2(\tilde{\omega}_b+\tilde{\omega}_c)+3\tilde{\omega}_d)}\Bigg] \end{aligned}$
D_{14}	$\begin{aligned} &\frac{8!}{5!}\Bigg[\frac{-30x_ax_bx_cx_d}{(\tilde{\omega}_a+\tilde{\omega}_b+\tilde{\omega}_c+\tilde{\omega}_d)(\tilde{\omega}_a+\tilde{\omega}_b+\tilde{\omega}_c+3\tilde{\omega}_d)(\tilde{\omega}_a+\tilde{\omega}_b+\tilde{\omega}_c+5\tilde{\omega}_d)}-\frac{10x_ax_bx_cx_d^3}{(\tilde{\omega}_a+\tilde{\omega}_b+\tilde{\omega}_c+3\tilde{\omega}_d)(\tilde{\omega}_a+\tilde{\omega}_b+\tilde{\omega}_c+5\tilde{\omega}_d)} \\ &-\frac{x_ax_bx_cx_d^5}{\tilde{\omega}_a+\tilde{\omega}_b+\tilde{\omega}_c+5\tilde{\omega}_d}\Bigg] \end{aligned}$

Table 3. *Cont.*

	Expression for D_i Coefficients
D_{15}	$\frac{8!}{3!3!}\left[\frac{-18(\tilde{\omega}_a+\tilde{\omega}_b+2(\tilde{\omega}_c+\tilde{\omega}_d))x_ax_bx_cx_d}{(\tilde{\omega}_a+\tilde{\omega}_b+\tilde{\omega}_c+\tilde{\omega}_d)(\tilde{\omega}_a+\tilde{\omega}_b+3\tilde{\omega}_c+\tilde{\omega}_d)(\tilde{\omega}_a+\tilde{\omega}_b+\tilde{\omega}_c+3\tilde{\omega}_d)(\tilde{\omega}_a+\tilde{\omega}_b+3(\tilde{\omega}_c+\tilde{\omega}_d))}-\frac{x_ax_bx_c^3x_d^3}{\tilde{\omega}_a+\tilde{\omega}_b+3(\tilde{\omega}_c+\tilde{\omega}_d)}-\frac{3x_ax_bx_c^3x_d}{(\tilde{\omega}_a+\tilde{\omega}_b+3\tilde{\omega}_c+\tilde{\omega}_d)(\tilde{\omega}_a+\tilde{\omega}_b+3(\tilde{\omega}_c+\tilde{\omega}_d))}-\frac{3x_ax_bx_cx_d^3}{(\tilde{\omega}_a+\tilde{\omega}_b+\tilde{\omega}_c+3\tilde{\omega}_d)(\tilde{\omega}_a+\tilde{\omega}_b+3(\tilde{\omega}_c+\tilde{\omega}_d))}\right]$
D_{16}	$\frac{8!}{2!2!2!}\left[\frac{-x_ax_b}{8\tilde{\omega}_c\tilde{\omega}_d(\tilde{\omega}_a+\tilde{\omega}_b+2(\tilde{\omega}_c+\tilde{\omega}_d))\tilde{\omega}_e}+\frac{x_ax_b}{8\tilde{\omega}_c\tilde{\omega}_d\tilde{\omega}_e(\tilde{\omega}_a+\tilde{\omega}_b+2\tilde{\omega}_e)}-\frac{x_ax_b}{8\tilde{\omega}_c\tilde{\omega}_d\tilde{\omega}_e(\tilde{\omega}_a+\tilde{\omega}_b+2(\tilde{\omega}_c+\tilde{\omega}_e))}-\frac{x_ax_b}{8\tilde{\omega}_c\tilde{\omega}_d\tilde{\omega}_e(\tilde{\omega}_a+\tilde{\omega}_b+2(\tilde{\omega}_d+\tilde{\omega}_e))}+\frac{x_ax_b}{8\tilde{\omega}_c\tilde{\omega}_d\tilde{\omega}_e(\tilde{\omega}_a+\tilde{\omega}_b+2(\tilde{\omega}_c+\tilde{\omega}_d+\tilde{\omega}_e))}-\frac{x_ax_bx_c^2x_d^2x_e^2}{\tilde{\omega}_a+\tilde{\omega}_b+2(\tilde{\omega}_c+\tilde{\omega}_d+\tilde{\omega}_e)}-\frac{2x_ax_bx_c^2(\tilde{\omega}_a+\tilde{\omega}_b+2\tilde{\omega}_c+\tilde{\omega}_d+\tilde{\omega}_e)}{(\tilde{\omega}_a+\tilde{\omega}_b+2\tilde{\omega}_c)(\tilde{\omega}_a+\tilde{\omega}_b+2\tilde{\omega}_c+2\tilde{\omega}_d)(\tilde{\omega}_a+\tilde{\omega}_b+2\tilde{\omega}_c+2\tilde{\omega}_e)(\tilde{\omega}_a+\tilde{\omega}_b+2\tilde{\omega}_c+2\tilde{\omega}_d+2\tilde{\omega}_e)}+\frac{x_ax_b}{8\tilde{\omega}_c(\tilde{\omega}_a+\tilde{\omega}_b+2\tilde{\omega}_c)\tilde{\omega}_d\tilde{\omega}_e}-\frac{2x_ax_bx_d^2(\tilde{\omega}_a+\tilde{\omega}_b+\tilde{\omega}_c+2\tilde{\omega}_d+\tilde{\omega}_e)}{(\tilde{\omega}_a+\tilde{\omega}_b+2\tilde{\omega}_d)(\tilde{\omega}_a+\tilde{\omega}_b+2\tilde{\omega}_c+2\tilde{\omega}_d)(\tilde{\omega}_a+\tilde{\omega}_b+2\tilde{\omega}_d+2\tilde{\omega}_e)(\tilde{\omega}_a+\tilde{\omega}_b+2\tilde{\omega}_c+2\tilde{\omega}_d+2\tilde{\omega}_e)}+\frac{x_ax_b}{8\tilde{\omega}_c\tilde{\omega}_d(\tilde{\omega}_a+\tilde{\omega}_b+2\tilde{\omega}_d)\tilde{\omega}_e}-\frac{2x_ax_bx_e^2(\tilde{\omega}_a+\tilde{\omega}_b+\tilde{\omega}_c+\tilde{\omega}_d+2\tilde{\omega}_e)}{(\tilde{\omega}_a+\tilde{\omega}_b+2\tilde{\omega}_e)(\tilde{\omega}_a+\tilde{\omega}_b+2\tilde{\omega}_c+2\tilde{\omega}_e)(\tilde{\omega}_a+\tilde{\omega}_b+2\tilde{\omega}_d+2\tilde{\omega}_e)(\tilde{\omega}_a+\tilde{\omega}_b+2\tilde{\omega}_c+2\tilde{\omega}_d+2\tilde{\omega}_e)}-\frac{x_ax_b}{8(\tilde{\omega}_a+\tilde{\omega}_b)\tilde{\omega}_c\tilde{\omega}_d\tilde{\omega}_e}-\frac{x_ax_bx_c^2x_d^2}{(\tilde{\omega}_a+\tilde{\omega}_b+2\tilde{\omega}_c+2\tilde{\omega}_d)(\tilde{\omega}_a+\tilde{\omega}_b+2\tilde{\omega}_c+2\tilde{\omega}_d+2\tilde{\omega}_e)}-\frac{x_ax_bx_d^2x_e^2}{(\tilde{\omega}_a+\tilde{\omega}_b+2\tilde{\omega}_d+2\tilde{\omega}_e)(\tilde{\omega}_a+\tilde{\omega}_b+2\tilde{\omega}_c+2\tilde{\omega}_d+2\tilde{\omega}_e)}-\frac{x_ax_bx_c^2x_e^2}{(\tilde{\omega}_a+\tilde{\omega}_b+2\tilde{\omega}_c+2\tilde{\omega}_e)(\tilde{\omega}_a+\tilde{\omega}_b+2\tilde{\omega}_c+2\tilde{\omega}_d+2\tilde{\omega}_e)}\right]$
D_{17}	$\frac{8!}{2!3!}\left[\frac{-6x_ax_bx_cx_e(\tilde{\omega}_a+\tilde{\omega}_b+\tilde{\omega}_c+\tilde{\omega}_d+2\tilde{\omega}_e)}{(\tilde{\omega}_a+\tilde{\omega}_b+\tilde{\omega}_c+\tilde{\omega}_e)(\tilde{\omega}_a+\tilde{\omega}_b+\tilde{\omega}_c+2\tilde{\omega}_d+\tilde{\omega}_e)(\tilde{\omega}_a+\tilde{\omega}_b+\tilde{\omega}_c+3\tilde{\omega}_e)(\tilde{\omega}_a+\tilde{\omega}_b+\tilde{\omega}_c+2\tilde{\omega}_d+3\tilde{\omega}_e)}-\frac{3x_ax_bx_cx_d^2x_e}{(\tilde{\omega}_a+\tilde{\omega}_b+\tilde{\omega}_c+2\tilde{\omega}_d+\tilde{\omega}_e)(\tilde{\omega}_a+\tilde{\omega}_b+\tilde{\omega}_c+2\tilde{\omega}_d+3\tilde{\omega}_e)}-\frac{x_ax_bx_cx_e^3}{(\tilde{\omega}_a+\tilde{\omega}_b+\tilde{\omega}_c+3\tilde{\omega}_e)(\tilde{\omega}_a+\tilde{\omega}_b+\tilde{\omega}_c+2\tilde{\omega}_d+3\tilde{\omega}_e)}-\frac{x_ax_bx_cx_d^2x_e^3}{\tilde{\omega}_a+\tilde{\omega}_b+\tilde{\omega}_c+2\tilde{\omega}_d+3\tilde{\omega}_e}\right]$
D_{18}	$\frac{8!}{4!}\left[\frac{-6x_ax_bx_cx_d}{(\tilde{\omega}_a+\tilde{\omega}_b+\tilde{\omega}_c+\tilde{\omega}_d)(\tilde{\omega}_a+\tilde{\omega}_b+\tilde{\omega}_c+\tilde{\omega}_d+2\tilde{\omega}_e)(\tilde{\omega}_a+\tilde{\omega}_b+\tilde{\omega}_c+\tilde{\omega}_d+4\tilde{\omega}_e)}-\frac{x_ax_bx_cx_dx_e^4}{\tilde{\omega}_a+\tilde{\omega}_b+\tilde{\omega}_c+\tilde{\omega}_d+4\tilde{\omega}_e}-\frac{6x_ax_bx_cx_dx_e^2}{(\tilde{\omega}_a+\tilde{\omega}_b+\tilde{\omega}_c+\tilde{\omega}_d+2\tilde{\omega}_e)(\tilde{\omega}_a+\tilde{\omega}_b+\tilde{\omega}_c+\tilde{\omega}_d+4\tilde{\omega}_e)}\right]$
D_{19}	$\frac{8!}{3!}\left[\frac{-3x_ax_bx_cx_dx_ex_f}{\left(\tilde{\omega}_a+\tilde{\omega}_b+\tilde{\omega}_c+\tilde{\omega}_d+\tilde{\omega}_e+\tilde{\omega}_f\right)\left(\tilde{\omega}_a+\tilde{\omega}_b+\tilde{\omega}_c+\tilde{\omega}_d+\tilde{\omega}_e+3\tilde{\omega}_f\right)}-\frac{x_ax_bx_cx_dx_ex_f^3}{\tilde{\omega}_a+\tilde{\omega}_b+\tilde{\omega}_c+\tilde{\omega}_d+\tilde{\omega}_e+3\tilde{\omega}_f}\right]$
D_{20}	$\frac{8!}{2!2!}\left[\frac{-2\left(\tilde{\omega}_a+\tilde{\omega}_b+\tilde{\omega}_c+\tilde{\omega}_d+\tilde{\omega}_e+\tilde{\omega}_f\right)x_ax_bx_cx_d}{(\tilde{\omega}_a+\tilde{\omega}_b+\tilde{\omega}_c+\tilde{\omega}_d)(\tilde{\omega}_a+\tilde{\omega}_b+\tilde{\omega}_c+\tilde{\omega}_d+2\tilde{\omega}_e)\left(\tilde{\omega}_a+\tilde{\omega}_b+\tilde{\omega}_c+\tilde{\omega}_d+2\tilde{\omega}_f\right)\left(\tilde{\omega}_a+\tilde{\omega}_b+\tilde{\omega}_c+\tilde{\omega}_d+2\left(\tilde{\omega}_e+\tilde{\omega}_f\right)\right)}-\frac{x_ax_bx_cx_dx_e^2}{(\tilde{\omega}_a+\tilde{\omega}_b+\tilde{\omega}_c+\tilde{\omega}_d+2\tilde{\omega}_e)\left(\tilde{\omega}_a+\tilde{\omega}_b+\tilde{\omega}_c+\tilde{\omega}_d+2\left(\tilde{\omega}_e+\tilde{\omega}_f\right)\right)}-\frac{x_ax_bx_cx_dx_f^2}{\left(\tilde{\omega}_a+\tilde{\omega}_b+\tilde{\omega}_c+\tilde{\omega}_d+2\tilde{\omega}_f\right)\left(\tilde{\omega}_a+\tilde{\omega}_b+\tilde{\omega}_c+\tilde{\omega}_d+2\left(\tilde{\omega}_e+\tilde{\omega}_f\right)\right)}-\frac{x_ax_bx_cx_dx_e^2x_f^2}{\left(\tilde{\omega}_a+\tilde{\omega}_b+\tilde{\omega}_c+\tilde{\omega}_d+2\left(\tilde{\omega}_e+\tilde{\omega}_f\right)\right)}\right]$
D_{21}	$\frac{8!}{2!}\left[\frac{-x_ax_bx_cx_dx_ex_f}{\left(\tilde{\omega}_a+\tilde{\omega}_b+\tilde{\omega}_c+\tilde{\omega}_d+\tilde{\omega}_e+\tilde{\omega}_f\right)\left(\tilde{\omega}_a+\tilde{\omega}_b+\tilde{\omega}_c+\tilde{\omega}_d+\tilde{\omega}_e+\tilde{\omega}_f+2\tilde{\omega}_g\right)}-\frac{x_ax_bx_cx_dx_ex_fx_g^2}{\tilde{\omega}_a+\tilde{\omega}_b+\tilde{\omega}_c+\tilde{\omega}_d+\tilde{\omega}_e+\tilde{\omega}_f+2\tilde{\omega}_g}\right]$
D_{22}	$\frac{-8!\ x_ax_bx_cx_dx_ex_fx_gx_h}{\tilde{\omega}_a+\tilde{\omega}_b+\tilde{\omega}_c+\tilde{\omega}_d+\tilde{\omega}_e+\tilde{\omega}_f+\tilde{\omega}_g+\tilde{\omega}_h}$

Now, for finding the complexity, we represent the N oscillator wavefunction in the following way:

$$\psi^{s=0}_{0,0,\cdots 0}(\tilde{x}_0,\cdots,\tilde{x}_{N-1}) \approx \exp\left[-\frac{1}{2}v_a A^{s=1}_{ab} v_b\right] \tag{59}$$

Once again, we have to choose a particular basis. Now, there are many choices for bases, but we consider the choice of bases in the following way:

$$\begin{aligned}\vec{v} = \{&\tilde{x}_0,\cdots\tilde{x}_{N-1},\tilde{x}_0^2,\cdots,\tilde{x}_{N-1}^2,\cdots,\tilde{x}_a\tilde{x}_b,\cdots,\tilde{x}_0^3,\cdots,\tilde{x}_{N-1}^3,\cdots,\tilde{x}_a\tilde{x}_b\tilde{x}_c,\cdots,\tilde{x}_0^4,\cdots,\tilde{x}_{N-1}^4,\cdots,\\ &\tilde{x}_a\tilde{x}_b\tilde{x}_c\tilde{x}_d,\cdots,\tilde{x}_a^2\tilde{x}_b^2\cdots,\tilde{x}_0^5,\cdots,\tilde{x}_{N-1}^5,\tilde{x}_0^6,\cdots,\tilde{x}_{N-1}^6,\cdots,\tilde{x}_a\tilde{x}_b\tilde{x}_c\tilde{x}_d\tilde{x}_e\tilde{x}_f,\cdots,\tilde{x}_a^3\tilde{x}_b^3,\cdots,\\ &\tilde{x}_a\tilde{x}_b\tilde{x}_c\tilde{x}_d\tilde{x}_e\tilde{x}_f\tilde{x}_g\tilde{x}_h,\cdots,\tilde{x}_a^{1/2}\tilde{x}_b\tilde{x}_c^{1/2},\cdots\}\end{aligned} \tag{60}$$

Here, a, b, c, d, e, f, g, and h are indices that can have any value in the range from 0 to $N-1$ and must not be equal to each other. In the last term in $\vec{v}$, we mention a term that can be used to kill off-diagonal entries just as we did for the two-oscillator case. There will be many more terms like this on this basis. Expressing them explicitly is not necessary for our current work, and so we have not mentioned them.

Now, we will represent the matrix $A(s=1)$ for N oscillators in a block diagonal fashion. In this format, the matrix will look like this:

$$A^{s=1}_{ab} = \begin{pmatrix} A_1 & 0 \\ 0 & A_2 \end{pmatrix} \tag{61}$$

where A_1 and A_2 are the so-called *unambiguous* and *ambiguous* blocks. Once we fix the target or reference stats, the coefficients in the *unambiguous* blocks are fixed. However, this is not the case for *the ambiguous* block, as it contains numerous parameters which are not fixed beforehand.

In the *unambiguous* block A_1, we have all of the coefficients of terms such as x_a^2 and $x_a x_b$ in Equation (54) multiplied by -2. On the other hand, the coefficients (multiplied by -2) for terms such as

$$x_a^2x_b^2,\, x_a^2x_b^2x_c^2,\, x_ax_bx_cx_d \tag{62}$$

are there on the A_2 block.

To compute the complexity, we choose a particular non-entangled reference state for arbitrary N oscillators:

$$\psi^{s=0}(x_1,x_2,\ldots,x_n) = \mathcal{N}^{s=0}\exp\Big[-\sum_{i=0}^{N-1}\frac{\tilde{\omega}_{ref}}{2}\Big(x_i^2+\lambda_4^0x_i^4+\lambda_6^0x_i^6+\lambda_8^0x_i^8\Big)\Big] \tag{63}$$

which can be represented as follows: S

$$\psi^{s=0}(\tilde{x}_1,\tilde{x}_2,\ldots,\tilde{x}_n) = \mathcal{N}^{s=0}\exp\Big[-\frac{1}{2}\Big(v_aA^{s=0}_{ab}v_b\Big)\Big] \tag{64}$$

where the matrix $A^{s=0}_{ab}$ can be written as in the normal mode basis:

$$A^{s=0}_{ab} = \begin{pmatrix} \tilde{\omega}_{ref}\mathbb{I}_{N\times N} & 0 \\ 0 & A_2^{s=0} \end{pmatrix} \tag{65}$$

Here, $\mathbb{I}_{N\times N}$ is the N dimensional unit matrix. We are assuming that all the natural frequencies are (i.e., for all x_i it is true that $\omega_0 = \tilde{\omega}_{ref}$). However, $A_2^{s=0}$ cannot be represented as easily as the first block because there are many undetermined parameters. Nevertheless, we can choose these parameters in such a way that the $A_2^{s=0}$ block becomes diagonal, just as we did for the two-oscillator case.

The complexity functional depends on the particular cost function that we choose. For the different cost functions mentioned in Equation (5), we find a different expression for the complexity functional. However, we will work with the following cost function for the rest of the paper:

$$\mathcal{F}_\kappa(s) = \sum_I p_I |Y^I|^\kappa \tag{66}$$

With respect to this particular choice for the cost function, the complexity functional becomes

$$\mathcal{C}_\kappa = \int_{s=0}^{1} \mathcal{F}_\kappa \, ds \tag{67}$$

Here, we set all the p_I variables to be one to put all directions in the circuit space on equal footing. Now, if we choose the parameters of $A_2^{s=0}$ such that $A^{s=0}$ is diagonal, then obviously, $A^{s=1}$ and $A^{s=0}$ will commute. If this is the case, then all $\mathcal{C}_\kappa$ can be written in a single equation as mentioned in [18]:

$$\begin{aligned} \mathcal{C}_\kappa &= \mathcal{C}_\kappa^{(1)} + \mathcal{C}_\kappa^{(2)} \\ &= \frac{1}{2^\kappa} \sum_{i=0}^{N-1} \left| \log\left(\frac{\lambda_i^{(1)}}{\tilde{\omega}_{ref}}\right)\right|^\kappa + \mathcal{C}_\kappa^{(2)} \end{aligned} \tag{68}$$

Here, $\lambda_i^{(1)}$ represents the eigenvalues of the unambiguous block of the $A^{s=1}$ matrix and $\mathcal{C}_\kappa^{(1)}$ and $\mathcal{C}_\kappa^{(2)}$ denote the contributions to the complexity functional for the unambiguous and ambiguous blocks, respectively. From here on, we will use the $\mathcal{C}_1$ complexity functional.

Commenting on $\mathcal{C}_1^{(2)}$ and the Ambiguous Block

Here, we comment on the difficulties and issues with defining the ambiguous block A_2, as has also been discussed in [18] for the ϕ^4 interaction theory. One of the reasons for calling the A_2 matrix ambiguous is that there is a lot of arbitrariness in defining this block of the matrix; that is, there are many possible choices for defining the coefficients of the A_2 block, such as some terms which can be defined in the diagonal entries as well as in the off-diagonal entries and several higher-order cross terms, including $\tilde{x}_a\tilde{x}_b\tilde{x}_c\tilde{x}_d\tilde{x}_e\tilde{x}_f\tilde{x}_g\tilde{x}_h$, which can be defined in several forms. One possible solution to this is to try to define the A_2 matrix with the most general entries in which the coefficients are placed among all possible places in the A_2 block so that the determinant of the matrix should be positive definite. For the ambiguous block, the complexity $\mathcal{C}_1^{(2)}$ can be defined with eigenvalues $\lambda_j^{(2)}$, and the total complexity will be given by Equation (68). However, due to the great arbitrariness or ambiguities in defining the A_2 block, we cannot easily define the complexity $\mathcal{C}_1^{(2)}$. One could think of using the renormalization approach to find the general form of $\mathcal{C}_1^{(2)}$, as was performed in [18] for the ϕ^4 interaction, but the theory in our case is non-renormalizable beyond the ϕ^4 term, so it is also not possible to use the standard renormalization procedure for our case.

Here, we calculate the complexity of the unambiguous block, which is easy to analyze. We use this expression to evaluate the complexity functional in the next section.

6. Numerical Evaluation of the Complexity Functional

Up to this point, we have always set the value of $M = 1$ in the two-oscillator Hamiltonian and N oscillator Hamiltonian. However, for a generic analysis and also for the continuum limit, we need to put the M factor back in H. If we reinstate the factor of M in the Hamiltonian, we obtain the following expression for the Hamiltonian:

$$H = \frac{1}{M}\sum_{\vec{n}}\left\{\frac{P(\vec{n})^2}{2} + \frac{1}{2}M^2\left[\omega^2 X(\vec{n})^2 + \Omega^2\sum_i (X(\vec{n}) - X(\vec{n}-\hat{x}_i))^2 + 2\left\{\lambda_4 X(\vec{n})^4 + \lambda_6 X(\vec{n})^6 + \lambda_8 X(\vec{n})^8\right\}\right]\right\} \quad (69)$$

The overall factor in front of the Hamiltonian does not have any effect on the structure of the eigenfunctions of this Hamiltonian. However, some of the factors need to be rescaled in presence of the M factor, which are given below:

$$\omega \to \frac{\omega}{\delta} \quad \Omega \to \frac{\Omega}{\delta} \quad \lambda_4 \to \frac{\lambda_4}{\delta^2} \quad \lambda_6 \to \frac{\lambda_6}{\delta^2} \quad \lambda_8 \to \frac{\lambda_8}{\delta^2} \quad \tilde{\omega}_{ref} \to \frac{\tilde{\omega}_{ref}}{\delta} \quad \lambda_4^0 \to \frac{\lambda_4^0}{\delta}$$

$$\lambda_6^0 \to \frac{\lambda_6^0}{\delta} \quad \lambda_8^0 \to \frac{\lambda_8^0}{\delta}$$

Here, we would like to mention again that $M = \frac{1}{\delta}$. Using these rescaled parameters, we assume that the general form of the eigenvalues of A_1 represent the N oscillator Hamiltonian with first-order perturbative correction:

$$\begin{aligned} \Lambda_{i_k} &= \Lambda_{4_{i_k}} + \lambda_6 f_{i_k}\left(N, \tilde{\omega}_{i_p}\right) + \lambda_8 g_{i_k}\left(N, \tilde{\omega}_{i_p}\right), \quad N\text{: Even} \\ &= \Lambda_{4_{i_k}} + \lambda_6 f'_{i_k}\left(N, \tilde{\omega}_{i_p}\right) + \lambda_8 g'_{i_k}\left(N, \tilde{\omega}_{i_p}\right), \quad N\text{: Odd} \end{aligned} \quad (70)$$

where N denotes the number of lattice points in each spatial dimension and the i_k indices run from 0 to $N-1$ for each dimension. Then, the $d-1$ dimensional spatial volume becomes $L^{d-1} = (N\delta)^{d-1}$.

Here, $\Lambda_{4_{i_k}}$ is the contribution from the ϕ^4 interaction, and f, g, f', and g' denote the additional contributions to the eigenvalues in the presence of ϕ^6 and ϕ^8 interaction. The form of $\Lambda_{4_{i_k}}$, as mentioned in [18], is

$$\begin{aligned} \Lambda_{4_{i_k}} &= \frac{\tilde{\omega}_{i_k}}{\delta} + \frac{3\lambda_4}{2N}\left(\frac{2}{\tilde{\omega}_{i_k}(\tilde{\omega}_{i_k} + \tilde{\omega}_{N-i_k})} + \frac{2}{\tilde{\omega}_{i_k}(\tilde{\omega}_{i_k} + \tilde{\omega}_{\frac{N}{2}-i_k})}\right), \quad N\text{: Even} \\ &= \frac{\tilde{\omega}_{i_k}}{\delta} + \frac{3\lambda_4}{2N}\left(\frac{2}{\tilde{\omega}_{i_k}(\tilde{\omega}_{i_k} + \tilde{\omega}_{N-i_k})}\right), \quad N\text{: Odd} \end{aligned} \quad (71)$$

These additional terms f, g, f', and g' cannot be calculated analytically. Therefore, we resort to numerical methods to calculate these.

The work carried out in [18] had a proper analytical expression for the eigenvalues, which made it easier to study the RG flows. However, when we consider higher-order interactions such as ϕ^6 and ϕ^8, such analytic expressions for the RG flows and complexity cannot be found. This makes it difficult for us to study the RG flows and MERA and is beyond the scope of our model. Instead, we will focus only on complexity. The eigenvalues we obtained were small corrections to the one obtained in [18], so the connection they made will not be affected by the addition of higher interacting terms. Now, we will resort to numerical methods in the next section.

Numerical Analysis of the Complexity Functional

We will calculate the complexity for the unambiguous block first for an increasing number of oscillators. We have found the wavefunction for the Hamiltonian in Equation (47). As we reinserted the M term, we will just update the complexity using the rescaled parameters mentioned in the previous subsection. We set the following relevant parameter values:

$$\lambda_4 = 0.5 \qquad \lambda_6 = 0.2 \qquad \lambda_8 = 0.001 \qquad \omega_0 = m = 4.0$$
$$\Omega = 0.25 \qquad L = 200 \qquad \tilde{\omega}_{ref} = 1.6$$

where L is the length of the periodic chain. We chose N and δ so that $N\delta = L$ was always satisfied. We will use the $\mathcal{C}_1^{(1)}$ functional for the unambiguous block.

Case I: Increasing the Interactions

In Figure 2, we have plotted numerically the behavior of the complexity of the unambiguous block as a function of N, which is the number of oscillators in $d = 2$ dimensions. In Figure 2a, we have two complexities, where the points in blue represent the complexity of the theory, which has no interaction term, and this complexity is due to the self-interaction between pairs of oscillators. We also see the points in orange and light orange, which represent the complexity of the theory with $\lambda_4\phi^4$ interaction. We notice that there is a bump initially in the graph for small N values, but in Figure 2a–c, we can observe that the values of the complexity with the free theory and the complexity with interactions became the same as we increased the value of N. We see that $\mathcal{C}_1^{(1)}$ grew linearly with increasing N values, and the contributions to $\mathcal{C}_1^{(1)}$ due to even interaction terms became negligible, while the behavior of the complexity for the unambiguous block would be same as if we were dealing only with the free theory. In Figure 2d, we have plotted $\mathcal{C}_1^{(1)}$ for N being an odd number of oscillators for even interactions of $\lambda_4\phi^4 + \lambda_6\phi^6 + \lambda_8\phi^8$, and we see that the initial values of the complexity increased as we included higher-order terms in the theory, but when we increased N, the contribution from these perturbative terms died out, and the graph followed a ϕ^2 linear pattern of $\mathcal{C}_1^{(1)}$.

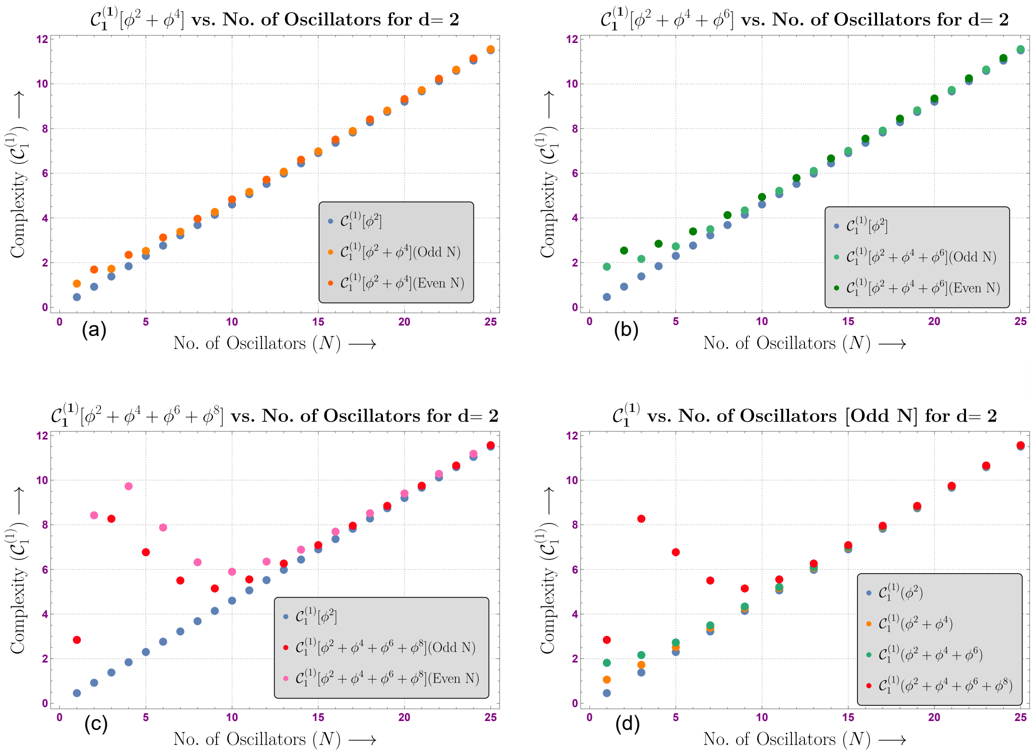

Figure 2. Plot: (**a**–**c**) represents the complexity $\mathcal{C}_1^{(1)}$ (from the unambiguous block) vs. the number of oscillators (N) for $d = 2$ dimensions with different interactions. In plot (**d**), complexity $\mathcal{C}_1^{(1)}$ vs. an odd number of oscillators (even resembling the same pattern) from all the interactions are placed together in the same plot, showing the contribution from each interaction.

Case II: Increasing the Dimension

In Figure 3, we show six different plots. In the first two plots, the complexity for the unambiguous block (up to ϕ^4 interaction) is plotted with respect to the number of oscillators in dimensions $d = 3$ and 4. Here, we notice that as we increased the dimensions, the contribution to $\mathcal{C}_1^{(1)}$ due to the interaction term increased, and we saw a similar pattern as we included other higher-order even terms (i.e, the third and fourth graphs have $(\lambda_4\phi^4 + \lambda_6\phi^6)$ interactions, and the fifth and sixth graphs contain $(\lambda_4\phi^4 + \lambda_6\phi^6 + \lambda_8\phi^8)$ interactions). However, in higher dimensions, the contributions of these interactions to the complexity $\mathcal{C}_1^{(1)}$ also became negligible when we increased the value of N, and the behavior of this complexity became similar to the case where we had only the ϕ^2 term and it grew linearly.

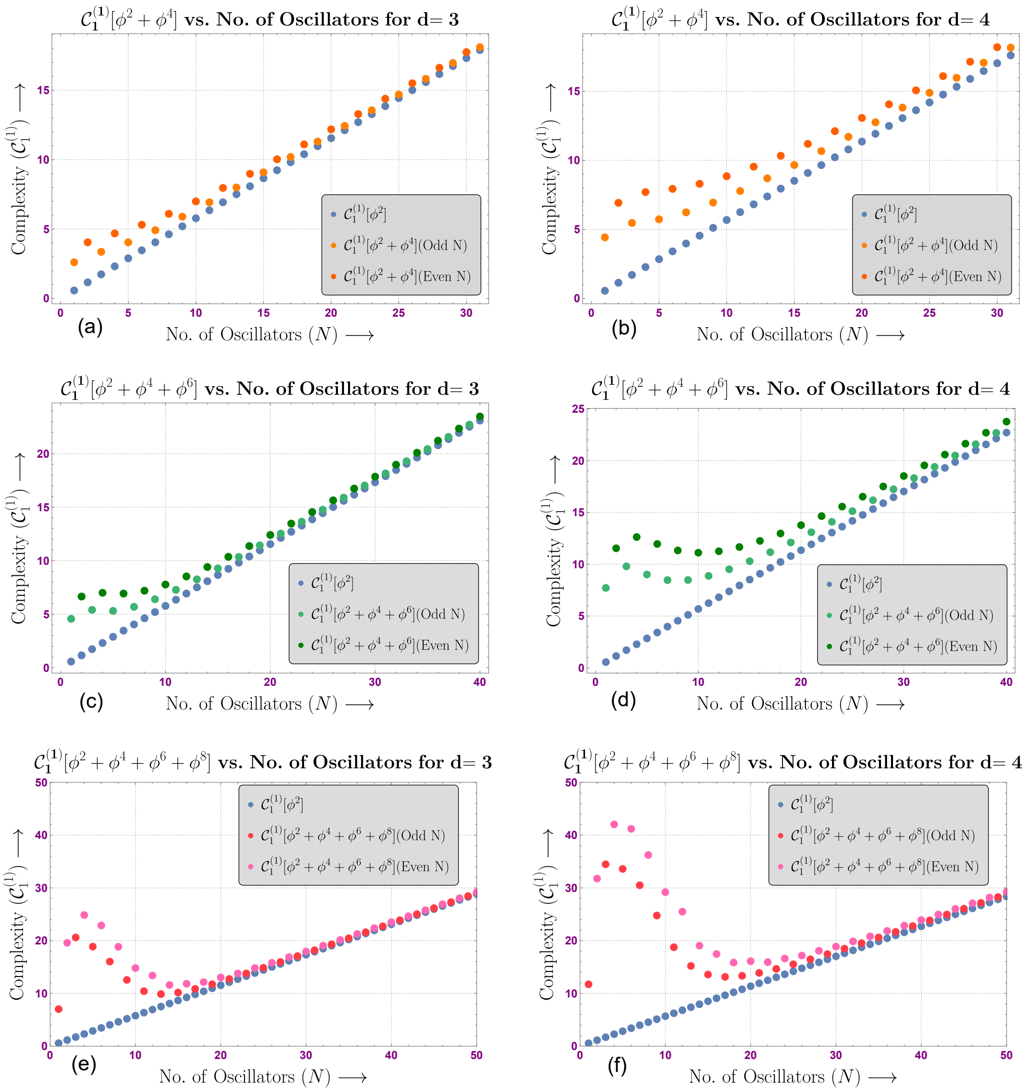

Figure 3. Plot of complexity $\mathcal{C}_1^{(1)}$ vs. number of oscillators in $d = 3$ and $d = 4$, respectively, is shown in (**a**–**f**) for $(\lambda_2\,\phi^2 + \lambda_4\,\phi^4 + \lambda_6\,\phi^6 + \lambda_8\,\phi^8)$.

Case III: $\mathcal{C}_1^{(1)}$ vs. ω_0

In Figure 4 , we have plotted the variation in the complexity $\mathcal{C}_1^{(1)}$ versus ω_0 for a particular value of oscillators $N = 15$, and we also show the variation in the same plot for different dimensions $(d = 2, 3, 4)$. As we increased the number of dimensions, the complexity of the unambiguous block $\mathcal{C}_1^{(1)}$ increased, and in a particular dimension, the complexity value increased as we increased the number of interactions, which was noticeable for low values of ω_0. However, as we increased the value of ω_0, the behavior became similar to the free scalar theory.

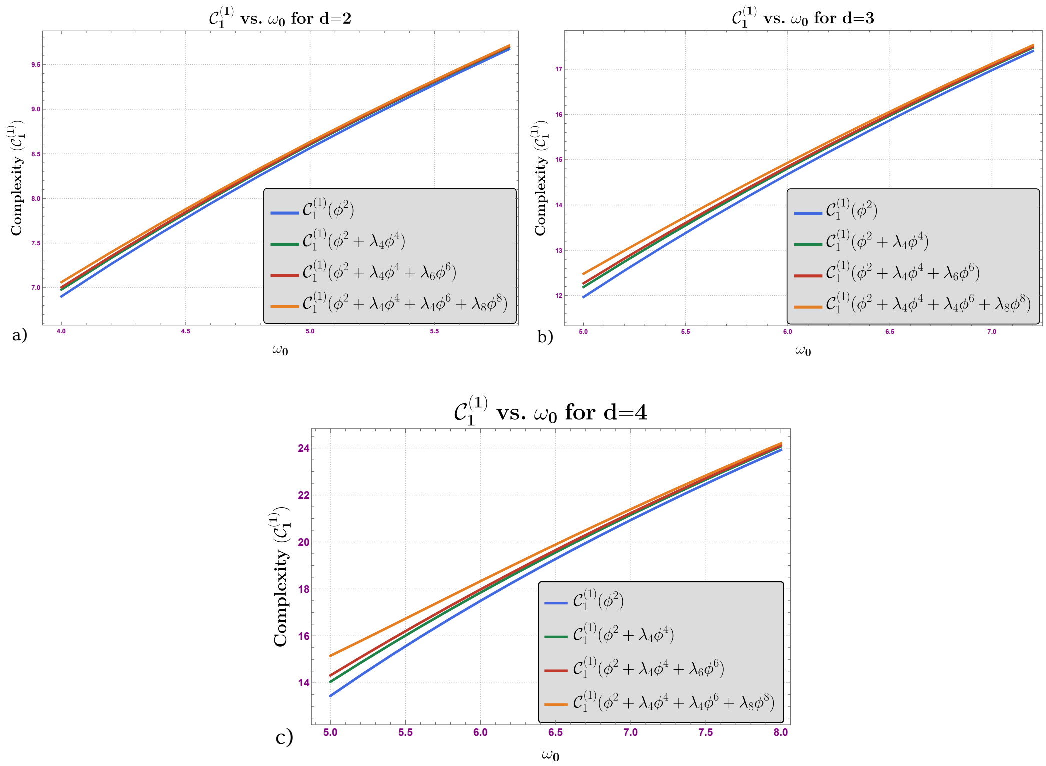

Figure 4. Plot of complexity $\mathcal{C}_1^{(1)}$ vs. ω_0 (**a**) for $d=2$, (**b**) for $d=3$, and (**c**) for $d=4$.

Case IV: Fractional Change in $\mathcal{C}_1^{(1)}$

We define the fractional change in complexity $\mathcal{C}_1$ for a particular N value as

$$\frac{\mathcal{C}_1(N+2)-\mathcal{C}_1(N)}{\mathcal{C}_1(N)}$$

Here, we have an increment of two in the definition because odd and even branches of N can possibly show different behavior, as was the case for the complexity.

For small values of N, the even and odd complexities were different from each other. This is directly related to the fact that one can distinguish the system with an even or odd number of oscillators, but as we went for a large number of oscillators or in the continuum limit, the distinction between the even and odd numbers of oscillators faded away. In Figure 5, we have plotted the complexity of the unambiguous block, and we find that, initially, the fractional change in complexity was large for small N values, but it decreased continuously as we moved toward a large number of oscillators.

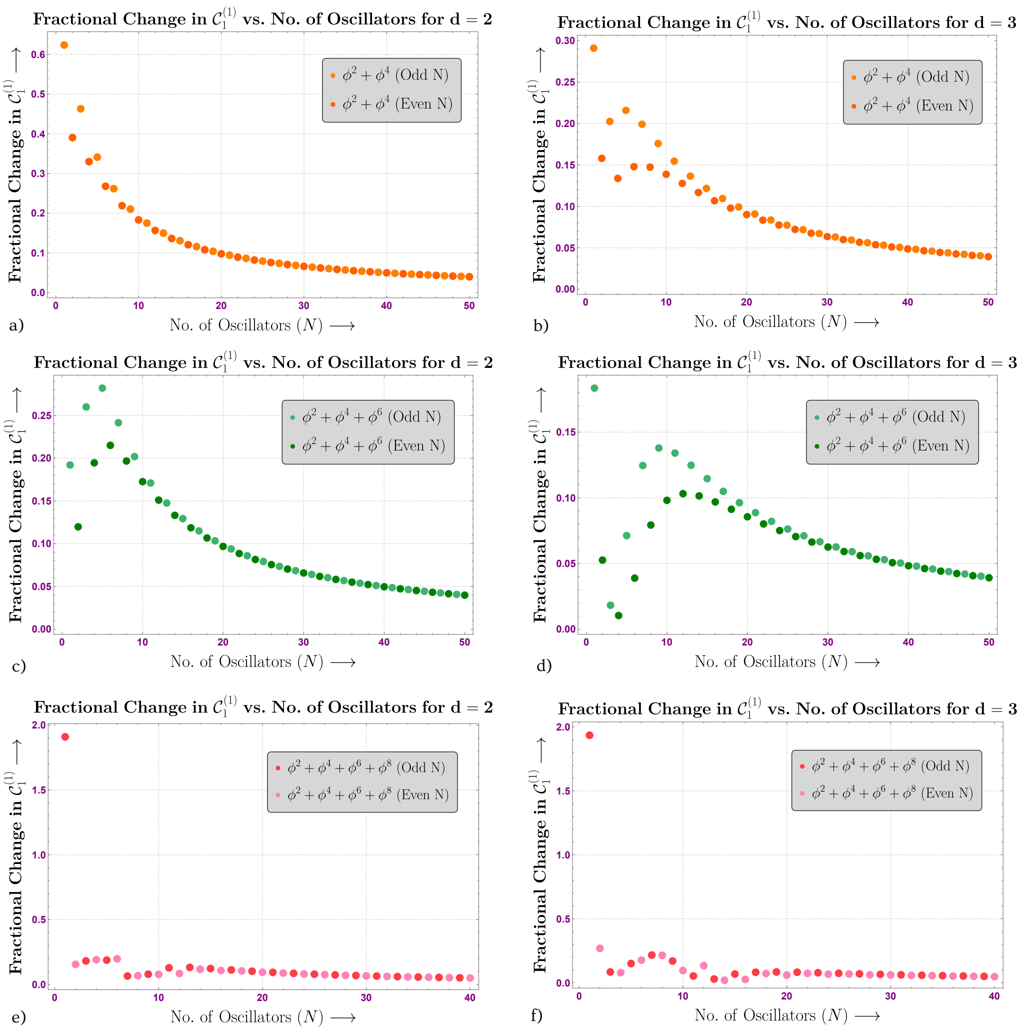

Figure 5. The Plot of fractional change in complexity vs. number of oscillators.

7. Conclusions and Future Prospects

This work studied the circuit complexity for weakly interacting scalar field theory with ϕ^4, ϕ^6, and ϕ^8 Wilsonian operators coupled via λ_4, λ_6, and λ_8 to a free scalar field theory, respectively. The values of the coupling constants were chosen in the framework of an EEFT such that the perturbation analysis was valid. The reference state was an unentangled, nearly Gaussian state, and the target state was an entangled, nearly Gaussian state which was calculated using a first-order perturbation theory. First, we worked with the case of two oscillators, where the unitary evolution $\mathbb{U}$, which took us from the reference state to the target state, was parameterized using the AdS parameters. With this, we calculated the line element and found the complexity functional by imposing the appropriate boundary conditions. Then, we proceeded to the N oscillator case. Here, the circuit complexity depended on the ratio of the eigenvalues of the target to the reference states of the N oscillators. Since we could not observe any analytical expression of the eigenvalues of the target state of the N oscillators, we resorted to numerical analysis. The target matrix for N oscillators had a part where the bases could be uniquely determined (unambiguous part) and another part where the bases could not be determined (ambiguous part). The contribution to the total complexity came from the ambiguous as well as the unambiguous parts. In our work, we focused mainly on the computation of the complexity for the unambiguous part, denoted by the A_2 matrix. The following are the results that we observed:

1. From our numerical analysis, the QCC with $\kappa = 1$ for the free field theory increased linearly with the number of oscillators. As we included the higher even Wilsonian terms, the growth of the complexity (contribution from the unambiguous part) was no longer linear for a small number of oscillators. For the large N limit, the contribution to the complexity from the interacting part vanished, and the linearity was restored.
2. From the graph of complexity vs. ω_0, we see that upon fixing the dimensions and the number of oscillators, the complexity from the unambiguous part increased with an increasing value for ω_0.
3. Another pattern inferred from our analysis is that as the dimension increases, the contribution to $\mathcal{C}_1^{(1)}$ due to the interaction term increases for a fixed number of oscillators. We observed this pattern using degenerate frequencies for higher dimensions. One would expect a similar pattern, even if the frequencies were non-degenerate.

In [18], the eigenvalues had a proper analytical expression, which makes it easier to study RG flows. On the other hand, after adding higher-order corrections, there is no analytical expression of the eigenvalues. This makes it very challenging to study the RG and MERA connection. The eigenvalues we obtained were small corrections to the one obtained in [18], so the connection they made would not be affected by the addition of higher interacting terms. In upcoming works, we will address this issue.

In our analysis, we used $\kappa = 1$ in our complexity functional $\mathcal{C}_\kappa$, but there are other different and useful kinds of measures that one can explore to gain new insights into circuit complexity.

Our approach to computing complexity is based on Nielsen's geometric approach, which suffers from ambiguity in choosing the elementary quantum gates and states. Recent works have attempted to develop a new notion of complexity that is independent of these choices. As for our future goals, we have in mind the following:

- We can calculate the circuit complexity for odd Wilsonian terms in the effective theory, such as ϕ^3, ϕ^4, and ϕ^7. We can further generalize the study by adding both even and odd interaction terms together.
- We can study the behavior of circuit complexity in a similar theory when there is a quantum quench in the interaction and mass. We have already performed this for a ϕ^4 interacting theory [119].
- We can further analyze circuit complexity in fermionic field theories and gauge theories.
- We can explore this problem in the context of the Krylov complexity [95,103,120], which is currently a melting pot in this research area.
- We can compare the Krylov complexity and circuit complexity for such theories to know which is a better measure of information for such cases.

Author Contributions: Conceptualization, S.C.; Methodology, S.C., S.M., N.P., A.R., S.S. and S.S.S.; Software, K.A., S.K., S.M., N.P., A.R., S.S., P.S. and S.S.S.; Validation, S.C.; Formal analysis, K.A., S.C., S.K., S.M., N.P., A.R., S.S., P.S. and S.S.S.; Investigation, S.C.; Writing—original draft, K.A., S.C., S.K., S.M., N.P. and A.R.; Writing—review & editing, S.C.; Supervision, S.C. All authors have read and agreed to the published version of the manuscript.

Funding: This research received no external funding.

Institutional Review Board Statement: Not applicable.

Informed Consent Statement: Not applicable.

Data Availability Statement: Not applicable.

Acknowledgments: S.C. would like to thank the work friendly environment and all the members of CCSP, SGT University. The research fellowship of S.C. was supported by the J. C. Bose National Fellowship of Sudhakar Panda. S.C. also would like to thank the School of Physical Sciences at the National Institute for Science Education and Research (NISER) in Bhubaneswar for providing a work-friendly environment. S.C. also thanks all the members of our newly formed virtual international non-profit consortium "Quantum Structures of the Space-Time & Matter"

(QASTM) for their elaborative discussions. S.C. would also like to thank all the speakers of the QASTM zoominar series from different parts of the world (For the uploaded YouTube link, see https://www.youtube.com/playlist?list=PLzW8AJcryManrTsG-4U4z9ip1J1dWoNgd) for supporting the research forum by giving outstanding lectures and their valuable time during the COVID pandemic time. Kiran Adhikari would like to thank TTK, RWTH, JARA, and the Institute of Quantum Information for the fellowships. Saptarshi Mandal, Nilesh Pandey, Abhishek Roy, Soumya Sarker, Partha Sarker, and Sadaat Salman Shariff would like to express their heartiest thanks to Jadavpur University, the University of Dhaka, NIT Karnataka, IIT Jodhpur, the University of Madras, and Delhi Technological University, respectively, for imparting knowledge and their enthusiasm for this research. Abhishek Roy would like to thank Sujit Damase for the discussions related to group generators. Partha Sarker would like to thank Syed Hasibul Hasan Chowdhury for the relevant discussions. K.A. would also like to thank David Di Vincenzo for his help in understanding quantum information theoretic concepts such as entanglement entropy and complexity. Finally, we would like to acknowledge our debt to the people belonging to various parts of the world for their generous and steady support for research in the natural sciences.

Conflicts of Interest: The authors declare no conflict of interest.

Appendix A. Interacting Part of the Hamiltonian in a Fourier Basis

The interacting part in the N oscillator Hamiltonian is

$$H' = \sum_{a=0}^{N-1} \lambda_4 x_a^4 + \lambda_6 x_a^6 + \lambda_8 x_a^8 = H'_{\phi^4} + H'_{\phi^6} + H'_{\phi^8} \tag{A1}$$

Now, we apply the discrete Fourier transform as in Equation (48) to find the ϕ^4 interaction:

$$H'_{\phi^4} = \sum_{a=0}^{N-1} \frac{\lambda_4}{N^2} \sum_{k',k_1,k_2,k_3=0}^{N-1} \exp\left[i\frac{2\pi a}{N}(k'+k_1+k_2+k_3)\right] \tilde{x}_{k'}\tilde{x}_{k_1}\tilde{x}_{k_2}\tilde{x}_{k_3} \tag{A2}$$

We apply the sum over index a and use the relation

$$\sum_{a=0}^{N-1} \exp\left[-i\left(\frac{2\pi a(k-k')}{N}\right)\right] = N\delta_{k,k'} \tag{A3}$$

to obtain

$$H'_{\phi^4} = \frac{\lambda_4}{N} \sum_{k',k_1,k_2,k_3=0}^{N-1} \delta_{k'+k_1+k_2+k_3,0}\tilde{x}_{k'}\tilde{x}_{k_1}\tilde{x}_{k_2}\tilde{x}_{k_3} \tag{A4}$$

Now, the Kronecker delta will reduce one of the indices, such as k' to $-k_1-k_2-k_3$. Now, k' only runs from $[0, N-1]$, whereas $-k_1-k_2-k_3$ has possible values in the range $[-3N, 0]$. To obtain a valid index value for k', we use the relation $\tilde{x}_{k+N} = \tilde{x}_k$ and write $k' = N - k_1 - k_2 - k_3 \; modN$. This will return a valid index value for k'. Then, we have

$$H'_{\phi^4} = \frac{\lambda_4}{N} \sum_{k_1,k_2,k_3=0}^{N-1} \tilde{x}_\alpha\tilde{x}_{k_1}\tilde{x}_{k_2}\tilde{x}_{k_3} \tag{A5}$$

Using similar arguments, we can find H'_{ϕ^6} and H'_{ϕ^8}.

Appendix B. $\mathcal{C}_2$ in Terms of the Ratio of the Target and Reference Matrix Eigenvalues

We claimed in Equation (46) that $\mathcal{C}_2$ can be expressed in terms of the ratio of eigenvalues of the target and reference matrix (i.e., $A(s=1)$ and $A(s=0)$, respectively). This was due to the nature of the unitary operator U and the diagonal block structure of $A(s=1)$ and $A(s=0)$.

To prove this, let us look at the complexity functional in Equation (44). The parameters in the 2×2 blocks on the U matrix have AdS parametrization, and they appear in $2[dy_i(1)^2 +$

$d\rho_i(1)^2]$ in $\mathcal{C}_2$, where $i = 1,3,5,7,9$. We can find these values for $y_i(1)$ and $\rho_i(1)$ from the boundary conditions we obtained in Equation (42). These values can be represented by the eigenvalues of $A(s=0)$ and $A(s=1)$ in the following way:

$$y_i = \frac{1}{4}\log\left[\frac{\lambda_1\lambda_2}{\Omega_1\Omega_2}\right]$$
$$\rho_i = \frac{1}{2}\cosh^{-1}\left[\frac{\lambda_1+\lambda_2}{2\sqrt{\lambda_1\lambda_2}}\right] \tag{A6}$$

Here, λ_1 and λ_2 are the eigenvalues of the 2×2 block in the $A(s=1)$ matrix corresponding to the block in U, whereas Ω_1 and Ω_2 are diagonal elements of the similar block 2×2 in $A(s=0)$. We can use the relation

$$\cosh^{-1}(x) = \ln(x+\sqrt{x^2-1}) \tag{A7}$$

to find the following for ρ_i:

$$\rho_i = \frac{1}{4}\ln\left[\frac{\lambda_2}{\lambda_1}\right] \tag{A8}$$

Then, our desired part in $\mathcal{C}_2$ will be

$$2(y_i(1)^2+\rho_i(1))^2 = 2\left[\ln\left[\frac{\lambda_1}{\Omega_1}\right]^2 + \ln\left[\frac{\lambda_2}{\Omega_2}\right]^2\right] \tag{A9}$$

Now, $i = 2,4,6,8$, and we have a different scenario. These are the lone diagonal parameters in the U matrix and have boundary conditions such as

$$y_i = \frac{1}{2}\ln\left[\frac{\lambda_T}{\Omega_R}\right] \tag{A10}$$

Here, λ_T and Ω_R denote the particular diagonal elements in $A(s=0)$ and $A(s=1)$, respectively, corresponding to the parameter y_i here. With these parameter values in hand, we can find from the complexity functional in Equation (44) the expression for Equation (46).

References

1. Harlow, D. TASI Lectures on the Emergence of Bulk Physics in AdS/CFT. *arXiv* **2018**, arXiv:1802.01040.
2. Ryu, S.; Takayanagi, T. Holographic derivation of entanglement entropy from AdS/CFT. *Phys. Rev. Lett.* **2006**, *96*, 181602. [CrossRef] [PubMed]
3. Hubeny, V.E.; Rangamani, M.; Takayanagi, T. A Covariant holographic entanglement entropy proposal. *JHEP* **2007**, *7*, 062. [CrossRef]
4. Rangamani, M.; Takayanagi, T. *Holographic Entanglement Entropy*; Springer: Berlin/Heidelberg, Germany, 2017; Volume 931. [CrossRef]
5. Susskind, L. Computational Complexity and Black Hole Horizons. *Fortsch. Phys.* **2016**, *64*, 24–43. Addendum: *Fortsch. Phys.* **2016**, *64*, 44–48. [CrossRef]
6. Stanford, D.; Susskind, L. Complexity and Shock Wave Geometries. *Phys. Rev. D* **2014**, *90*, 126007. [CrossRef]
7. Susskind, L.; Zhao, Y. Switchbacks and the Bridge to Nowhere. *arXiv* **2014**, arXiv:1408.2823.
8. Susskind, L. Entanglement is not enough. *Fortsch. Phys.* **2016**, *64*, 49–71. [CrossRef]
9. Brown, A.R.; Roberts, D.A.; Susskind, L.; Swingle, B.; Zhao, Y. Complexity, action, and black holes. *Phys. Rev. D* **2016**, *93*, 086006. [CrossRef]
10. Brown, A.R.; Roberts, D.A.; Susskind, L.; Swingle, B.; Zhao, Y. Holographic Complexity Equals Bulk Action? *Phys. Rev. Lett.* **2016**, *116*, 191301. [CrossRef]
11. Brown, A.R.; Susskind, L.; Zhao, Y. Quantum Complexity and Negative Curvature. *Phys. Rev. D* **2017**, *95*, 045010. [CrossRef]
12. Couch, J.; Fischler, W.; Nguyen, P.H. Noether charge, black hole volume, and complexity. *JHEP* **2017**, *3*, 119. [CrossRef]
13. Susskind, L. *Three Lectures on Complexity and Black Holes*; Springer: Berlin/Heidelberg, Germany, 2020.
14. Jefferson, R.; Myers, R.C. Circuit complexity in quantum field theory. *JHEP* **2017**, *10*, 107. [CrossRef]
15. Chapman, S.; Heller, M.P.; Marrochio, H.; Pastawski, F. Toward a Definition of Complexity for Quantum Field Theory States. *Phys. Rev. Lett.* **2018**, *120*, 121602. [CrossRef] [PubMed]

16. Khan, R.; Krishnan, C.; Sharma, S. Circuit Complexity in Fermionic Field Theory. *Phys. Rev. D* **2018**, *98*, 126001. [CrossRef]
17. Hackl, L.; Myers, R.C. Circuit complexity for free fermions. *JHEP* **2018**, *7*, 139. [CrossRef]
18. Bhattacharyya, A.; Shekar, A.; Sinha, A. Circuit complexity in interacting QFTs and RG flows. *JHEP* **2018**, *10*, 140. [CrossRef]
19. Haferkamp, J.; Faist, P.; Kothakonda, N.B.T.; Eisert, J.; Halpern, N.Y. Linear growth of quantum circuit complexity. *Nat. Phys.* **2022**, *18*, 528–532. [CrossRef]
20. Bhattacharyya, A.; Chemissany, W.; Haque, S.S.; Murugan, J.; Yan, B. The Multi-faceted Inverted Harmonic Oscillator: Chaos and Complexity. *SciPost Phys. Core* **2021**, *4*, 002. [CrossRef]
21. Ali, T.; Bhattacharyya, A.; Haque, S.S.; Kim, E.H.; Moynihan, N.; Murugan, J. Chaos and Complexity in Quantum Mechanics. *Phys. Rev. D* **2020**, *101*, 026021. [CrossRef]
22. Eisert, J. Entangling Power and Quantum Circuit Complexity. *Phys. Rev. Lett.* **2021**, *127*, 020501. [CrossRef]
23. Roberts, D.A.; Yoshida, B. Chaos and complexity by design. *JHEP* **2017**, *4*, 121. [CrossRef]
24. Camilo, G.; Melnikov, D.; Novaes, F.; Prudenziati, A. Circuit Complexity of Knot States in Chern-Simons theory. *JHEP* **2019**, *7*, 163. [CrossRef]
25. Couch, J.; Fan, Y.; Shashi, S. Circuit Complexity in Topological Quantum Field Theory. *Fortsch. Phys.* **2022**, *70*, 9–10. [CrossRef]
26. Chagnet, N.; Chapman, S.; de Boer, J.; Zukowski, C. Complexity for Conformal Field Theories in General Dimensions. *Phys. Rev. Lett.* **2022**, *128*, 051601 [CrossRef]
27. Flory, M.; Heller, M.P. Conformal field theory complexity from Euler-Arnold equations. *JHEP* **2020**, *12*, 091 [CrossRef]
28. Jaiswal, N.; Gautam, M.; Sarkar, T. Complexity and information geometry in the transverse XY model. *Phys. Rev. E* **2021**, *104*, 024127. [CrossRef]
29. Barbon, J.L.F.; Rabinovici, E. Holographic complexity and spacetime singularities. *JHEP* **2016**, *1*, 084. [CrossRef]
30. Alishahiha, M. Holographic Complexity. *Phys. Rev. D* **2015**, *92*, 126009. [CrossRef]
31. Yang, R.Q. Strong energy condition and complexity growth bound in holography. *Phys. Rev. D* **2017**, *95*, 086017. [CrossRef]
32. Chapman, S.; Marrochio, H.; Myers, R.C. Complexity of Formation in Holography. *JHEP* **2017**, *1*, 062. [CrossRef]
33. Carmi, D.; Myers, R.C.; Rath, P. Comments on Holographic Complexity. *JHEP* **2017**, *3*, 118. [CrossRef]
34. Reynolds, A.; Ross, S.F. Divergences in Holographic Complexity. *Class. Quant. Grav.* **2017**, *34*, 105004. [CrossRef]
35. Zhao, Y. Complexity and Boost Symmetry. *Phys. Rev. D* **2018**, *98*, 086011. [CrossRef]
36. Flory, M. A complexity/fidelity susceptibility g-theorem for $AdS_3/BCFT_2$. *JHEP* **2017**, *6*, 131. [CrossRef]
37. Reynolds, A.; Ross, S.F. Complexity in de Sitter Space. *Class. Quant. Grav.* **2017**, *34*, 175013. [CrossRef]
38. Carmi, D.; Chapman, S.; Marrochio, H.; Myers, R.C.; Sugishita, S. On the Time Dependence of Holographic Complexity. *JHEP* **2017**, *11*, 188. [CrossRef]
39. Couch, J.; Eccles, S.; Fischler, W.; Xiao, M.L. Holographic complexity and noncommutative gauge theory. *JHEP* **2018**, *3*, 108. [CrossRef]
40. Yang, R.Q.; Niu, C.; Zhang, C.Y.; Kim, K.Y. Comparison of holographic and field theoretic complexities for time dependent thermofield double states. *JHEP* **2018**, *2*, 082. [CrossRef]
41. Abt, R.; Erdmenger, J.; Hinrichsen, H.; Melby-Thompson, C.M.; Meyer, R.; Northe, C.; Reyes, I.A. Topological Complexity in AdS_3/CFT_2. *Fortsch. Phys.* **2018**, *66*, 1800034. [CrossRef]
42. Swingle, B.; Wang, Y. Holographic Complexity of Einstein-Maxwell-Dilaton Gravity. *JHEP* **2018**, *09*, 106. [CrossRef]
43. Reynolds, A.P.; Ross, S.F. Complexity of the AdS Soliton. *Class. Quant. Grav.* **2018**, *35*, 095006. [CrossRef]
44. Fu, Z.; Maloney, A.; Marolf, D.; Maxfield, H.; Wang, Z. Holographic complexity is nonlocal. *JHEP* **2018**, *2*, 072. [CrossRef]
45. An, Y.S.; Peng, R.H. Effect of the dilaton on holographic complexity growth. *Phys. Rev. D* **2018**, *97*, 066022. [CrossRef]
46. Bolognesi, S.; Rabinovici, E.; Roy, S.R. On Some Universal Features of the Holographic Quantum Complexity of Bulk Singularities. *JHEP* **2018**, *6*, 016. [CrossRef]
47. Chen, B.; Li, W.M.; Yang, R.Q.; Zhang, C.Y.; Zhang, S.J. Holographic subregion complexity under a thermal quench. *JHEP* **2018**, *7*, 034. [CrossRef]
48. Abt, R.; Erdmenger, J.; Gerbershagen, M.; Melby-Thompson, C.M.; Northe, C. Holographic Subregion Complexity from Kinematic Space. *JHEP* **2019**, *1*, 012. [CrossRef]
49. Hashimoto, K.; Iizuka, N.; Sugishita, S. Thoughts on Holographic Complexity and its Basis-dependence. *Phys. Rev. D* **2018**, *98*, 046002. [CrossRef]
50. Flory, M.; Miekley, N. Complexity change under conformal transformations in AdS_3/CFT_2. *JHEP* **2019**, *5*, 003. [CrossRef]
51. Couch, J.; Eccles, S.; Jacobson, T.; Nguyen, P. Holographic Complexity and Volume. *JHEP* **2018**, *11*, 044. [CrossRef]
52. Hosseini Mansoori, S.A.; Jahnke, V.; Qaemmaqami, M.M.; Olivas, Y.D. Holographic Complexity of Anisotropic Black Branes. *Phys. Rev. D* **2019**, *100*, 046014. [CrossRef]
53. Chapman, S.; Marrochio, H.; Myers, R.C. Holographic complexity in Vaidya spacetimes. Part I. *JHEP* **2018**, *6*, 046. [CrossRef]
54. Chapman, S.; Marrochio, H.; Myers, R.C. Holographic complexity in Vaidya spacetimes. Part II. *JHEP* **2018**, *6*, 114. [CrossRef]
55. Caceres, E.; Chapman, S.; Couch, J.D.; Hernandez, J.P.; Myers, R.C.; Ruan, S.M. Complexity of Mixed States in QFT and Holography. *JHEP* **2020**, *3*, 012. [CrossRef]
56. Ben-Ami, O.; Carmi, D. On Volumes of Subregions in Holography and Complexity. *JHEP* **2016**, *11*, 129. [CrossRef]
57. Abad, F.J.G.; Kulaxizi, M.; Parnachev, A. On Complexity of Holographic Flavors. *JHEP* **2018**, *1*, 127. [CrossRef]
58. Brown, A.R.; Susskind, L. Second law of quantum complexity. *Phys. Rev. D* **2018**, *97*, 086015. [CrossRef]

59. Bernamonti, A.; Galli, F.; Hernandez, J.; Myers, R.C.; Ruan, S.M.; Simón, J. First Law of Holographic Complexity. *Phys. Rev. Lett.* **2019**, *123*, 081601. [CrossRef]
60. Bernamonti, A.; Galli, F.; Hernandez, J.; Myers, R.C.; Ruan, S.M.; Simón, J. Aspects of The First Law of Complexity. *J. Phys. A Math. Theor.* **2020**, *53*, 294002. [CrossRef]
61. Cai, R.G.; Ruan, S.M.; Wang, S.J.; Yang, R.Q.; Peng, R.H. Action growth for AdS black holes. *JHEP* **2016**, *9*, 161. [CrossRef]
62. Lehner, L.; Myers, R.C.; Poisson, E.; Sorkin, R.D. Gravitational action with null boundaries. *Phys. Rev. D* **2016**, *94*, 084046. [CrossRef]
63. Moosa, M. Evolution of Complexity Following a Global Quench. *JHEP* **2018**, *3*, 031. [CrossRef]
64. Moosa, M. Divergences in the rate of complexification. *Phys. Rev. D* **2018**, *97*, 106016. [CrossRef]
65. Hashimoto, K.; Iizuka, N.; Sugishita, S. Time evolution of complexity in Abelian gauge theories. *Phys. Rev. D* **2017**, *96*, 126001. [CrossRef]
66. Chapman, S.; Eisert, J.; Hackl, L.; Heller, M.P.; Jefferson, R.; Marrochio, H.; Myers, R.C. Complexity and entanglement for thermofield double states. *SciPost Phys.* **2019**, *6*, 034. [CrossRef]
67. Guo, M.; Hernandez, J.; Myers, R.C.; Ruan, S.M. Circuit Complexity for Coherent States. *JHEP* **2018**, *10*, 011. [CrossRef]
68. Camargo, H.A.; Caputa, P.; Das, D.; Heller, M.P.; Jefferson, R. Complexity as a novel probe of quantum quenches: Universal scalings and purifications. *Phys. Rev. Lett.* **2019**, *122*, 081601. [CrossRef]
69. Doroudiani, M.; Naseh, A.; Pirmoradian, R. Complexity for Charged Thermofield Double States. *JHEP* **2020**, *1*, 120. [CrossRef]
70. Chapman, S.; Chen, H.Z. Charged Complexity and the Thermofield Double State. *JHEP* **2021**, *2*, 187. [CrossRef]
71. Bhattacharyya, A.; Nandy, P.; Sinha, A. Renormalized Circuit Complexity. *Phys. Rev. Lett.* **2020**, *124*, 101602. [CrossRef]
72. Bhargava, P.; Choudhury, S.; Chowdhury, S.; Mishara, A.; Selvam, S.P.; Panda, S.; Pasquino, G.D. Quantum aspects of chaos and complexity from bouncing cosmology: A study with two-mode single field squeezed state formalism. *SciPost Phys. Core* **2021**, *4*, 026 [CrossRef]
73. Lehners, J.L.; Quintin, J. Quantum Circuit Complexity of Primordial Perturbations. *Phys. Rev. D* **2021**, *103*, 063527. [CrossRef]
74. Bhattacharyya, A.; Das, S.; Haque, S.S.; Underwood, B. Rise of cosmological complexity: Saturation of growth and chaos. *Phys. Rev. Res.* **2020**, *2*, 033273. [CrossRef]
75. Choudhury, S.; Dutta, A.; Ray, D. Chaos and Complexity from Quantum Neural Network: A study with Diffusion Metric in Machine Learning. *JHEP* **2021**, *4*, 138. [CrossRef]
76. Choudhury, S.; Chowdhury, S.; Gupta, N.; Mishara, A.; Selvam, S.P.; Panda, S.; Pasquino, G.D.; Singha, C.; Swain, A. Circuit Complexity From Cosmological Islands. *Symmetry* **2021**, *13*, 1301. [CrossRef]
77. Adhikari, K.; Choudhury, S.; Chowdhury, S.; Shirish, K.; Swain, A. Circuit complexity as a novel probe of quantum entanglement: A study with black hole gas in arbitrary dimensions. *Phys. Rev. D* **2021**, *104*, 065002. [CrossRef]
78. Adhikari, K.; Choudhury, S.; Pandya, H.N.; Srivastava, R. $\mathcal{PGW}$ Circuit Complexity. *arXiv* **2021**, arXiv:2108.10334.
79. Choudhury, S.; Selvam, S.P.; Shirish, K. Circuit Complexity from Supersymmetric Quantum Field Theory with Morse Function. *Symmetry* **2022**, *14*, 1656 [CrossRef]
80. Bai, C.; Li, W.H.; Ge, X.H. Towards the non-equilibrium thermodynamics of the complexity and the Jarzynski identity. *arXiv* **2021**, arXiv:2107.08608.
81. Caputa, P.; Kundu, N.; Miyaji, M.; Takayanagi, T.; Watanabe, K. Liouville Action as Path-Integral Complexity: From Continuous Tensor Networks to AdS/CFT. *JHEP* **2017**, *11*, 097. [CrossRef]
82. Caputa, P.; Magan, J.M. Quantum Computation as Gravity. *Phys. Rev. Lett.* **2019**, *122*, 231302. [CrossRef]
83. Boruch, J.; Caputa, P.; Takayanagi, T. Path-Integral Optimization from Hartle-Hawking Wave Function. *Phys. Rev. D* **2021**, *103*, 046017. [CrossRef]
84. Boruch, J.; Caputa, P.; Ge, D.; Takayanagi, T. Holographic path-integral optimization. *JHEP* **2021**, *7*, 016. [CrossRef]
85. Nielsen, M.A. A Geometric Approach to Quantum Circuit Lower Bounds. *arXiv* **2005**, arXiv:quant-ph/0502070.
86. Nielsen, M.A. Quantum Computation as Geometry. *Science* **2006**, *311*, 1133–1135 [CrossRef]
87. Dowling, M.R.; Nielsen, M.A. The Geometry of Quantum Computation. *Quantum Inf. Comput.* **2008**, *8*, 861–899 [CrossRef]
88. Nielsen, M.A.; Dowling, M.R.; Gu, M.; Doherty, A.C. Optimal control, geometry, and quantum computing. *Phys. Rev. A* **2006**, *73*, 062323 [CrossRef]
89. Watrous, J., Quantum Computational Complexity. In *Encyclopedia of Complexity and Systems Science*; Meyers, R.A., Ed.; Springer: New York, NY, USA, 2009; pp. 7174–7201.
90. Aaronson, S. The Complexity of Quantum States and Transformations: From Quantum Money to Black Holes. *arXiv* **2016**, arXiv:1607.05256.
91. Orús, R. Tensor networks for complex quantum systems. *APS Phys.* **2019**, *1*, 538–550. [CrossRef]
92. Nishioka, T.; Ryu, S.; Takayanagi, T. Holographic Entanglement Entropy: An Overview. *J. Phys. A* **2009**, *42*, 504008. [CrossRef]
93. Almheiri, A.; Dong, X.; Harlow, D. Bulk Locality and Quantum Error Correction in AdS/CFT. *JHEP* **2015**, *4*, 163. [CrossRef]
94. Swingle, B. Entanglement Renormalization and Holography. *Phys. Rev. D* **2012**, *86*, 065007. [CrossRef]
95. Caputa, P.; Magan, J.M.; Patramanis, D. Geometry of Krylov complexity. *Phys. Rev. Res.* **2022**, *4*, 013041. [CrossRef]
96. Parker, D.E.; Cao, X.; Avdoshkin, A.; Scaffidi, T.; Altman, E. A Universal Operator Growth Hypothesis. *Phys. Rev. X* **2019**, *9*, 041017. [CrossRef]
97. Roberts, D.A.; Stanford, D.; Streicher, A. Operator growth in the SYK model. *JHEP* **2018**, *6*, 122. [CrossRef]

98. Rabinovici, E.; Sánchez-Garrido, A.; Shir, R.; Sonner, J. Operator complexity: A journey to the edge of Krylov space. *JHEP* **2021**, *6*, 062. [CrossRef]
99. Barbón, J.L.F.; Rabinovici, E.; Shir, R.; Sinha, R. On The Evolution of Operator Complexity Beyond Scrambling. *JHEP* **2019**, *10*, 264. [CrossRef]
100. Jian, S.K.; Swingle, B.; Xian, Z.Y. Complexity growth of operators in the SYK model and in JT gravity. *JHEP* **2021**, *3*, 014. [CrossRef]
101. Dymarsky, A.; Gorsky, A. Quantum chaos as delocalization in Krylov space. *Phys. Rev. B* **2020**, *102*, 085137. [CrossRef]
102. Dymarsky, A.; Smolkin, M. Krylov complexity in conformal field theory. *Phys. Rev. D* **2021**, *104*, L081702. [CrossRef]
103. Balasubramanian, V.; Caputa, P.; Magan, J.; Wu, Q. A new measure of quantum state complexity. *arXiv* **2022**, arXiv:2202.06957.
104. Shankar, R. *Effective Field Theory in Condensed Matter Physics*; Cambridge University Press: Cambridge, MA, USA, 1998.
105. Cheung, C.; Creminelli, P.; Fitzpatrick, A.L.; Kaplan, J.; Senatore, L. The Effective Field Theory of Inflation. *JHEP* **2008**, *3*, 014. [CrossRef]
106. Weinberg, S. Effective Field Theory for Inflation. *Phys. Rev. D* **2008**, *77*, 123541. [CrossRef]
107. Agarwal, N.; Holman, R.; Tolley, A.J.; Lin, J. Effective field theory and non-Gaussianity from general inflationary states. *JHEP* **2013**, *5*, 085. [CrossRef]
108. Burgess, C.P. Intro to Effective Field Theories and Inflation. *arXiv* **2017**, arXiv:1711.10592.
109. Choudhury, S. Field Theoretic Approaches to Early Universe. Ph.D. Thesis, Indian Statistical Institute, Calcutta, India, 2016,
110. Choudhury, S. Can Effective Field Theory of inflation generate large tensor-to-scalar ratio within Randall–Sundrum single braneworld? *Nucl. Phys. B* **2015**, *894*, 29–55. [CrossRef]
111. Naskar, A.; Choudhury, S.; Banerjee, A.; Pal, S. EFT of Inflation: Reflections on CMB and Forecasts on LSS Surveys. *arXiv* **2017**, arXiv:1706.08051.
112. Pich, A. Effective field theory: Course. Les Houches Summer School in Theoretical Physics, Session 68: Probing the Standard Model of Particle Interactions. *arXiv* **1998**, arXiv:hep-ph/9806303.
113. Burgess, C.P. Introduction to Effective Field Theory. *Ann. Rev. Nucl. Part. Sci.* **2007**, *57*, 329–362. [CrossRef]
114. Donoghue, J.F. Introduction to the effective field theory description of gravity. *arXiv* **1995**, arXiv:gr-qc/9512024.
115. Donoghue, J.F. The effective field theory treatment of quantum gravity. *AIP Conf. Proc.* **2012**, *1483*, 73–94. [CrossRef]
116. Dubovsky, S.; Hui, L.; Nicolis, A.; Son, D.T. Effective field theory for hydrodynamics: Thermodynamics, and the derivative expansion. *Phys. Rev. D* **2012**, *85*, 085029. [CrossRef]
117. Crossley, M.; Glorioso, P.; Liu, H. Effective field theory of dissipative fluids. *JHEP* **2017**, *9*, 095. [CrossRef]
118. Choudury, S. Cosmic Microwave Background from Effective Field Theory. *Universe* **2019**, *5*, 155 [CrossRef]
119. Choudhury, S.; Gharat, R.M.; Mandal, S.; Pandey, N. Circuit Complexity in an interacting quenched Quantum Field Theory. *arXiv* **2022**, arXiv:2209.03372.
120. Adhikari, K.; Choudhury, S.; Roy, A. Krylov Complexity in Quantum Field Theory. *arXiv* **2022**, arXiv:2204.02250.